Chromatin Immunoprecipitation in Fused Silica Capillaries

A Miniaturization Approach to Mapping Protein-DNA Interaction in Cells

Dissertation

Olaf Selchow

Vom Fachbereich Physik der Universität Kaiserslautern zur Verleihung des akademischen Grades "Doktor der Naturwissenschaften" genehmigte Dissertation

durchgeführt am
European Molecular Biology Laboratory (EMBL)
in Heidelberg

unter Anleitung von
Prof. Dr. Christiane Ziegler
Fachbereich Physik der Universität Kaiserslautern

Zweitgutachter: apl. Prof. Dr. René Beigang

Datum der wissenschaftlichen Aussprache: 19. April 2002

D 386

Abstract

Microsystem technology has been a fast evolving field over the last few years. Its ability to handle volumes in the sub-microliter range makes it very interesting for potential application in fields such as biology, medicine and pharmaceutical research. However, the use of micro-fabricated devices for the analysis of liquid biological samples still has to prove its applicability for many particular demands of basic research. This is particularly true for samples consisting of complex protein mixtures.

The presented study therefore aimed at evaluating if a commonly used glass-coating technique from the field of micro-fluidic technology can be used to fabricate an analysis system for molecular biology. It was ultimately motivated by the demand to develop a technique that allows the analysis of biological samples at the single-cell level.

Gene expression at the transcription level is initiated and regulated by DNA-binding proteins. To fully understand these regulatory processes, it is necessary to monitor the interaction of specific transcription factors with other elements - proteins as well as DNA sites - in living cells. One well-established method to perform such analysis is the Chromatin Immunoprecipitation (CHIP) assay. To map protein-DNA interactions, living cells are treated with formaldehyde *in vivo* to cross-link DNA-binding proteins to their resident sites. The chromatin is then broken into small fragments, and specific antibodies against the protein of interest are used to immunopurify the chromatin fragments to which those factors are bound. After purification, the associated DNA can be detected and analyzed using Polymerase Chain Reaction (PCR).

Current CHIP technology is limited as it needs a relatively large number of cells while there is increasing interest in monitoring DNA-protein interactions in very few, if not single cells. Most notably this is the case in research on early organism development (embryogenesis).

To investigate if microsystem technology can be used to analyze DNA-protein complexes from samples containing chromatin from only few cells, a new setup for fluid transport in glass capillaries of 75μm inner diameter has been developed, forming an array of micro-columns for parallel affinity chromatography. The inner capillary walls were antibody-coated using a silane-based protocol. The remaining surface was made chemically inert by saturating free binding sites with suitable biomolecules. Variations of this protocol have been tested. Furthermore, the sensitivity of the PCR method to detect immunoprecipitated protein-DNA complexes was improved, resulting in the reliable detection of about 100 DNA fragments from chromatin. The aim of the study was to successively decrease the amount of analyzed chromatin in order to

investigate the lower limits of this technology in regard to sensitivity and specificity of detection.

The *Drosophila* GAGA transcription factor was used as an established model system. The protein has already been analyzed in several large-scale CHIP experiments and antibodies of excellent specificity are available.

The results of the study revealed that this approach is not easily applicable to "real-world" biological samples in regard to volume reduction and specificity. Particularly, material that non-specifically adsorbed to capillary surfaces outweighed the specific antibody-antigen interaction, the system was designed for. It became clear that complex biological structures, such as chromatin-protein compositions, are not as easily accessible by techniques based on chemically modified glass surfaces as pre-purified samples.

In the case of the investigated system, it became evident that there is a need for more research that goes beyond the scope of this work. It is necessary to develop novel coatings and materials to prevent non-specific adsorption. In addition to improving existing techniques, fundamentally new concepts, such as microstructures in biocompatible polymers or liquid transport on hydrophobic stripes on planar substrates to minimize surface contact, may also help to advance the miniaturization of biological experiments.

Zusammenfassung

Die Mikrosystemtechnologie hat sich in den letzten Jahren mit unvorhergesehener Dynamik entwickelt. Vor allem die Möglichkeit, in Mikrostrukturen und Kanälen Flüssigkeitsvolumen von weniger als einem Mikroliter zu manipulieren und zu transportieren begründet ihr großes Potential für Anwendungen in Bereichen wie der Biologie, der Medizin und der pharmazeutischen Forschung. Der Einsatz der Mikrofluidik bei der Analyse biologisch relevanter Proben, zum Beispiel von komplexen Mischungen mehrerer Proteine, ist jedoch noch sehr begrenzt. Der wesentliche limitierende Faktor sind Wechselwirkungen der Proteine mit den Wänden der Mikrokanäle.

Vor diesem Hintergrund untersucht die vorliegende Arbeit die Anwendung einer in der Mikrofluidik verbreiteten Methode zur Beschichtung von Glasoberflächen auf ein Analyseverfahren der Molekularbiologie.

Auf der Ebene der Transkription wird die Regulierung der Genexpression vor allem von DNA-bindenden Proteinen kontrolliert. Um diesen Vorgang ganz zu verstehen ist es notwendig, die Wechselwirkung spezifischer Transkriptionsfaktoren mit bestimmten Elementen - Proteinen wie auch DNA-Sequenzen - in lebenden Zellen zu untersuchen. Eine etablierte Methode zur Erforschung solcher Fragestellungen ist der *Chromatin Immunoprecipitation* (CHIP) *assay*. Um Protein-DNA-Wechselwirkungen zu bestimmen werden lebende Zellen mit Formaldehyd behandelt um die Proteine an ihre Bindungsstellen *in vivo* zu fixieren. Anschließend wird das Chromatin in kleine Fragmente geschnitten und mit spezifischen Antikörpern, an die der spezifische Faktor gebunden ist, aufgereinigt. Die assoziierte DNA kann mit der *Polymerase Chain Reaction* (PCR) analysiert werden.

CHIP-Analysen benötigen relativ viele Zellen. Es besteht aber ein großes Interesse, Protein-DNA-Wechselwirkungen in wenigen oder sogar einzelnen Zellen zu untersuchen. Dies betrifft vor allem die Forschung an frühen Entwicklungsstadien von Organismen (Embryogenese).

Mit dem Ziel, Protein-DNA-Komplexe von wenigen Zellen zu analysieren wurde ein Array von Mikrosäulen für Affinitätschromatographie entwickelt. Der Kern dieses neuen Aufbaus für den Transport von Flüssigkeiten besteht aus 8 parallelen Glaskapillaren mit einem Innendurchmesser von 75 μm. Die inneren Wände der Kanäle sind mit Antikörpern beschichtet. Das auf Silanisierung basierende Protokoll bindet jedes beliebige Protein kovalent an die Glasoberfläche und erlaubt gleichzeitig, die Beschichtung gegen unspezifische Adsorption abzuschirmen. Mehrere Parameter dieser Beschichtung wurden variiert. Weiterhin wurde die Empfindlichkeit der PCR-Detektion der immunoprezipitierten Protein-DNA Komplexe verbessert,

wodurch ein zuverlässiger Nachweis von etwa 100 DNA Fragmenten aus Chromatin möglich ist. Das Ziel der Arbeit ist, die Menge an eingesetztem Chromatin schrittweise zu verringern um die Grenzen in Bezug auf Nachweisgrenze und Spezifizität zu charakterisieren.

Als molekulares Modellsystem für diesen Miniaturisierungsansatz wurde der GAGA Transkriptionsfaktor in *Drosophila* gewählt, da dieses Protein schon in vielen CHIP-Experimenten untersucht wurde und Antikörper mit sehr guter Affinität zur Verfügung stehen.

Die experimentellen Ergebnisse dieser Studie zeigen die Grenzen des beschriebenen Ansatzes bezüglich Volumenreduzierung und Spezifizität auf. Die Effekte von unspezifisch an den Oberflächen adsorbierendem Probenmaterial überdecken die spezifische Wechselwirkung mit der Antikörperbeschichtung. Im Gegensatz zu vorher aufgereinigten Proben sind komplexe biologische Strukturen wie Chromatin offensichtlich schwer zugänglich für Analysetechniken, die auf chemisch modifizierten Glasoberflächen basieren.

Es ist deutlich geworden, daß im Falle biologischer Systeme wie dem hier beschriebenen ein Bedarf für weitere Forschungssarbeit besteht, der über den Rahmen dieser Arbeit hinausgeht. Es werden vor allem neue Materialien und Beschichtungen mit wesentlich besseren Eigenschaften gegen unspezifische Adsorption benötigt. Auch grundsätzlich neue Ansätze und Konzepte - wie Mikrostrukturen aus biokompatiblen Polymermaterialien oder Flüssigkeitstransport auf hydrophoben Streifen auf planaren Substraten zur Minimierung des Proben-Oberflächen-Kontakts - können helfen, miniaturisierte Experimente mit biologischen Proben voranzubringen.

Contents

Chapter 1

Introduction

From an application point of view, miniaturization of bioanalytical techniques means reduction of sample material and volume as well as a potential increase in sensitivity. These very promising properties of microfabricated analysis devices strongly attract a great scientific interest in basic molecular biology research. In particular, the potential of investigating and biochemically analyzing single cells is very attractive.

So far, techniques used to examine single cells are mostly based on fluorescence staining (cell sorting or microscopical analysis), microinjection (in situ -techniques like in situ PCR for detection of specific gene sequences) and micro-dissection. Biochemical separation of cellular compounds and their biochemical analysis on the molecular level is not realized yet. Extraction and examination of the molecular compounds of single cells will provide new insights on all those biological processes which are not accessible so far due to restricted amount of sample cells or molecules available. Standard laboratory techniques for (cell-)biological experiments usually require many thousands of cells of the same type. Therefore, results obtained from large-scale experiments are but averages and most if not all information on the individual object is lost.

Also, for many types of experiments only few cells are available, e.g. because a rare cell type is investigated or due to experimental manipulation. Experimental techniques based on microstructures have the potential to approach these situations.

During the last years, microsystem technology has evolved to a vast field of research comprising many disciplines like microfabrication technique development, microhydrodynamics, micro-optics, capillary electrophoresis, micro-separation research, to name only a few. The progress in design and fabrication technology of miniaturized and highly integrated biochemical analysis devices, known as "Lab-on-a-Chip" or Micro Total Analysis Systems (μTAS) systems, has now reached a qualitatively

new level. Many (bio-)chemical analytical techniques have been demonstrated in microfluidic devices, involving microliter to picoliter sample volumes. Amongst these are micro-chip implementations of continuous flow PCR, integrated nanoliter DNA analysis, integrated multi-step genotyping assays, highly paralleled high speed DNA separation, high throughput cell handling, cell sorting and many more. The specific fields of microarray technology and microfabricated biosensors have already entered the stage of commercialization.

However, the long anticipated and advertised potential applications of microfluidics in fields such as analytical chemistry, medical diagnostics, environmental monitoring, drug discovery and evaluation of new pharmaceuticals could be realized to a limited extend only. So far, resulting off-the-shelf and ready-to-use applications are still few.

In particular, implementations of miniaturized concepts for basic biological research are now put to test at a progressive rate. It is clear that direct evaluation of the available technology in the research laboratory is needed to bring microsystem developers and potential users together.

In this context, this thesis investigates the application of the miniaturization concept to basic molecular biology research from a most practical point of view: The project goal is to fabricate a microchannel-based immunoaffinity chromatographic tool that enables the biologist to carry out a highly sensitive molecular separation from minute amount of sample material and thereby allows him to address qualitatively new questions on the organism he is working on.

As a model system for a demonstration of the concept the *in vivo* DNA-binding site identification and analysis of the GAGA transcription factor (GAF) in the fruitfly *Drosophila Melanogaster* was chosen. The key step of such a protein-DNA interaction analysis is a highly selective and sensitive immunoaffinity chromatographic separation of the target from its cellular environment. The GAF protein has been studied for many years and basic knowledge on its function is available.

A collaboration with a laboratory working on chromatin remodeling and gene expression regulation was established. With their expertise and the supply of the relevant chemicals (i.e. a good anti-GAF antibody and chromatin material from *Drosophila*) the problems concerning the biochemistry of this model system were considerably reduced.

The molecular complexity of the chromatin samples increases the demands on selectivity of experimental manipulation and detection methods tremendously. The sheer number of molecular species and their variety of chemical and physical properties in such a "real-world" sample makes separation selectivity and background signal in detection a challenge. Non-specifically adsorbed sample material to the substrate is known to be another source of background signal from immunoaffinity separation

techniques and therefore surface property control was one of the concerns of the presented work.

It is a key issue in all microanalysis applications involving cellular extracts or complex protein mixtures to either reliably control the surface properties of the used containers and channels or to ensure that contact with the confining walls is prevented. This requirement, which is due to the increased surface-to-volume ratio in microchannels, puts high and in many aspects new demands on the properties of the microstructures used.

Also, the total amount of target GAF molecules in the sample is dramatically reduced when approaching the few-cell-level. This is a big step ahead in comparison to most of the work on immunoassays in microsystems that has been presented in the literature so far.

The project involves immobilized antibodies in microchannels (capillaries) of 75 μm inner diameter. The antibody modified inner surfaces of these capillaries serve as stationary phase for the immunoaffinity purification of the target protein-DNA and Polymerase Chain Reaction (PCR) was chosen as highly sensitive detection method for the DNA sequence bound to the precipitated protein.

The following steps were carried out in the process of the presented work:

Addressing the critical subject of the project idea first, a suitable surface modification technique was chosen to covalently immobilize antibodies on fused silica glass surfaces. Two silane-based protocols for protein immobilization and surface blocking against non-specific adsorption of sample material were evaluated. A coating procedure for commercially available glass capillaries was established an the successful coating of capillaries with functional antibodies was monitored by confocal fluorescence imaging of labeled antibodies and antigen on the inner channel surfaces.

Then, performance of the large-scale separation technique that was chosen for miniaturization was assessed quantitatively. Protocols and the used chemicals were tested by performing the large-scale chromatin immunoprecipitation (CHIP) assay in the way it is routinely carried out in molecular biology laboratories and reported in the literature.

A fluidics setup arrangement was designed that allows a parallel mounting of eight capillaries, simultaneous flushing with buffer and individual low-dead-volume sample injection. Special care had to be taken of homogeneous temperature control for all eight columns with an array of high power Peltier elements.

The PCR amplification of the specific target DNA fragment and a control fragment was optimized by choosing a well-amplifying amplicon and the respective primers. The cycling times and temperatures were fine tuned as well.

As a next step, the concept of the fluidic setup was tested by performing a simple affinity separation of biotinylated DNA fragments from non-biotinylated DNA fragments with an anti-biotin coated capillary.

Finally, experiments with antibodies attached directly to the glass walls were performed.

Chapter 2

Literature Review, Theory and Background

In this chapter, the main aspects of microsystem technology and miniaturized analysis systems with relevance to the presented work and biological science in general are discussed (section 2.1). Furthermore, the basics and some theoretical background on affinity chromatography are presented in section 2.2 and the biological motivation for this project is introduced in section 2.3. Section 2.4 explains the principles of the *Polymerase Chain Reaction* (PCR). The experiments carried out during the work for this thesis rely on the extreme sensitivity of PCR as an indirect method for the detection of DNA fragments.

2.1 Bioanalysis in Microsystems

During the last years, microfabricated analytical devices (also referred to as "Lab-on-a-chip" or "Micro Total Analysis Systems" (μTAS) have experienced a phenomenal increase in popularity and the potential for their application is still enthusiastically advertised (*Khandurina and Guttman* (2002), *Wang* (2000), *Becker and Gärtner* (2000), *Kopp et al.* (1997), *Li et al.* (2001)). Interestingly, the founders of the concept of microanalytical devices adopt now a more pragmatic position, critically assess and consider the practical needs and specific applications for this technology (*Harrison et al.* (2000), *Wilding and Kricka* (1999) and *de Mello and Wootton* (2002)). Only recently, miniaturization and microfluidics technology are about to enter basic biological and molecular biology research (*Khandurina and Guttman* (2002) and *Jakeway et al.* (2000)).

An overview on the history of microsystem technology in general is given in sec-

tion 2.1.1, followed by examples on existing technologies for microfabricated analytical devices in the field of the life sciences (section 2.1.2). Section 2.1.3 introduces microfluidics, followed by a brief review of the most common substrate materials for microstructures, namely glass and polymers, in section 2.1.4. Finally, section 2.1.5 stresses the importance of chemical surface property control in miniaturized sample containers. In this context, the presented project has been taken up, and from this point of view the following section provides an introducing to bioanalysis in microsystems.

Generally, microanalysis devices can be classified in two categories based on the complexity of the fluidics involved: microarray-based (DNA or protein molecules immobilized in a micro-chip) and microfluidic-based (DNA or proteins being transported, reacted and analyzed on a chip). Of these two types of such systems, the latter is of greater relevance for this work and therefore will be emphasized in the following introduction.

2.1.1 General Historical Overview

The field of Micro Electro Mechanical Systems (MEMS) has evolved during the last twenty years from the techniques developed for microelectronics industry. The technology for fabrication of microstructures in silicon clearly played a key role in the revolutionizing impact microelectronics had on society. The fact that computers, that once had the size of entire rooms, have been replaced by small laptop computers of much higher performance illustrates this in a striking way.

Three-dimensional structures with dimensions of the order of micrometers, e.g. first MEMS devices such as ink jet nozzle arrays (at Hewlett Packard, *Kuhn et al.* (1978)) and the first micro-fabricated gas chromatograph on a silicon waver (*Terry* (1975)), came up in the late seventies, initiating the microsystems technology which nowadays is a popular and rapidly proliferating field. In 1982, the use of silicon as a mechanical material was reviewed for the first time by *Petersen* (1982).

But it was only in the beginning of the 90s that advanced engineering technologies developed for the microelectronics industry were systematically applied to develop fluidic handling systems for minute volumes of liquids (*Gravesen et al.*, 1993). This mainly happened in analytical chemistry. Pioneering work has been carried out by A. Manz (*Manz et al.* (1990), *Effenhauser et al.* (1993)) by bringing up the concept of μTAS. The basis of this concept was to integrate micro-fabricated channels for liquid handling, chemical reaction chambers and detection systems into a single device.

The major advantages of developing miniaturized devices for (bio-)analytical and chemical applications have already been outlined in the work of *Manz et al.* (1990).

The most important advantages are:

- Reduction of reaction and separation times
- Reduction of chemical and reagent consumption
- Potential for easy scale up by parallel systems
- Reduction of sample (analyte) material
- Portability of devices

Apart from more comfortable, easier and faster procedures in the laboratory there are other, more specific advantages to introducing miniaturization and integration techniques to biology:

- Qualitatively new experiments become possible
- Precise manipulation of minute liquid volumes (down to the range of $\approx$ femtoliter)
- Potential to reach the level of single molecule analysis/detection

Meanwhile many groups all over the world and several companies have taken up the ideas, aiming to produce easy-to-use tools that will make chemical and biochemical analysis cheaper, faster, portable and more reliable (*Gilman and Ewing* (1995), *Waters et al.* (1998) and *Harrison et al.* (1993)).

The main fields of application of microstructures in the life sciences are without any doubt the chemical, pharmaceutical and biomedical industry. The potentials reach from microsurgery devices to high throughput screening of medical compounds in the development of new pharmaceutical molecules (*Mitchell et al.* (2000), *Polla et al.* (2000) and *Brischwein et al.* (1996)).

With the completion of the human genome project, which was substantially speeded up by microchannel DNA sequencing technology and capillary electrophoresis, and the advent of DNA microarrays (*Chipping Forecast*, 1999), microsystem technology has more and more become a focus of interest for the basic biological research (*Khandurina and Guttman*, 2002). Important progress in biochemical analysis, both quantitatively and qualitatively, is expected from new methods based on the idea of downscaling existing methods with respect to the sample amount and instrumentation size.

Albeit the many advantages of working in microstructures (mentioned above) there are also downsides of this technology. One of them is the need to precisely control the surface properties of the sample containing volumes. This is particularly important

when working with biological material. To avoid unwanted reactions with microchannel walls, rendering the channel walls inert is a big concern in most microsystem applications with sensitive biomolecular sample material (see also section 2.1.5).

2.1.2 Existing Microfabricated Devices in Biotechnology and Biochemical Analysis

Before focussing on the particular aspects of microfluidics, the following will briefly list the "state of the art" of biomolecular analysis in microdevices. A comprehensive review on the current status of development of microfabricated reaction and separation systems is given by *Krishnan et al.* (2001).

Many of the more complex integrated systems, such as the "Lab-on-a-Chip", are still under development and their application is still restraint to research projects where economical aspects or production are secondary. However, some applications are already available, such as a broad variety of miniaturized biosensors (e.g. for blood analysis or biochemical warfare detection), capillary electrophoresis (in glass capillaries and on micro-fabricated silicon structures), nanoliter well plates and DNA microarrays and many more. The following is a list of examples of reported, and in part commercially available, miniaturized (bio-)analytical devices (in arbitrary order):

1. Integrated DNA analysis in microsystems (*Burns et al.*, 1998)
2. On-chip continuous-flow PCR (*Kopp et al.*, 1998)
3. On-chip PCR with integrated electrophoretical separation (*Woolley et al.*, 1996)
4. Cell handling in microsystems (*Harrison* (1997) and *Fuhr et al.* (1995))
5. Highly paralleled on-chip capillary electrophoresis (*Shi et al.*, 1999)
6. Micro-immunoassays (*Chiem and Harrison* (1998), *Ensing and Paulus* (1996) and *Rowe et al.* (1999))
7. Microfilters (*Andersson et al.*, 2001)
8. Waveguide biosensors for ricin (*Narang et al.*, 1997)
9. High throughput protein identification with capillary electrophoresis coupled to mass spectrometry (*Li et al.*, 2001)
10. A portable blood analyzer with multiple electrochemical sensors (i-STAT, Kanata, Canada)

2.1.3 Microfluidics

Fluid and molecular transport in channels of micrometer dimensions often follow different physical rules compared to hydrodynamics at the macroscopic scale. Fluid control has emerged as an important consideration in microanalytical devices, and thus, understanding the principles of microfluidics is essential when developing new complex applications. Although the fluidics of the newly developed setup in this thesis is rather simple, the relevant topics of microfluidic transport are summarized in this section. A review was recently published by *Polson and Hayes* (2001).

Controlling Fluids in Microsystems

Sample transport for analytical purposes in microchannels involves volumes of microliters to picoliters (for the relation of volume to channel-diameter see table in appendix D). This means that even for reasonable concentrations[1], there are only a few molecules at the start, and hence, each molecule must be conserved. Loss of molecules can happen by uncontrolled interactions with the walls (see section 2.1.5) or by dispersion of the sample, i.e. diffusional dilution along the flow direction.

One important aspect of microfluidics is the existence of laminar flow up to high flow rates and high pressures. Laminar flow is the hydrodynamic regime where liquid layers glide smoothly along each other without any turbulences. The hydrodynamic parameter describing the transition from laminar to turbulent flow is the Reynolds number which depends on liquid density and viscosity as well as flow speed and channel dimensions. The small channel dimensions in microfluidics keep the flow regime below critical values for virtually all realistic and applicable situations (*Manz et al.*, 1990).

As a consequence, mixing of solutions in microchannels relies entirely on diffusion due to missing convection or turbulence.

Pumping systems are usually either electroosmotic or pressure-induced devices.

Electroosmosis is a rather recent technology that had its breakthrough with the increasing applications of capillary electrophoresis (CE). The driving force for the flow is produced by the ionic interaction of the solution layers near the solid/solution interface with an axial potential gradient. This axial potential gradient is also the basis for molecular separation by CE. (*Lacher et al.* (2001)) Electroosmotic transport can be ideal because it minimizes dispersive effects and works in the smallest channels; however, it is difficult to control it and it is influenced by fluid and channel wall surface

[1] A typical (rather high) molecular concentration in biological analysis is 10 μM which is 10^{17} molecules per liter and thus, only 10^5 molecules per picoliter.

properties (*Polson and Hayes*, 2001).

For this work, pressure driven pumping has been chosen since the effects of high voltages on the structural conformation of proteins attached to the walls ar not easily predictable. The consequences of such high voltages on the functionality of antibodies is not sufficiently investigated yet (*Chiem and Harrison* (1998) and *Ensing and Paulus* (1996)). As discussed in section 2.3.3 and 2.2.2, functionally intact antibodies attached to glass capillary walls are essential for the experiments in this thesis.

Pressure Effects and Flow Rates in Microchannels

The properties of pressure-induced flow can be explained by classical hydrodynamics and are therefore fully understood, and the technique successfully generates large-volume flow rates and is simple to control from external sources.

When using pressure driven pumping, the major aspects that have to be considered are:

A most practical aspect is that channels, connectors and interfaces need to be well sealed to ensure proper flow control (this is not the case for electroosmotic flow which works in open channel systems also).

Pressure driven flow induces dispersion from laminar flow profiles due to an inherent parabolic flow speed profile along the radius (see for example *Paul et al.* (1998)). Since this work focusses on solid substrate separation (section 2.2), dispersion was not considered a negative effect.

Pressure increases dramatically with increasing flow rates and decreasing channel diameters, considerably restricting throughput speed compared to electroosmotic flow.

Typical flow rates of the syringe pump used in the experiments in chapter 4 (Harvard Apparatus, USA) are 0.1 to 100 μl/min, using a syringe with 1 ml volume.

The relation of pressure and flow rate as a function of capillary length and diameter is described by equation 2.1.

$$Q = \frac{\pi(p_1 - p_2)R^4}{8\eta L}. \tag{2.1}$$

This is the law of *Hagen-Poiseuille*, where $Q = \frac{\partial V}{\partial t} = \dot{V}$ is the volume flow rate, $p_1 - p_2 = \Delta p$ is the pressure difference between the two capillary ends, R is the inner capillary radius, η the liquids viscosity (0.001025 Nsm^{-2} for water at 20 °C) and L the length of the capillary. This law assumes there is no slip between the liquid layer that is in contact with the capillary wall and the glass surface.

For water (diluted aqueous solutions) equation 2.1 becomes

$$\Delta p \text{ (in bar)} = C \times \frac{L \text{ (in m)} \; Q \; (\text{in}\frac{\text{nl}}{\text{min}})}{D^4 \text{ (in } \mu\text{m)}}. \tag{2.2}$$

with D being the capillary inner diameter and $C = 8488.26$

For channel diameters of 75 μm (see section 3.4) and a channel length of 1 meter this results in $\Delta p = 0.27$ bar at a flow rate of 1 μl/min. Keeping the pressure low enough to use standard liquid chromatography (LC) fittings, connectors and tubing as well as custom manufactured components ($\leq$ 20 bar) limits the flow rates to the range of $\approx$ 1 to 100 μl/min, depending in the channel length.

Diffusion in Microchannels

In microchannels, the surface-to-volume ratio is dramatically increased compared to larger diameter channels. Consequently, molecules dissolved in a fluid that passes through such a channel interact more frequently with the channel walls. The walls are simply "closer" to a particular molecule. This can be both advantageous and disadvantageous depending on the respective application. Disadvantageous, if the molecule adsorbs and gets lost for further reaction or analysis, or advantageous, if the wall properties are specifically modified and analytical reactions are supposed to take place at the surface. In both cases, it is important to know how long it takes for a molecule in the liquid flow before it has had contact with the confining surfaces. Transit times for the fluid (i.e. flow rates) have to be adjusted according to whether wall contact is desired or not.

Mixing and wall contact depends on the diffusion rate with which particles and molecules move in the volume.

The time t a particle or molecule diffuses an average distance r in a liquid (or gas) volume is given by the *Stokes-Einstein* equation (equation 2.3).

$$\langle r^2 \rangle = 6Dt \tag{2.3}$$

$\langle r^2 \rangle$ is the mean square displacement and D the diffusion coefficient. It can be derived from either a statistical approach (random walk) or from *Fick's* law and the related diffusion theory. Both approaches are explained in the textbooks of *Truskey et al.* (2000) and *Gerthsen* (2001), respectively.

This applies for the assumption of small particles in aqueous diluted solutions, i.e. for the ideal case. Thus, in the context of the present work it will serve only as an estimate.

Diffusion coefficients vary a lot between molecules and are hard to measure. But roughly, one can say, that proteins (the type of molecule that is of interest for this work) have diffusion coefficients between 10^{-6} and 10^{-8} cm^2/s (*Truskey et al.*, 2000). The first value applies for proteins in rather diluted solutions while the latter corresponds to protein diffusion in the plasma of a biological cell. From this it follows, that a macromolecule takes about 2.3 s to diffuse in an aqueous solution from the center to the walls of a 75 μm inner diameter microchannel. Since the volume of such a channel is 4.4 μl/m, flow rates of the order of 10 μl per minute guarantee several contacts of a dissolved molecule with the wall in a 50 cm long channel (see section 3.4 and the table in appendix D).

2.1.4 Microsystem Materials: Plastics and Glass

Microfabricated devices are currently manufactured from a variety of materials by processes adapted mainly from the microelectronics industry. Besides the commonly used glass and silica wafers, polymer-based materials, such as polydimethylsiloxane (PDMS), polymethylmethacrylate (PMMA), polycarbonate and polytetrafluorethylene (PTFE or Teflon), have been recently introduced. This section gives a very brief introduction to the two main types of material: glass an plastics (polymers). Reviews on microfabrication and the employed materials have been published for example by *Jakeway et al.* (2000) and *Chovan and Guttman* (2002).

For the work carried out during the presented Ph.D. project, fused silica glass capillaries were chosen as microchannels because protocols for covalent attachment of biomolecules to glass surfaces are well-established. Moreover, they are commercially available (and relatively cheap) and can be easily filled and rinsed.

Glass

Since microfabrication technology was derived from the electronics industry and focussed on machining silicon wafers, the first microfluidic systems were also fabricated from silicon. Standard photolithography and subsequent wet etching were used to produce microchannels on a planar substrate.

Electrokinetic pumping was established as the method of choice for transporting liquids in these microchannels. Since the conductivity of silicon proved problematic for the application of high voltages as are required for electroosmotic flow, various types of glass became more and more popular substrate materials.

Apart from the lower thermal and electrical conductivities, compared to silicon, also the optical transparency of glass and quartz glass made these materials attractive for

microstructures. This applies in particular to those systems that involve fluorescence or other optical detection methods.

There are some disadvantages of quartz and glass as substrate materials for microstructures: The costs can become prohibitive when making larger fluidic devices ($\geq$ 100 cm^2), harmful wet chemistry is involved in the fabrication, geometrical design is limited to simple channel profiles and the surface chemistry of glass can pose problems because it strongly interacts with charged molecules (which applies to most biomolecules, and especially to proteins). This is mainly due to the highly charged surfaces that glasses have in common.

Reviews on silicon, glass and quartz are given by *Petersen* (1982) and *Kopp et al.* (1997).

Plastic

Polymers as substrate material offer a possible solution to the fabrication challenges listed in the previous paragraph. Their wide range of material properties, their low costs and the development of suitable microfabrication techniques for plastics have made them more and more the material of choice for many applications.

Fabrication techniques for polymer microstructures are replica molding, microcontact printing, hot embossing and LIGA (Lithography Galvanoabformung).

The broad range of polymer types available also makes them potentially more suitable for biological and biomedical applications since the substrate material can easily be adapted for the particular application to eliminate unwanted sample-surface interaction.

Extensive and detailed reviews on microfabrication in plastic materials are *Boone et al.* (2002) and *Becker and Gärtner* (2000).

2.1.5 Functional Coatings and Unspecific Adsorption

The smaller a volume, the larger the surface-to-volume ratio. This parameter describes that there is "more surface per volume unit". A consequence of this rule is that solutes in a microvolume interact more frequently with the container walls. Without controlled surface properties these interactions tend to lead to unwanted effects like non-specific adsorption to microchannel walls and potentially to degradation of the solute. In the microfabrication field, a surface-to-volume ratio of 20 $\frac{\text{mm}^2}{\mu\text{l}}$ is considered as a threshold from where on (for small reactant concentrations) "the importance of inert surfaces becomes extreme" (*Wilding and Kricka* (1999)). For

surface-to-volume ratios of typical microchannel diameters see appendix D.

From an application point of view, the frequent interactions between samples and walls can also be exploited for the purposes of the particular application by modifying the inner surfaces of the microchannel in a specific way. Depending on whether such specific surface coating is required or only non-specific interaction has to be prevented, different chemical modification techniques are applied. Amongst others, the following parameters are involved in the choice of the chemical surface modification protocol:

- The type of substrate (e.g. plastic, glass, silicon, gold or ceramics)
- The functional unit that is attached to the channel walls (e.g. polymers, antibodies or other proteins or lipids)
- The type of sample (e.g. DNA, DNA-protein mixtures, pure protein or cells)
- The type of liquid transport (e.g. pressure driven or electroosmotic)

Biomolecular samples put particular demands on the system: While surface interactions of DNA are almost only electrostatic, proteins carry charges and at the same time have hydrophobic domains. Hence, for cellular extracts or other sample types that consist of a mixture of these two molecular species the search for the appropriate surface modification technique can become difficult.

For the present work, covalent antibody and protein attachment to fused silica glass surfaces was required. Versatile silane-based glass-modification techniques were chosen to accomplish the immobilization of antibodies for immunoaffinity separation and prevention of any non-specific sample-wall interaction simultaneously (see section 3.5.1 and 3.5.3).

Introductions in surface coating techniques and reviews can be found in *Ratner* (1995), *Mrksich and Whitesides* (1996), *Morgan et al.* (1995), *Seigel et al.* (1997), *Piehler et al.* (1996) and *Alcantar et al.* (2000).

2.2 Molecular Separation

Eukaryotic cells in higher organisms (e.g. humans) contain more than 10^5 distinct proteins an a much greater number of chemical species in general. Some of these molecules are present in only trace amounts (e.g. intermediates in enzyme mechanisms) while others are present in abundance (e.g. cytoskeletal proteins). Moreover, the concentration of some components depends on the stage of the cell cycle or the developmental stage of the organism. Other molecules are present at approximately constant levels. Therefore, the study of the chemical components of cells is a key

to gain insight into the dynamics of cell composition and function as well as the underlying processes.

One approach to the study of individual chemical components is to separate them from each other by chromatographic techniques.

This section gives an introduction to the basic concepts of chromatography with a focus on affinity chromatography and immunoseparation. These techniques form the basis of the *Chromatin Immunoprecipitation* (CHIP) *Assay* which is the central topic of this thesis.

Affinity chromatography can be studied in more detail in the book of *Matejtschuk* (1997) and a very practical introduction can be obtained from *Amersham Pharmacia* (2001). Recent reviews on affinity chromatography and immunoaffinity chromatography are *Hage and Nelson* (2001), *Gadgil et al.* (2001), *Muronetz et al.* (2001) and *Weller* (2000).

2.2.1 Introduction to Affinity Chromatography

The term chromatography stands for one of several separation techniques defined as differential migration from a narrow initial zone. Chromatography separates the components or solutes of a mixture on the basis of the relative amounts of each solute distributed between a moving solvent stream, called the mobile phase, and a contiguous stationary phase. The mobile phase may be either a liquid or a gas, while the stationary phase is either solid or liquid.

For a given species, the ratio of the times spent in the moving and stationary regions is equal to the ratio of its concentrations in these regions. The term adsorption isotherm is often used when a solid phase is involved (see below). A mixture of solutes is introduced into the system in a confined region or narrow zone (the origin), whereupon the different species are transported at different rates in the direction of fluid flow. The driving force for solute migration is the moving fluid, and the resistive force is the solute affinity for the stationary phase; the combination of these forces, as manipulated by the analyst, produces the separation.

There are two main types of chromatographic separation: Partition and adsorption. The first, summarized in figure 2.1, relies on the separation of the components of a mixture due to their different solubilities in the stationary phase. The equilibrium concentrations in the mobile and stationary phase are determined mostly by their respective solubilities and summarized in the partition coefficient $K_p = \frac{C_s}{C_m}$, where C_s and C_m are the equilibrium sample concentrations in the stationary and mobile phase, respectively. The higher the value of K_p for a particular solute, the slower it migrates along the separation column.

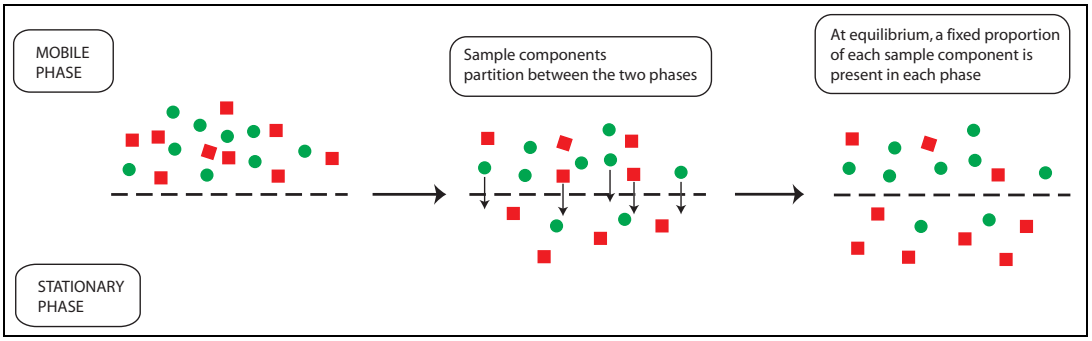

Figure 2.1: Partitioning of molecules in a two-phase system. Two components are represented by round and square shapes respectively. The two phases could be an aqueous buffer (mobile phase) and a solid stationary phase. The two components get separated by their different partition coefficients in this system. After *Sheehan* (2000), page 13.

Adsorption is the basis of "affinity chromatography" (and other techniques, such as ion exchange chromatography, see *Sheehan* (2000) and *Amersham Pharmacia* (2001)) and relies on the actual binding of the molecule of interest to a solid substrate, allowing for much higher selectivity of the separation. The concept is illustrated in figure 2.3 for the particular case of an immunoaffinity chromatographic assay. It was first described by *Cuatrecasas and Wilchek* (1968).

In affinity chromatography the components of a mixture are separated on the basis of the reversible interaction between a molecule (or complex) of interest and a specific ligand coupled to a chromatographic matrix. The binding between ligand and target molecule follows the basic thermodynamic principles of any reversible molecular interaction and can be described in terms of an equilibrium reaction: If $[T]$ and $[L]$ are the equilibrium concentration of unbound target and unbound ligand respectively, and $[T-L]$ is the concentration of target-ligand complex, also at equilibrium, then the "affinity constant" $K_a = \frac{[T-L]}{[T]\cdot[L]}$ is a measure for the strength of the target-ligand interaction. The actual amount of bound target still depends on geometrical boundary conditions and diffusion parameters (see section 2.1.3) which determine the time it will take for the binding reaction to reach equilibrium.

Affinity chromatography is unique in purification technology since it is the only technique that enables the purification of a biomolecule on the basis of its biological function or chemical structure. Affinity chromatography of biomolecules offers high selectivity and, in most cases, high capacity. It can yield purification factors of the order of thousands and the recoveries of active and structurally intact material are very high (*Amersham Pharmacia*, 2001).

Biological interactions between ligand and target molecule can be a result of electrostatic or hydrophobic interactions, van der Waals forces and/or hydrogen bonding.

To elute the target molecule from the affinity medium the interaction can be reversed, either specifically using a competitive ligand, or non-specifically, by changing the pH, ionic strength, polarity or temperature. Through this, in a single step small amounts of biological material can be purified from high levels of contaminating (background) substances.

Successful affinity purification requires a biospecific ligand that can be covalently attached to a chromatographic matrix. The coupled ligand must retain its specific binding affinity for the target molecules and, after washing away unbound material, the binding between the ligand and target molecule must be reversible to allow the target molecules to be removed in an active form. Any component can be used as a ligand for its respective binding partner. Some typical biological interactions, frequently used in affinity chromatography, are listed below:

- enzyme ⇔ substrate analogue, inhibitor, cofactor
- antibody ⇔ antigen, virus, cell
- lectin ⇔ polysaccharide, glycoprotein, cell surface receptor, cell
- nucleic acid ⇔ complementary base sequence, histones, nucleic acid polymerase, nucleic acid binding protein
- hormone, vitamin ⇔ receptor, carrier protein
- metal ions ⇔ poly (His) fusion proteins, native proteins with histidine, cysteine and/or tryptophan residues on their surfaces

For the experiments in this work, immunoaffinity was chosen for the separation of a particular protein-DNA complex from its cellular context (see section 2.3 and 3.3). This choice is justified by the relative simplicity and selectivity of immunoaffinity assays compared to other separation methods (*Hage and Nelson*, 2001).

2.2.2 Antibodies - Immunoaffinity Chromatography

The specificity of the affinity medium derives from the selectivity of the ligand (and the use of selective elution conditions). One of the most selective interactions known in biochemistry is the interaction of antibodies with their antigen. Its diversity and its strength (affinity constants see below), have created many uses for antibodies and antibody fragments both in therapeutic and diagnostic applications as well as for immunochemical techniques in basic research.

The technical possibilities to design specific antibodies against virtually any antigen, be it a particular protein, a fragment of a protein, another biomolecule or even metal particles (*Wylie et al.*, 1992), makes them the most popular tool for molecular separation where high specificity is required. A very good and detailed summary of antibody properties is available from *Harlow and Lane* (1988). In the following, only the most important aspects for this work are briefly summarized.

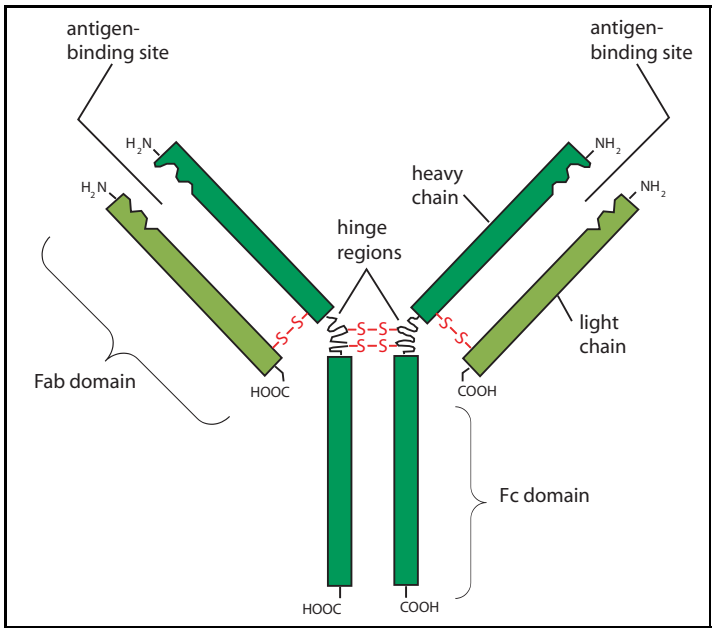

Figure 2.2: Schematic of an IgG molecule

Antibodies are an essential part of the immune system of animals. They are proteins produced in response to the presence of foreign molecules in the body. Synthesized by a particular lymphocyte type they circulate throughout the blood where they bind to the foreign antigens and induce the antigens removal from the circulation by marking it for cells specialized in phagocytosis.

Antibodies are a large family of glycoproteins. All the members of this family share key features both functional (i.e., the binding to antigens) and structural. Structurally, the various classes (IgG, IgM, IgA, IgE and IgD — Ig standing for "immunoglobulin") all are multimers which consist of various combinations of a Y-shaped subunit. The simplest antibody, IgG, consists of only one of these subunits. It is also the most abundant antibody in blood serum and since it is the type that is used for the immunoassay in this work the following discussion is restricted to this particular antibody family.

IgG molecules are proteins that are made of three domains, two identical Fab domains that form the arms of the Y shaped structure and one Fc domain that forms

the stem (see figure 2.2). The domains are linked by a flexible hinge that allows the antigen binding Fab domains freedom to interact with different antigen conformations. The Fc domain, pointing away from the antigen binding sites, is important for the immune response of the host organism. In immuno-biochemistry it is the preferred end of the molecule for attachment or labeling avoiding interference with or steric hindrance of the specific antibody-antigen interaction.

IgGs are all formed by two pairs of identical polypeptides, the shorter "light chains" and the longer "heavy chains" that are held together mainly by disulfide-bonds as shown in figure 2.2. At the ends, the heavy and the light chains carry variable regions that make the specific binding sites for the respective antigen. Altogether an IgG molecule has a molecular weight of about 160 Kilodalton.

IgG molecules are amongst the most robust proteins known. They can withstand harsh buffer conditions and even after extended time at room temperature they do not denature nor loose their specificity and affinity for their antigen.

Antibody Production

Large amounts of antibodies with specific affinity for a given antigen are usually obtained from blood serum of a host animal that was injected with that antigen. The immune system of the host recognizes the molecule as a foreign species and produces antibodies against it which can be purified from the blood. Amongst the most common animals used for this purpose are rabbit, mouse, goat, sheep and donkey. More details about antibody production and the immune system can be found in the books of *Benjamini et al.* (2000) and *Janeway et al.* (2001).

Affinity Constants

The affinity constants of antibodies for their respective target vary over a range that extends from below 10^5 M^{-1} to above 10^{12} M^{-1} (*Hage and Nelson* (2001) and *Harlow and Lane* (1988)). Good antibodies can reach affinity strength that is only surpassed by the ligand-target pair Biotin-Avidin which has an affinity constant of 10^{15} M^{-1}. Biotin-Avidin is the strongest non-covalent biomolecular binding known (*Green* (1975), *Moy et al.* (1994) and *Florin et al.* (1994)).

Immunoaffinity Chromatography

As antibodies became more and more popular as analytical reagents they were soon considered for chromatographic separation (*Campbell et al.*, 1951). With the devel-

opment of suitable support materials and immobilization methods, antibodies were soon placed into columns and used as stationary phases. Immobilization of antibodies to a solid support was first reported in 1967 (*Catt and Niall*, 1967). The strong and at the same time specific interaction of antibodies with their antigen made immunoaffinity chromatography the widely used analytical technique it is today (*Hage and Nelson*, 2001). Figure 2.3 is an illustration of its principle, indicating the high separation power by the theoretical purification result of 100% (no non-specific molecule is left in the eluate). While partition-based chromatography (see section 2.2.1) cannot even theoretically yield a 100% purification, a highly specific (immuno-) affinity chromatography often comes close to that ultimate limit.

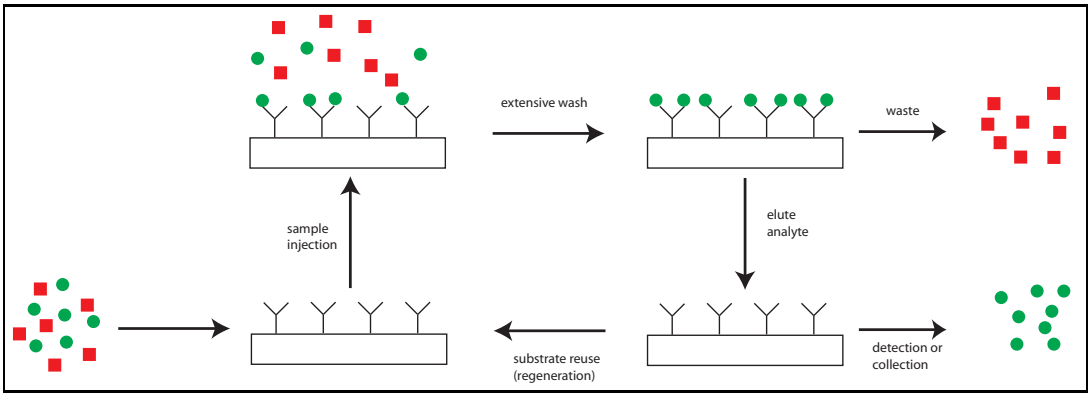

Figure 2.3: The principle of a chromatographic immunoassay

2.3 Chromatin Immunoprecipitation and Transcription Regulation

The biological question on which this work is focussing is the function of the GAGA transcription factor (GAF) in *Drosophila Melanogaster*. GAF is an important DNA-binding protein involved in the regulation of chromatin structure and chromatin remodeling in *Drosophila*. To understand its role in gene expression regulation it is essential to map the specific DNA-binding sites of GAF *in vivo*. The *Chromatin Immunoprecipitation* (CHIP) *Assay* is a well-established method to carry out this mapping and has already been successfully applied to GAF (*Strutt et al.* (1997) and *Orlando et al.* (1997)). This section gives an overview on the biological background of the presented work and explains why the CHIP assay from GAF has been chosen as a model system for a miniaturization approach.

Section 2.3.1 briefly summarizes the general mechanisms of gene transcription control. In the following section 2.3.2 GAF and its function in the development of

Drosophila Melanogaster is introduced. Section 2.3.3 gives a more technical introduction in the established method of chromatin immunoprecipitation and section 2.3.4 discusses the need of downscaling and miniaturization of this particular technique in biological research and motivates the choice of GAF as a model system for this project.

2.3.1 Chromatin Structure and Gene Expression Regulation

Gene expression in eukaryotic cells is regulated at several independent levels which are illustrated in figure 2.4. These are the levels of a) RNA transcription from DNA, b) post-transcriptional RNA processing and modification, c) control of RNA transport out of the nucleus, d) the control of RNA inactivation and e) the translation of the RNA sequence to the respective protein. Another, later step can be protein activity control. On the first of these levels, transcription of the genomic DNA sequence to RNA is mainly controlled by the accessibility of the promoter regions of the genes for the RNA polymerase enzyme.

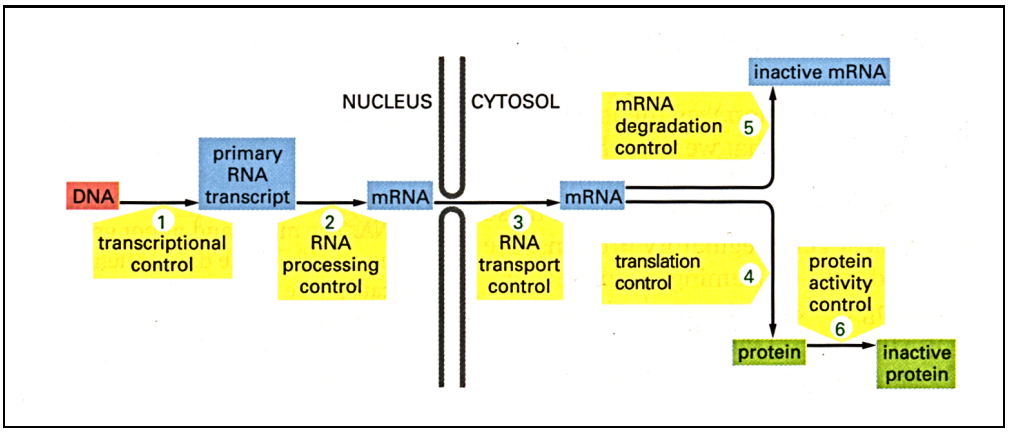

Figure 2.4: The distinct levels of gene control (*Alberts et al.* (1994), page 403).

The DNA in the cell nucleus is wound around nucleosomes, complexes formed by a particular type of protein, the histones. In the inactive state, these nucleosomes are densely packed in a fiber that is wound in itself in several higher order structures, as schematized in figure 2.5. This complex structure of packed DNA, together with its associated, structure-maintaining and structure-regulating proteins is called chromatin. Packed in chromatin the entire genomic DNA strand (there is one meter of DNA in a typical animal cell, which corresponds to 3×10^9 nucleotides) is safely stowed in chromosomes of the size of only a few micrometers. Figure 2.5 shows these different levels of DNA packing.

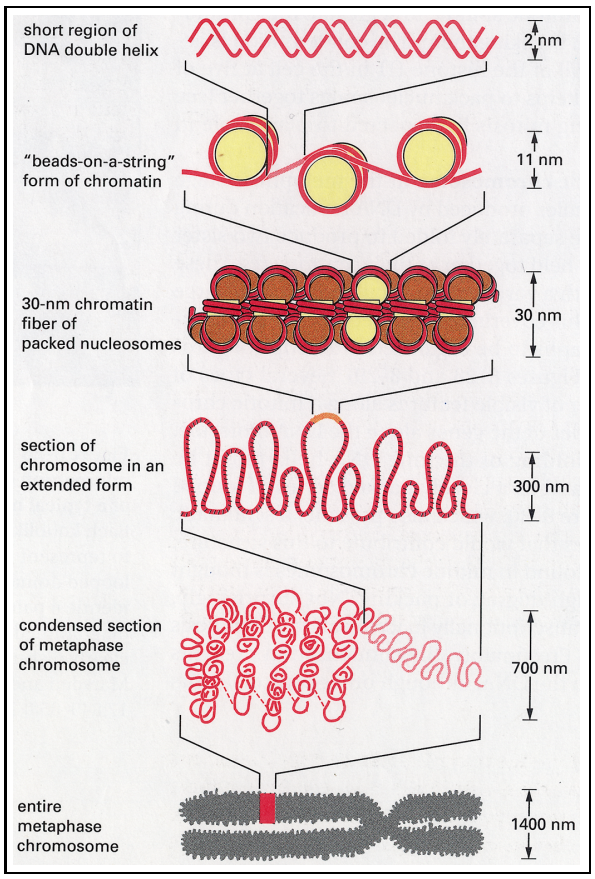

Figure 2.5: The levels of DNA packing in chromatin (*Alberts et al.* (1994), page 354).

Changes in the chromatin structure, induced by the binding of regulatory proteins, so-called "transcription factors", to key sequences on the DNA and to the nucleosomes, influence the accessibility of genes for the RNA polymerase, the enzyme that transcribes the DNA sequence into an RNA molecule. Hence to understand the function of transcription factors is crucial to gain insight in gene expression control on the first of the described levels.

2.3.2 The GAGA - Factor in *Drosophila Melanogaster*

In the development of *Drosophila Melanogaster* the GAGA transcription factor (GAF) is a protein of general importance and within the research on chromatin structure and remodeling it has been a focus of interest for years (*Becker* (1995), *Granok et al.* (1995), *Strutt et al.* (1997) and *Benyajati et al.* (1997)). GAF is a sequence-specific DNA-binding protein involved in the expression regulation of many housekeeping

and developmentally regulated genes such as heat shock genes, and "homeotic" [2] genes. It also has functions in early *Drosophila* development other than transcription regulation, e.g., it is required for nuclear division (*Bhat et al.* (1996)).

Drosophila GAF is encoded by the *Trithorax-like* gene (*Farkas et al.*, 1994). The protein structure of the DNA-binding domain of GAF has been resolved by *Omichinski et al.* (1997). It is clear that it generally binds GA(CT)-rich sequences in the regulatory regions of genes. Although experiments *in vitro* show binding of GAF to a base triplet (GAG) (*Wilkins and Lis*, 1998), the minimal sequence motif required for GAF binding *in vivo* is not clearly established.

Baricheva et al. (1997) have mapped tissue specific expression and activity of GAF in *Drosophila* embryos while recent studies on GAF and its functions *in vivo* in cultured *Drosophila* cells revealed new insight on the mutual interaction of GAF with the Polycomb protein, a counteractor of GAF in gene expression activation (*Strutt et al.*, 1997). In the latter case they found co-localization of the two proteins in a binding site analysis based on chromatin immunopurification (see section 2.3.3). The established method for binding site analysis in cells has been adapted for mapping DNA target sites of chromatin-associated proteins in *Drosophila* embryos by *Cavalli et al.* (1999).

This shows, that although research on GAF is long established, it still represents an active focus of research.

2.3.3 The Chromatin Immunoprecipitation (CHIP) Assay

The *Chromatin Immunoprecipitation* (CHIP) *Assay* has become an established method for mapping modifications of chromatin associated proteins (e.g. histone acetylation (*Crane-Robinson et al.*, 1999)) as well as binding sites for specific protein-DNA interaction (*Horak et al.* (2002), *Strutt et al.* (1997) and *Cavalli et al.* (1999)). These depend strongly on the state of development of the cells and protein-DNA interactions are weak and transient in time. Therefore one crucial aspect of such analysis it to avoid any influence of sample preparation on the parameters of interest. Fast fixing of chromatin in the living target cells, preferentially with formaldehyde, (see *Hecht and Grunstein* (1999) and *Solomon and Varshavsky* (1985)) is required.

Traditional CHIP methodology involves cross-linking of proteins to DNA in living cells, shearing the chromatin into short fragments, separating the protein-DNA complexes by immunoprecipitation with antibodies against the protein of interest and subsequent analysis of the associated DNA.

[2] "Homeotic" genes maintain the spatial information generated by early patterning mechanisms in the embryo. Their activity varies with cell and tissue type.

Protocols are described in detail in *Cavalli et al.* (1999) and *Strutt and Paro* (1999).

In brief, cells (or, as in the context of the presented work, 12 - 14 hours old fly embryos) are incubated with a formaldehyde cross-linking buffer (typically ca. 11% HCHO for 1 hour at 4°C). After stopping the fixation with several washing steps, the embryos are sheared by sonication and then again washed with sarcosyl buffer. Cell debris are removed by spinning in a microfuge before the chromatin is purified in an ultracentrifugation step in a CsCl-gradient. This chromatin fraction, ready for immunoprecipitation, is frozen for storage at -80°C and can be kept for many months.

To purify a specific protein of interest, in the case of the presented work the GAGA transcription factor cross-linked to DNA fragments, a specific antibody is added to the chromatin. To allow efficient binding of this antibody to its target, a long incubation step with a sufficiently high antibody concentration is important. Then, the chromatin is mixed with protein A coated agarose beads and incubated for typically 3 hours on ice to allow the specific binding of protein A and IgG antibodies to form (see section 3.5.2). Incubation is followed by extensive washing with detergent-modified and high salt buffers. For this purpose, the agarose beads are spun down in a minifuge, supernatant buffer is taken off and the pellet is resuspended in fresh buffer. Finally, after repeated washing, the sample is heated in a Tris-based buffer to 65°C. This reverses the formaldehyde cross-links due to the pH-drop that Tris buffer shows upon heating. Now the DNA fragments are detached from their associated proteins and are accessible for analysis techniques such as *Polymerase Chain Reaction* (PCR, see section 2.4), ligation-mediated PCR and identification by blotting, electrophoresis or sequencing. For the detailed protocol of the immunoprecipitation see also appendix B.

If the experimental boundary conditions require it, this reliable technique for immunoprecipitation can be modified by using specific secondary antibodies instead of protein A and by replacing agarose beads by other solid substrates such as paramagnetic styrene beads (section 3.3.2) or glass surfaces (section 2.4 and 3.6).

2.3.4 Limited Target Material - Single Cell Experiments?

The common CHIP technology is limited because it requires relatively large amounts of cells ($\geq 10^7$ cells per 100 μl sample, see section 3.3.1) and involves lengthy procedures. Consequently, biological questions for which only very little sample material is available, e.g., because a rare cell type has been chosen or the introduction of a lethal mutation resulted in only few surviving embryos, are currently not addressable. Also, some cell types are naturally only available in small quantities, as in early embryonic stages.

In the process of pattern formation in an embryo (and cell differentiation in general), obviously, gene expression is different from one cell to the next. This is particularly true for the regulation of homeotic genes. Since GAF is a key factor in the control of homeotic genes (see section 2.3.2), an analysis of its function comparing cells in successive developmental stages, different tissue types or even adjacent cells is of great scientific interest.

The fact that many functions and properties of GAF are already well known makes it a very useful model system for new methodological developments such as the one presented in this thesis. In particular the availability of a GAF-specific polyclonal antibody (rabbit IgG) with proven affinity (*Bonte* (1998), *Becker* (1998) and *Strutt et al.* (1997)) for GAF makes this antibody-antigen system an ideal candidate for the development of a highly sensitive micro-structure based immunoassay.

At present, CHIP assays are done from 100 μl chromatin containing a maximum of 10^8 copies of a particular target gene (see 3.3.1). The ultimate goal to perform DNA binding site analysis from single cells requires to overcome two major experimental restrictions: The detection sensitivity for purified DNA fragments needs to be improved. The detection of few target molecules in CHIP assays needs a highly efficient PCR amplification (see section 3.7).

Secondly, to enhance immunoprecipitation (IP) specificity, a considerably improved control of sample-surface interactions compared to standard techniques (see section 2.1) is required. This focus on sample-surface interactions is due to the increased surface to volume ratio of miniaturized vessels that can handle samples in the sub-nanoliter range (the typical volume of a cell is about 1 picoliter).

Therefore, the first challenge of the development of single cell CHIP analysis technique is to solve these two major obstacles.

2.4 Polymerase Chain Reaction (PCR)

The optimization of a suitable PCR protocol for detection of few target DNA fragments fished from chromatin is one of the essential steps towards CHIP assays from low amounts of target material (see also section 2.3.4).

In this section, the principles of PCR amplification are introduced (section 2.4.1). Section 2.4.2 describes the detection and identification of PCR products by agarose gel electrophoresis. In section 2.4.3 the principles of real time PCR and its importance for the presented application are explained.

2.4.1 What is PCR?

In most organisms the genetic code is carried by the deoxyribonucleic acid (DNA). It is a polymer composed of units of phosphate and deoxyribose (pentose sugar) molecules which form a "backbone" to which nitrogenous bases are attached. There are four different nitrogenous bases, thymine (T), adenine (A), cytosine (C) and guanine (G) that make up DNA and with their sequence in which they are arranged along the DNA strand they are coding for the genetic information. The bases can form complementary pairs, thymine binding with adenine and cytosine with guanine. DNA usually exists in the form of a double helix which is tightly packaged and forms part of the chromosomes. Genetic information is transcribed from DNA to RNA from which it is eventually translated into proteins (see section 2.3.1). In these processes, a single DNA strand serves as a template and by adding the fitting nucleotides a complementary 'daughter' strand is produced. In a living cell the complete genome is replicated by a highly complex process involving many different proteins.

PCR copies DNA in the test tube and uses only the basic elements of the natural DNA replication machinery (*Mullis et al.* (1986) and *Saiki et al.* (1988)). In a simple buffer system a region of a template DNA molecule is copied by an enzyme, the DNA polymerase, that uses free deoxynucleotides (dNTPs) as building blocks of the new strand. Sequence-specific oligonucleotides ("primer") define the starting point for the DNA polymerase by binding to the single strand template according to normal base-pairing rules. These primers are custom-designed to flank the region on the target DNA that is to be amplified and they are therefore defining sequence and size of the PCR amplicon (i.e., the product fragment). The polymerase works only in one direction along the template strand (from the so-called 5' end to the 3' end, an asymmetry introduced into the DNA polymer by the chemical structure of the monomer bases).

Figure 2.6 sketches the 3 steps of a PCR reaction. First, the DNA strands are separated by heat ($\approx 95°C$), a step also called denaturation. Next it is cooled to the annealing temperature, permitting the primers to bind to their complementary sequence on the template. In the third step the temperature changes to the optimum working temperature for the polymerase enzyme (e.g. $\approx 72°C$). By using a pair of primers, one for each strand of DNA both strands are duplicated during the reaction. Repeating this temperature cycle doubles number of the DNA target again. Figure 2.7 illustrates the exponential amplification by successive cycling. Theoretically, 25 cycles would result in an amplification by a factor of $2^{25} \approx 3 \times 10^6$. But the process is not 100% efficient and it is usually necessary to carry out between 25 and 40 reaction cycles. The fact that the real amplification factor is less than 2^n, with n being the cycle number, is due to decrease of resource availability, reactant and enzyme degradation and the influence of changing concentrations of reactants and reaction

products on the reaction kinetics.

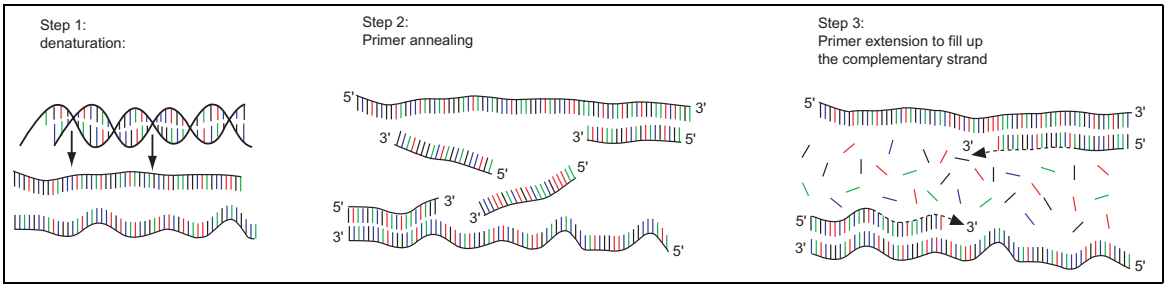

Figure 2.6: The 3 steps of PCR amplification: 1) denaturation at 95°C, 2) primer annealing at 50 to 60°C and 3) extension of the primer by the DNA polymerase (≈ 72°C). The colors symbolize the different bases.

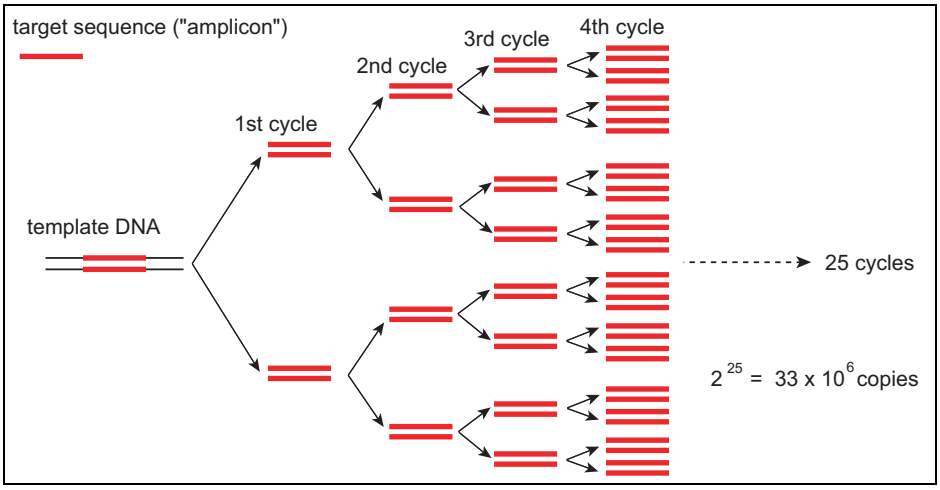

Figure 2.7: In the ideal case of 100% efficiency, the exponential amplification of the target sequence yields a 3×10^7-fold increase of the amount of DNA after 25 cycles.

Only the discovery of thermostable enzymes, such as *Taq polymerase*, that resist the series of exposure to 95°C made it possible to avoid the need to add fresh enzyme after each cycle. Good polymerase enzymes can reliably resist more than 35 cycles (obviously depending on cycle times). This considerably improved speed and reliability of the technique and allowed it becoming a routine method in biological science and DNA analysis.

For further reading and a more detailed, but still comprehensive explanation see *McPherson et al.* (1996) and *McPherson and Møller* (2000).

2.4.2 Agarose Gel Electrophoresis and Detection Limits

Once large numbers of amplicons have been produced they can easily be detected by gel electrophoresis. This detection method is illustrated in figure 2.8: The PCR product is placed in a gel prepared from agarose and, when subject to an electric field, the negatively charged DNA molecules migrate through the gel towards the positive electrode. Since the rate of migration of the amplicons through the agarose matrix is inversely proportional to their size, they will be separated into bands of molecules, each band containing molecules of the same length. The bands are traditionally stained with ethidium bromide, a UV-fluorescent dye that intercalates with the double-helix of DNA. Pictures of UV illuminated gels are taken with a CCD camera.

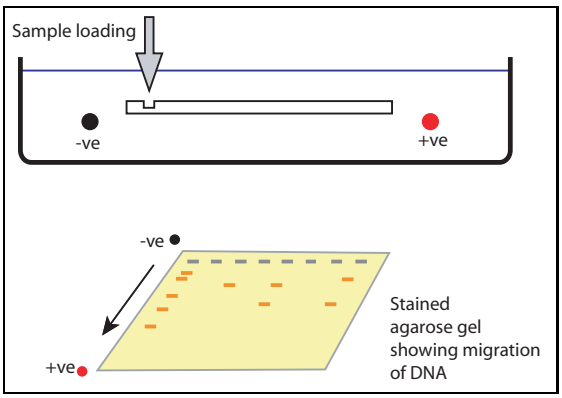

Figure 2.8: PCR product detection by agarose gel electrophoresis

The detection limit for bands on such an ethidium bromide stained gel is roughly in the range of $1-50$ ng of DNA, depending on the employed staining and illumination method.

The molecular weight (MW) of a double stranded DNA fragment is $\approx 660\ \frac{\mathrm{g}}{\mathrm{mol}\times\mathrm{basepair}}$ Hence, a 200 basepair (bp) fragment has a MW of 132000 $\frac{\mathrm{g}}{\mathrm{mol}}$. From this it follows directly that 50 ng of a 200 bp fragment contains 2.25×10^{11} molecules.

Consequently, to detect 100 template molecules an amplification factor of at least 10^9 is required (assuming 100% efficiency), which corresponds to about 32 PCR cycles. For a single template at least 39 cycles are required.

This shows the limitations of agarose gel electrophoresis as detection method for PCR products from very few template molecules. For better detection and also for quantitation of PCR product, a method called Real Time PCR, discussed in section 2.4.3, is required.

Single template PCR is frequently used in immunology (e.g., *Küpper et al.* (1996),

Daniels et al. (1996) and *Chan and Delabie* (1996)), but from entire cells. They usually involve two subsequent PCR reactions in which the product of the first is taken as template for the second. These protocols do not allow prior protein immunopurification and thus are not suitable for CHIP assays.

PCR has also been successfully performed on silicon microstructures (*Waters et al.* (1998), *Wilding et al.* (1994), *Northrup et al.* (1998), *Kopp et al.* (1998) and *Woolley et al.* (1996)), potentially allowing for on-column and low volume detection in capillaries for immuno-affinity separation. But these approaches start with relatively high amounts of starting material concentrations and mostly avoid effects of present protein on PCR and microchannel transport by using purified DNA (unspecific adsorption, see section 2.1.5).

Thus, for downscaling the CHIP assays, there was a need to optimize the PCR procedure to reliably detect very few DNA fragments purified from *Drosophila* chromatin.

2.4.3 PCR Kinetics and Real Time PCR

Traditionally, DNA product quantitation is carried out by band intensity analysis of ethidium bromide stained agarose gels or UV absorption measurements. Theoretically, there is a quantitative relationship between amount of starting target material and amount of PCR product. In practice, though, this relationship is influenced by many parameters and often it is impossible to quantitate the amount of starting nucleic acid material by traditional end-point analysis.

The development of real-time quantitative PCR has eliminated this problem by monitoring the amount of PCR product after every single cycle allowing the reliable quantitation of PCR products and starting material. Another advantage of real-time PCR is that the PCR tubes do not need to be opened after the amplification reaction is complete. This prevents contamination of the PCR products and reduces the amount of "false positive" results.

PCR can be looked at as having three phases of productivity: The early cycles, the mid cycles and the late cycles. Figure 2.9 illustrates these kinetics of product accumulation. In the early cycles (e) only relatively little product is produced (as expected from an exponential process) and during the mid cycles (m) the exponential amplification becomes significant in output and ideally doubles the number of product fragments in each cycle. Eventually, in the late cycles (l), the reaction reaches a plateau which is due to changes in relative resource concentrations (of dNTPs as well as polymerase and primers). Also, the processivity of the polymerase enzyme decreases with the time it is exposed to elevated temperatures. This finally leads to a

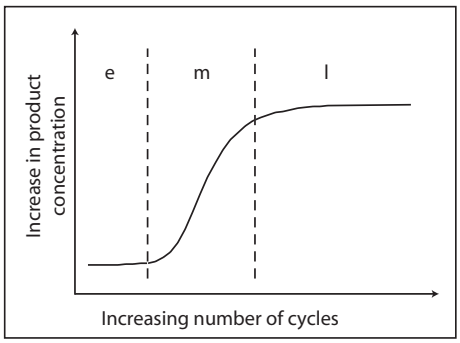

Figure 2.9: Three PCR phases: e) the early phase in which there is still little product, m) the mid phase during which product accumulates exponentially and l) the late or plateau phase where productivity slows down due to limitations of resources (after *McPherson and Møller* (2000), page 15).

stagnation in amplicon production as primers and dNTPs deplete and the polymerase denatures: the concentration curve reaches a plateau. The consequences for intensity comparison of bands of two products amplified by multiplex-PCR in the same reaction tube are obvious: After the reaction has been stopped at a certain cycle number, one of the reactions might be in a different phase of the kinetics curve compared to the second. It might have run in the plateau phase, depleting the resources, while the other reaction still did not reach the mid phase. The major cause for such a behavior would be a considerably different template number in the starting material which is inherently the case in the CHIP assays discussed in chapter 4 of this thesis.

Therefore, simple band intensity comparison should be used very carefully for quantitation of DNA fragments in the immunopurification eluates of CHIP assays when multiplex PCR has been carried out. Splitting the PCR reactions in two, with only one primer pair per reaction still does not avoid the problem that once the reaction has run in the plateau phase the information about the number of starting templates is lost.

Real-time PCR analysis detects nucleic acid amplification products as they accumulate in real-time, thus keeping the information on when the reaction runs into the plateau and on the amount of product accumulated at any cycle.

An introductory overview on real time PCR is given by *Giulietti et al.* (2001). Reviews have been published by *Lie and Petropoulos* (1998) and *Jung et al.* (2000).

There are two general methods for the quantitative detection of the amplicon: DNA-binding agents or fluorescent probes.

DNA-binding agents quantitate the amplicon production (including non-specific amplification and primer-dimer complex) by the use of a non-sequence specific intercalating agent that fluoresces only when bound to double stranded DNA. The detected

fluorescence signal from the reaction tube is directly proportional to the amount of amplified DNA. The major problem with this detection is that non-specific amplifications cannot be distinguished from specific amplifications and that obviously it can only be used in singleplex reactions.

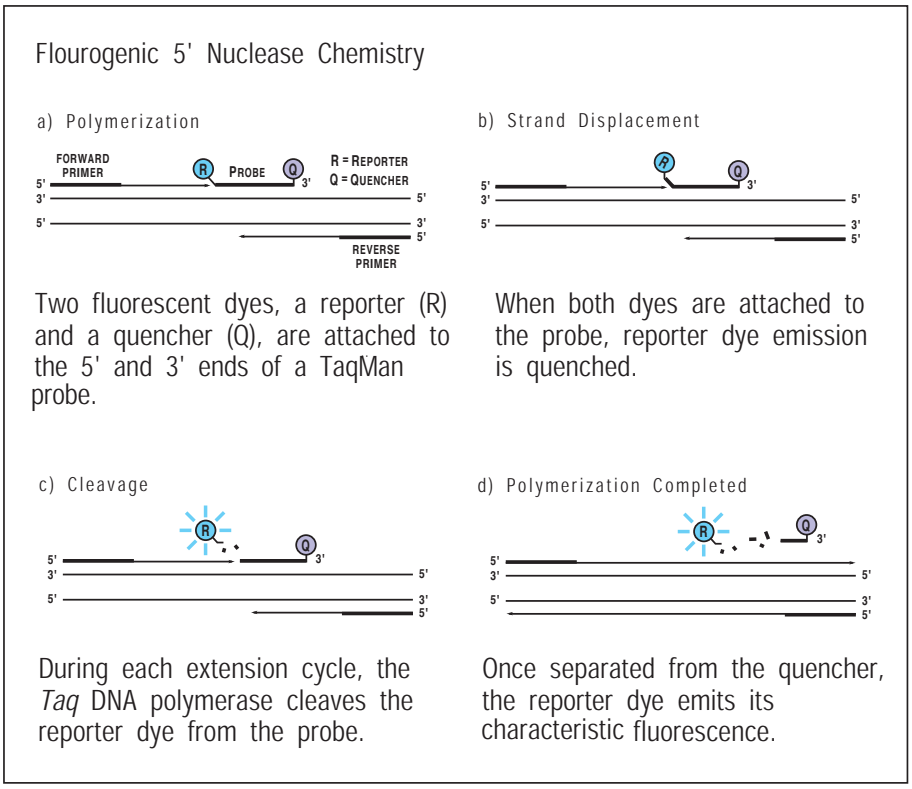

Figure 2.10: Illustration of the fluorescence signal generation in specific probe-based real time PCR. The reporter dye is cleaved off the probe and liberated from the quenching dye by the 5' to 3' nuclease activity of Taq DNA polymerase. From PE Biosystems.

In this work, sequence specific product detection with fluorescently labeled probe has been used: A reporter fluorescence dye and a quencher dye are attached to an oligonucleotide probe TaqMan^{R}. The probe sequence is complementary to the specific amplicon sequence and is added to the PCR reaction. Once both dyes are attached to the probe and the probe has annealed to its complementary site on the amplicon, only negligible fluorescence from the reporter is observed (figure 2.10 a) and b)). Once PCR amplification begins, DNA polymerase cleaves the probe, and the reporter dye is released from the probe (figure 2.10 c)). The reporter dye, which is separated from the quencher dye during every amplification cycle, generates a sequence-specific fluorescent signal (figure 2.10 d)). The signal increases in real time as PCR cycles continue; the fluorescence intensity increases proportionally. This mechanism, making use of the 5'→3' exonucleatic activity of Taq polymerase and of the sequence-specific

annealing of fluorescent probes ("TaqMan assay") was described for the first time by *Heid et al.* (1996).

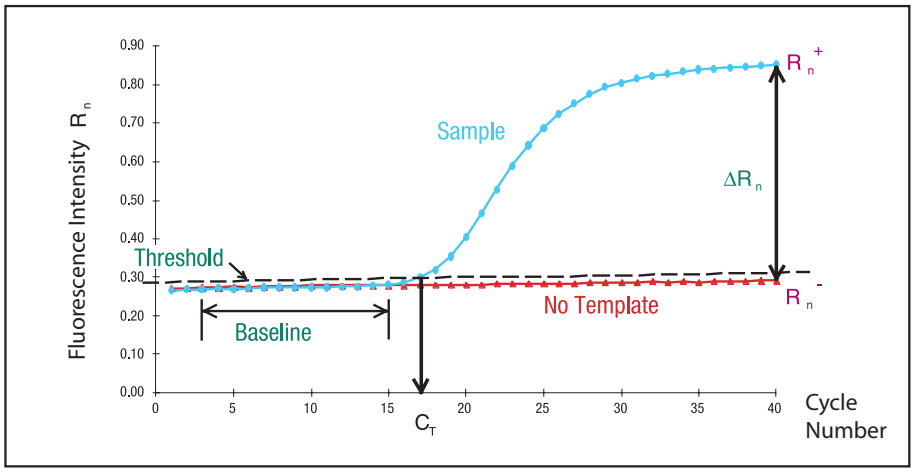

Figure 2.11: Model of a real time PCR amplification plot. From PE Biosystems. It shows the fluorescence signal versus cycle number.

Reactions are characterized by the point in time during cycling when amplification of a PCR product is first detected rather than the amount of PCR product accumulated after a fixed number of cycles. The higher the starting copy number of the nucleic acid target, the sooner a significant increase in fluorescence is observed.

Figure 2.11 shows a representative plot of fluorescence signal versus cycle number and defines the terms used in the quantitation analysis. In the initial cycles of PCR, there is little change in fluorescence signal. An increase in fluorescence above this baseline indicates the detection of accumulated PCR product. A fixed fluorescence threshold can be set above the baseline. The parameter C_T (threshold cycle) is defined as the fractional cycle number at which the fluorescence passes the fixed threshold. As shown by *Higuchi et al.* (1993), a plot of the log of initial target copy number for a set of standards versus C_T is a straight line. Target in unknown samples is quantified by measuring C_T and using the standard curve to determine starting copy number.

Chapter 3

Materials and Methods

This chapter introduces the techniques and materials for the experiments described in chapter 4. The detailed experimental protocols are also given.

At the start of this chapter, in section 3.1 the chemicals, materials and buffer solutions used in this thesis project are listed. The result of a "Western blot" is presented in section 3.2. It proves the functionality of the antibody used for GAF-CHIP experiments. In section 3.3 the large-scale chromatin immunoprecipitation (CHIP) experiment with magnetic beads is outlined, including an estimation of the target concentration in the chromatin samples (the "starting material"). Section 3.4 describes the custom designed setup for the fluidic handling in capillaries. Section 3.5 explains the chemistry that has been employed to fabricate a μm-scale immunoaffinity column by immobilization of antibodies on the inner channel walls of fused silica capillaries. It also includes a description of alternative glass surface coatings (section 3.5.2 and 3.5.3). The CHIP assay in capillaries is then specified in section 3.6 The PCR detection details are given in section 3.7. This is followed by a summary of confocal fluorescence microscopy in section 3.8. Confocal microscopy has been employed for the imaging of glass coatings (see section 4.1 and 4.2).

3.1 Chemicals and Buffer Solutions

This section introduces chemicals, buffer and components in the form of a summary list. It serves as a reference for the following chapters.

3.1.1 Chemicals

The chemicals and materials used for the coatings in all experimental work of this thesis were the following:

- Methanol (100%, anhydrous), toluene (100%, anhydrous), HCl 37% (fuming), dimethylformamide (DMF), sulfuric acid (H_2SO_4, 97%), hydrogen peroxide (H_2O_2, 37%) and KOH were all of analytical grade or higher from Fluka, Germany.
- Sodium acetate was from Fluka, Germany. Purity $\geq$ 99.5%, Prod.no. 71188
- NaCl, Na_2HPO_4, NaH_2PO_4, LiCl, glycin, acetic acid and ethanol (100%, anhydrous) were all analytical grade or higher from Merck, Germany.
- TE buffer (10 mM Tris pH 8.0 1 mM EDTA) was obtained as 100x pre-mix from Fluka.
- Triton-X-100, Na-deoxycholate and NP-40 were from Sigma, Germany.
- Dodecylsulfate-Na-salt (SDS) and AEBSF were from Serva, Germany (Invitrogen Corporation).
- Double distilled and sterilized water was used from the central laboratory facilities at EMBL Heidelberg.
- Argon (grade 5.0) and nitrogen (grade 5.0) were purchased from Messer Griesheim, Germany.
- 3-Mercaptopropyl-trimethoxysilane (MTS) was purchased from Gelest Inc., USA (Prod.-no. SIM6476.0).
- The heterobifunctional cross-linker N-gamma-Maleimidobutylryloxy Succinimide ester (GMBS) was from Pierce Corporation (Perbio Science Deutschland GmbH, Prod.-no. 22309).
- PEG-Silane with molecular weight of 5000 Dalton has been purchased from Shearwater Corporation, USA. (Prod.-no. 2M4HOH11)
- Bovine Serum Albumin (BSA), Fraction V, RIA and ELISA grade, was purchased from Calbiochem, Germany (Prod.-no. 126593).
- Recombinant Protein A (expressed in E. Coli) was purchased from Sigma (Prod.-no. P7837).
- Fused silica capillaries of various diameters (with standard polyimide coating on the outside, for capillary electrophoresis) were manufactured by Polymicro Technologies, Phoenix, USA, and purchased via Optronis, Germany.

- Paramagnetic beads were from Dynal, Norway:
  1. Streptavidin coated beads: Prod.no. 112.05
  2. Protein A coated beads: Prod.no. 100.01
  3. Sheep-anti-rabbit IgG coated beads: Prod.no. 112.03
- PCR primer were HPLC purified quality from Biospring, Germany.
- PCR reagents for multiplex PCR were from Epicentre, USA.
- PCR reagents for real time PCR (including TaqMan Probes) were from Applied Biosystems, Germany.
- Agarose (electrophoresis grade) was purchased from Gibco (Invitrogen Corporation, Prod.-no. H15510-027).

MTS, GMBS, DMF were handled under nitrogen ($\leq 1\%$ oxygen).

MTS was used for a maximum of 2 months after opening.

GMBS was used for maximal 1 week after opening.

Antibodies

The antibodies used for this work are the following (numbers are lab-internal numbering in arbitrary order):

antibody number	host	target	label or conjugate	company	Prod.-no.	note
# 6	rabbit	mouse	Alexa 546	Mol. Probes	A-11060	
# 8	goat	mouse	Alexa 546	Mol. Probes	A-11030	
# 9	rabbit	goat	Alexa 488	Mol. Probes	A-11078	
# 11	goat	rabbit	Alexa 488	Mol. Probes	A-11008	
# 12	goat	rabbit	none	Jackson	111-005-045	
# 13	goat	rabbit	Alk. Ph.	Promega	S3731	Fc specific
# 15	goat	Biotin	none	Sigma	B3640	

Mol. Probes stands for Molecular Probes, Europe.

Jackson stands for Jackson ImmunoResearch, USA.

Alexa 488 is a dye from Molecular Probes that is excited at 488 nm and emits at 520 nm. Alexa 546 absorbs at 546 nm and emits at 575 nm. Alexa dyes are very robust against buffer conditions and bleach very slowly.

Alk. Ph. stands for alkaline phosphatase. In the CHIP experiment in chapter 4, this antibody was employed for its high affinity against the Fc region of rabbit IgGs and not because of the conjugate.

3.1.2 Buffer Solutions

RIPA buffer:

- 1% Triton-X-100
- 0.1% Na-deoxycholate
- 0.1% SDS
- 140 mM NaCl
- 10 mM Tris pH 8.0
- 1 mM EDTA
- add AEBSF to 1 mM immediately before use.

LiCl buffer:

- 250 mM LiCl
- 10 mM Tris pH 8.0
- 1 mM EDTA
- 0.5% NP-40
- 0.5% Na-deoxycholate

TE buffer:

- 10 mM Tris HClpH 8.0
- 1 mM EDTA

Glycin buffer:

- 200 mM Glycin
- adjusted to pH 2.5 with 2 M HCl

PBS buffer:

- 100 mM NaCl
- 100 mM Na_2HPO_4 and NaH_2PO_4
- ratio of the latter: to obtain pH 7.6

Acetate Buffer:

- 100 mM $C_2H_3NaO_2$ and Acetic Acid
- ratio of the latter: to obtain pH 5

TAE buffer:

- 40 mM Tris acetate
- 1 mM EDTA

3.2 The anti-GAF Antibody - Western Blot

For the successful immunopurification of GAGA transcription factor (GAF) from *Drosophila* chromatin (section 2.3.3, chapter 4), the quality of the antibody against GAF is the most essential parameter. The antibody used for this work was produced by the group of Prof. Peter Becker, Munich, in rabbits. Its affinity for GAF is exceptionally high (*Becker*, 1998) and many chromatin immunoprecipitation (CHIP) studies were realized, based on this molecule (*Strutt et al.* (1997) and *Cavalli et al.* (1999)). For more information about antibodies and their function, see section 2.2.2.

The aliquot of anti-GAF used for the experiments in chapter 4 was stored at $-80°C$ for several years. Therefore, a Western Blot analysis of this antibody was carried out to verify the functionality and specificity for GAF protein.

In a Western Blot, electrophoretically separated proteins are transferred ("blotted") from a gel to a solid support and probed with specific antibodies. It is a very useful technique for the identification and quantitation of specific proteins in complex mixtures. In brief, the samples to be assayed are solubilized and separated by SDS-polyacrylamide gel electrophoresis. From this gel they are blotted by direct electrophoretic transfer to a nitrocellulose filter or nylon membrane. Non-specific interactions of antibodies with the membrane are avoided by saturating it with a neutral protein product (in this case, milk proteins). The membrane is subsequently exposed to unlabeled antibodies ("primary antibodies") specific for the target protein. In the case of this project, the primary antibody is the anti-GAF antibody that recognizes the bands corresponding to GAF. In a second step, the membrane is incubated with secondary antibodies raised against the conserved regions of the primary antibodies. Secondary antibodies carry an enzymatically active domain that can be used for their calorimetric detection. In this case, a goat-anti-rabbit, alkaline phosphatase-conjugated secondary antibody was used. The Western Blotting technique, originally published by *Towbin et al.* (1979) and *Burnette* (1981), is explained in detail in *Sambrook et al.* (1989).

Nuclear extract from 12 to 14 hours old *Drosophila* embryos was used in two concentrations (a1 and a2 in figure 3.1). Two more samples with GAF free extracts were added as controls (b1 and b2).

Protocol

Figure 3.1 is a scan of the resulting nylon membrane of the western blot that was carried out after the following protocol:

1. The nuclear extracts are electrophoretically separated on a common 12% SDS-

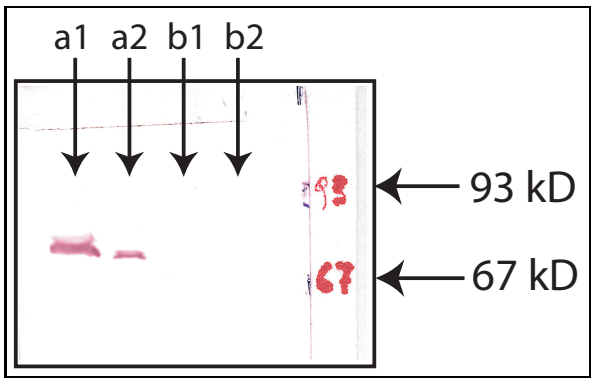

Figure 3.1: The western blot shows a clean, distinct band at a molecular weight of about 70 kD, which corresponds to the molecular weight of GAGA transcription factor. a1 and a2 are nuclear extract from 12-14 hours old embryos. a1 is 5× the concentration of a2. b1 and b2 are other nuclear extract samples with very low GAF expression, used as control.

polyacrylamide gel (following the standard protocol from *Sambrook et al.* (1989), page 18.47 and following).

2. Then, the gel is equilibrated in a "transfer buffer" (25 mM Tris, 192 mM glycine, 15% methanol) for 10 minutes to clean it from the protein denaturing detergent SDS.

3. The nylon membrane (Immobilon-P, 0.45 μm from Millipore) is activated in methanol for 1 minute and then equilibrated in transfer buffer for 5 minutes.

4. Electrotransfer of proteins from the gel to the membrane is done in a sandwich assembly (described in *Sambrook et al.* (1989), page 18.65) for 60 minutes at 60 volts.

5. It follows washing of the membrane with TBS buffer (20 mM Tris pH 7.4, 150 mM NaCl, 0.1% Triton-X-100) for 10 minutes an room temperature and 45 minutes to 1 hour in TBS with 5% milk powder.

6. The primary antibody against the protein of interest (anti-GAF in this case) is incubated in a 1/1500 dilution in milk-TBS for 2 hours at room temperature.

7. This is followed by 3 times 5 minutes wash with milk-TBS.

8. Now the secondary antibody is incubated on the membrane for 1 hour at room temperature (alkaline phosphatase-conjugated goat-anti-rabbit from Sigma, product no. A-3687, diluted according to manufacturers recommendation in milk-TBS).

9. Then the membrane is again thoroughly washed in milk-TBS (once for 5 minutes) and TBS (3 times 5 minutes) before the alkaline phosphatase reaction kit (from Biorad, product no. 88483) is applied according to the manufacturers specifications. The enzymatic reaction stains the bands where the primary antibody has recognized its target.

The results shown in figure 3.1 prove that the anti-GAF antibody has not degraded or decreased in functionality nor in specificity. Lanes a1 and a2 present a strong clean signal at the expected molecular weight of GAF (70 kD). Thus, anti-GAF has specifically recognized GAF.

3.3 Large Scale CHIP Assays

The transfer of chromatin immunoprecipitation (CHIP) assays to the miniaturized scale requires some modification and adjustment of the common protocols as well as some particular considerations on the sample concentrations of macromolecules involved. These points are presented in the following sections.

Section 3.3.1 gives an estimate on target gene concentration in the formaldehyde cross-linked chromatin and discusses the consequences for the downscaling approach. Section 3.3.2 lists the experimental steps for the large-scale CHIP experiment that has been carried out with paramagnetic beads (sample volume: 100 μl).

3.3.1 The Chromatin Sample

For the interpretation of experimental results of an immunopurification (IP) such as the core experiment of the presented work, described in chapter 4, it is essential to know the concentrations of potential targets in the starting material.

In the preparation of formaldehyde cross-linked chromatin (see *Cavalli et al.* (1999)), 5 grams of *Drosophila Melanogaster* embryos yielded 11 ml of chromatin for IP experiments (*Gilfillan*, 2000). This compares to 1 ml extract from 454 mg embryos.

The fly embryos were 12 to 14 hours old when collected for the chromatin preparation. Hence they are at their developmental stage 15. From the data on developmental stages of *Drosophila* and cell division numbers in the book of *Campos-Ortega and Hartenstein* (1997), it follows that a fly embryo of an age of 12 to 14 hours has roughly 20000 to 30000 cells, i.e. ≈ 50000 copies of each single-copy gene.

The embryo of *Drosophila Melanogaster* weighs 9.5 μg (*Mazur et al.*, 1988). Thus, 1 ml chromatin extract contains the material from $454000 : 9.5 \approx 47800$ embryos.

As a maximum estimate, assuming no losses in all preparation and purification steps it follows that in each ml extract there are $47800 \times 50000 \approx 2.4 \times 10^9$ gene copies.

This is a maximum concentration of

$$C_0 = 2 \times 10^6 \tag{3.1}$$

gene copies per microliter.

This concentration, together with the performance of the respective detection method (such as PCR, discussed in section 3.7) sets the frame for possible downscaling approaches of IP techniques.

3.3.2 CHIP Assay with Magnetic Beads

As a control for the downscaled experiments in capillaries, the following method was employed to reproduce a large-scale CHIP assay with the same biological sample material. This protocol is derived from the original CHIP protocol listed in appendix B. It uses monodisperse paramagnetic styrene beads from Dynal (Dynal Biotech, Norway) with a diameter of 2.8 μm ("Dynabeads").

The biological interest of the CHIP assay performed in this experiment is to monitor the specific protein-DNA interaction of the GAGA transcription factor and its target DNA binding sites *in vivo* (as discussed in section 2.3.2). The promoter sequence of the hsp26 gene ("Heat Shock Protein 26") in *Drosophila Melanogaster* has several prominent GAGA (hence GAF-binding) regions and is a specific binding target region for GAF (*O'Brien et al.* (1995), *Lu et al.* (1993) and *Wilkins and Lis* (1997)). This promoter is the specific target region for the GAF CHIP experiments in this work. Hence, this experiment aims for showing specific enrichment of DNA fragments from the hsp26 promoter (for short: "hsp26 fragments") in the eluates from the GAGA factor-CHIP assay.

Formaldehyde cross-linked and mechanically sheared chromatin from 12 to 14 hours old *Drosophila* embryos, provided by Prof. Peter Becker, Munich, was prepared according to standard CHIP assay protocols (see section 2.3.3). After buffer modification it was incubated with the rabbit-anti-GAF antibody over night at 4°C. Long incubation is important to ensure that the antibody has enough time to efficiently find and bind its target.

Dynabeads were washed in PBS buffer according to the manufacturers specifications. For this experiment (results in section 4.3), protein A beads were used as well as sheep-anti-rabbit coated beads. Both types of beads have a high specific affinity for rabbit IgG (such as the rabbit-anti-GAF). For protein A-antibody affinity see also section 3.5.2. The beads were incubated with the chromatin sample in a standard reaction tube. After the target, i.e. the complex of anti-GAF antibody with GAF and the cross-linked DNA fragments, is bound to the beads, the tube is placed on a magnet suitable for this kind of experiment in standard reaction tubes (from Dynal Biotech). The magnetic field drags the beads to the tube wall and the clear supernatant solution can easily be taken off and replaced with a washing buffer. The beads (with the target

bound to it) are now resuspended by removing the tube from the magnet and carefully shaking or vortexing it. Repetition of this washing-procedure (two or three times) leads to a considerable degree of purity. This technique is illustrated in figure 3.2.

The buffer conditions are important to ensure elimination of unspecific retention of sample material and at the same time keeping the specific antibody-antigen interaction intact. For CHIP assays a detergent modified Tris buffer ("RIPA") with high salt concentration is commonly used (*Orlando and Paro*, 1993). For its composition see section 3.1. The detergent neutralizes hydrophobic interaction and the high salt concentration shields electrostatic interactions. The concentrations are critical since the specific antibody-antigen interaction also relies mostly on hydrophobic and electrostatic forces (*Stryrer* (1995) page 371 and *Harlow and Lane* (1988) page 26) and a compromise has to be found between stringent washing and maintaining the specificity. The last wash step was performed with pure Tris buffer to remove detergent and salt leftover.

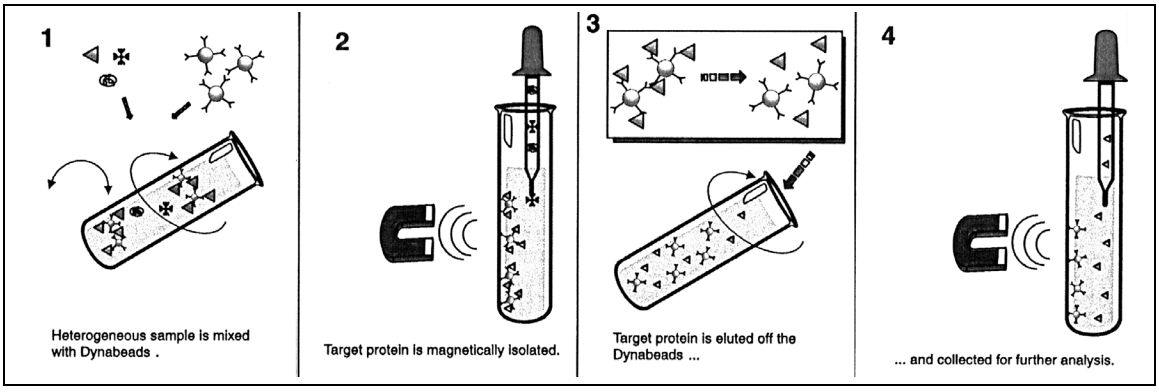

Figure 3.2: The principle of solid phase immunoprecipitation relies upon an paramagnetic-bead-bound antibody. The target antigen which, once bound, can be separated from a complex mixture such as a cell extract for further use. For biotin-labeled targets streptavidin is used instead of the antibody. The picture is taken from the "Technical Handbook for Cell Separation and Protein Purification", page 118 from Dynal Biotech.

After washing, the column was heated to 65°C in Tris buffer. Tris buffer lowers its pH dramatically upon heating. This pH-drop shifts the equilibrium of bound and free formaldehyde to the free state and thereby reverses the formaldehyde cross-links (*Solomon and Varshavsky* (1985) and *Orlando et al.* (1997)). The DNA fragments were now free from associated protein and could be detected by PCR as described in section 3.7.

After a successful immunoprecipitation, the PCR products of the target (GAF-associated) DNA fragment in the "+" sample is enriched compared to the product from the "−" sample.

Although paramagnetic beads are very practical and easy to use, a Dynabead-based assay for immunoprecipitation of protein-DNA complexes as described in this section is limited to large amounts of sample. Only recently, the combination of magnetic beads and microfluidics has become a focus of microsystem development (see for example *Hayes et al.* (2001), *Jiang and Harrison* (2000), *Oleschuk et al.* (2000), and *Ruzicka and Hansen* (2000)).

Protocol

The protocol for the immunopurification with magnetic beads is:

1. Adjust a 100 μl aliquot of chromatin to RIPA buffer conditions by adding 20 μl of each of the following: 10% Triton-X-100, 1% Na-deoxycholate, 1% SDS and 1.4 M NaCl. Then 10 μl of 0.1 M Tris pH 8.0 and 10 mM EDTA. Finally, add 2 μl of 100 mM AEBSF.

2. Split the resulting 200 μl in 2 $\times$ 100 μl. (anti-GAF + and $-$, as control). To one of them (+ sample) add 0.5 μl of the rabbit-anti-GAF antibody. The other serves as a control ($-$ sample). Incubate both rotating at 4 °C over night (o/n). The following steps are applied to both samples identically.

3. Dilute the chromatin 1 : 10 in RIPA buffer.

4. Take 100 μl of protein A-beads from Dynal and put them in a 1.5 ml reaction tube. Place the tube on the magnet (MPC-S, Prod. No. 120.20 from Dynal Biotech, Norway) and wait until the beads are all drawn to the back wall of the tube. Take off the clear buffer solution and resuspend the beads in fresh PBS buffer for washing. Mix well and repeat this step twice.

5. After the last wash, resuspend the magnetic beads in 100 μl chromatin (1 : 10 in RIPA, see above) and incubate them at 4°C for 3 hours (rotating).

6. Then put the tubes on a magnet, take off the buffer and wash with 1 ml fresh RIPA buffer. Repeat 3 times.

7. 3 washes (1 ml) with the 500 mM LiCl buffer in the same way as described above.

8. 2 washes with Tris buffer (Tris HCl pH 8.0).

9. Last resuspension in 100 μl Tris buffer.

10. Then, put the tubes to 65°C for 6 hours for cross-link reversal.

11. From this, take 4 μl as template for the PCR reactions and run the products on a 2% agarose gel (as described in 3.7).

3.4 The Setup

This section describes the experimental setup that was used to clean and coat the capillaries (section 3.4.1) as well as the fluidics setup designed to run 8 capillary CHIP assays in parallel (section 3.4.2). Also, the details of the new Peltier-sandwich for capillary temperature control are given in section 3.4.3.

3.4.1 Pressure Driven Coating Station

To efficiently treat the inner surface of fused silica capillaries with chemicals, a commercially available "solvent rinsing kit" (Supelco, Germany) for capillary electrophoresis applications was used. Figure 3.3 shows a schematic drawing of such a unit that can easily be parallelled.

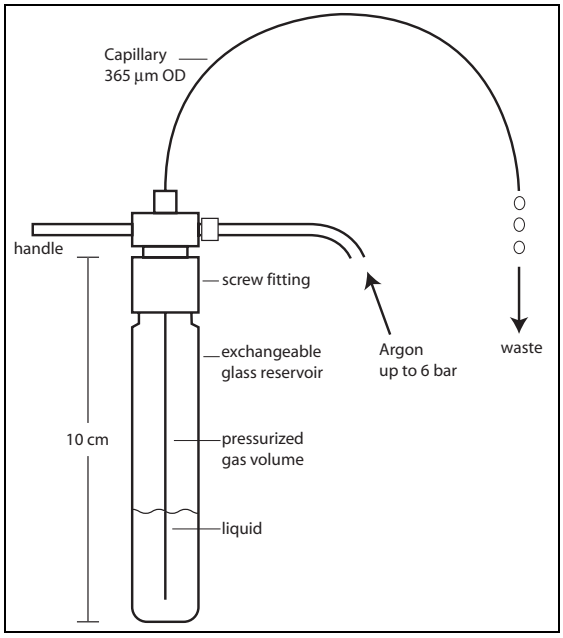

Figure 3.3: The pressure driven coating tool. (From Supelco, Germany)

The pressure inlet was connected to a 200 bar cylinder with high purity grade argon (grade 5.0). With a pressure control unit from Messer Griesheim, Germany, the pressure in the glass reservoir was regulated between 3 and 6 bar, depending on the viscosity of the applied solution (see section 2.1.3). This way the liquid is forced in the capillary that is inserted far enough to ensure its end is submerged below the liquid surface.

The major advantages of this tool for the requirements of the described thesis project are:

a) This device ensures fast and efficient passage of the chemicals and has been employed for all capillary treatment from the cleaning to the final PBS buffer rinse (section 3.5.1).

b) The reservoir is made of glass and thus chemically inert and very resistant to the employed corrosive chemicals (see section 3.5.1).

c) The glass reservoirs are easy to replace. This makes it easier to keep coating and cleaning solutions free from contaminants.

3.4.2 Capillary Manifold - the Fluidics

To control the fluidic samples and buffers in the immunoaffinity columns for the CHIP experiments, a new setup was designed that allows the controlled sample injection and rinsing with buffer in 8 parallel capillary columns with a length of 60 cm each. The total volume of a 60 cm long column with an inner diameter (ID) of 75 μm is 2.6 μl. (For tables of capillary diameter and volumes see appendix D.)

Figure 3.4 is a drawing of the setup. 8 columns are sandwiched between temperature controlled plates ensuring precise cooling and heating as required by the experimental protocol (section 3.6). The peltier device is described in section 3.4.3.

Each column is connected to the buffer reservoir via a PEEK micro-cross connector (figure 3.5, from Upchurch Scientific, USA). The intersecting channels have an ID of 152 μm. Thus, the total volume of the micro-cross body is $\leq$ 100 nl. The biocompatible material (PEEK) was chosen to reduce unspecific adsorption to a minimum. One of the 4 outlets stayed permanently plugged since only one sample injection capillary was connected at a time. To keep the drawing simple, figure 3.4 shows only the very left micro-cross in detail.

The PEEK micro-crosses and the buffer reservoir are connected by 5 cm long uncoated glass capillaries with an ID of 75 μm, i.e. a volume of 220 nl. This is the volume of buffer that still has to pass the columns after a buffer change in the reservoir has been carried out. The 5 cm are the minimum length required due to the type of the involved fittings.

The buffer reservoir is made from a 12 cm long PMMA block. PMMA was chosen for its transparency and its chemical inertness to the buffers as well as for its mechanical strength that was necessary for drilling fine bores and cutting the threads. It has a 2.5 mm ID horizontal channel from which 8 outlets (drilling ID 150 μm) go to the capillary ports on the bottom side of the block (see figure 3.4). The ratio of these

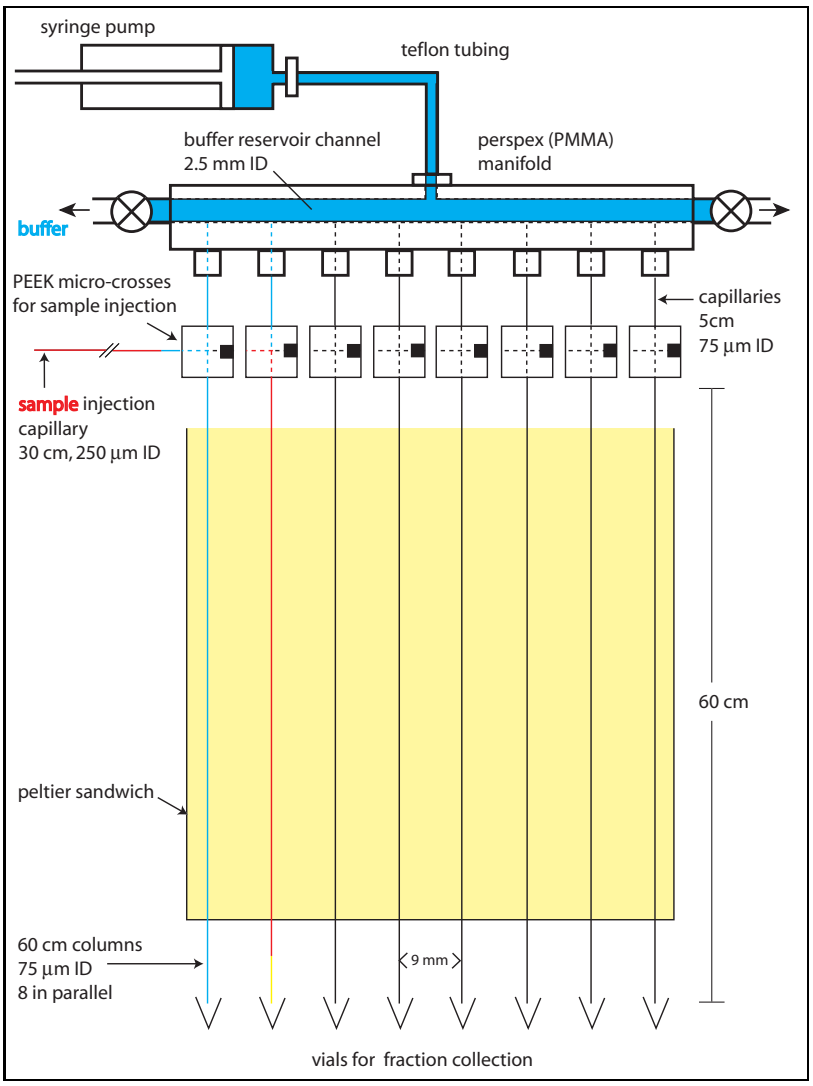

Figure 3.4: The fluidics setup for 8 paralleled capillaries.

two diameters is chosen to ensure constant pressure in the buffer reservoir and thus equal flow rates in all 8 capillaries.

The buffer reservoir is connected via teflon tubing (ID 2 mm) to a syringe that is mounted on a syringe pump (Harvard Apparatus, USA).

30 cm long injection capillaries with an ID of 250 μm (volume: $\approx$ 16 μl) are connected to Hamilton-microliter syringes (Hamilton Company, USA) and filled with the sample plug (e.g. 3 μl chromatin flanked by 3 μl buffer on each side) by simple suction. Immediately after filling, they are connected to the horizontal port of the micro-cross and the sample is injected into the column.

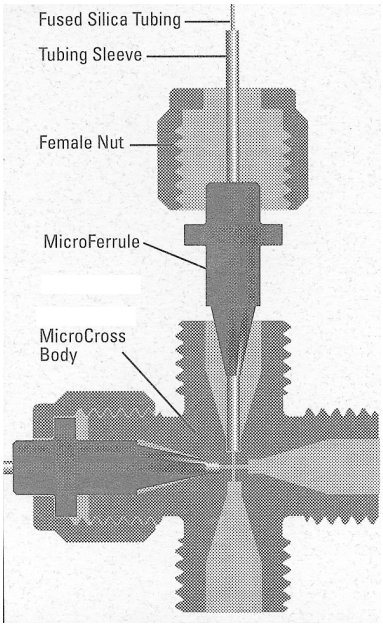

Figure 3.5: The low dead volume intersection for sample injection. From Upchurch Scientific, USA.

The micro-crosses and all fittings that come in contact with sample material were cleaned after each experiment. Cleaning of the components involves a 3 hour immersion in 5 N HCl, subsequent rinsing in double distilled water and 70% ethanol and drying in a vacuum oven.

All fittings and tubing were purchased from Upchurch Scientific, USA.

The PMMA manifold was designed in the process of this project and was manufactured at EMBL Heidelberg.

3.4.3 Temperature-Control in Capillaries

To control the temperature in the capillary columns as accurately as possible, a new peltier device was designed and built. 10 high power Peltier elements were arranged in a sandwich style array and controlled electronically by a feedback-thermistor driven power-amplifier. Figure 3.6 shows the design of the device that was built in the mechanical workshop at EMBL.

The capillaries are sandwiched between two aluminium plates. The aluminium plates are temperature controlled from the back by a stacked array of Peltier elements (figure 3.8). A heat sink is mounted to the outside of the assembly to provide efficient cooling and stability. The sandwich was held together by thermally insulated screws

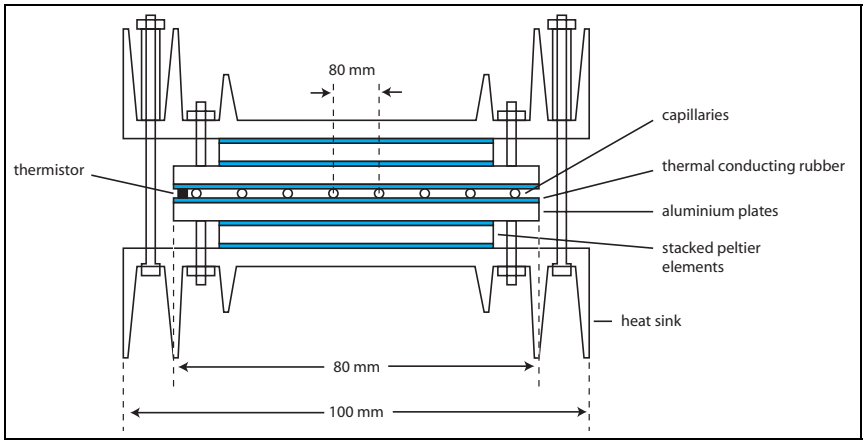

Figure 3.6: In house made Peltier array sandwich for capillary temperature control. The capillaries are clamped between two aluminium plates (4 mm thick). These plates are tempered by stacked peltier elements (62 × 62 mm in surface and 4.6 mm thick). The whole assembly is held together by heat sink plates to ensure heat removal from the system. Good thermal contact between the components is ensured by a thermally conducting rubber layer (0.2 mm thick). In the direction of the capillary length, the device measures 55 cm.

and between all stacked components a thermally conducting rubber layer was inserted to ensure optimal contact (both thermal and mechanical). The total length of the sandwich is 55 cm. For experimental work it was mounted upright on a rack, the injection micro-crosses placed at the top and the fraction collection tubes at the bottom.

An photo of the setup is shown in figure 3.7.

The Peltier elements (product number 284-826 from RS Components, UK) are 62 × 62 mm in surface and 4.6 mm thick. Each element has 120 Watts power. They are connected to an in-house made assembly of power supply units (PSU), amplifiers and control elements to provide the necessary power and feedback control.

The temperature control was realized by a "Control Module" from Wavelength Electronics, Inc (model MPT10000, product number at RS Electronics, UK: 218-6465). This control unit, powered by its own power supply, regulates the output of the main power amplifier via a signal attenuator (to slow down feedback reactions and avoid oscillations around the set temperature). A temperature switch set to the needed temperature (i.e. 4°C during IP experiments and 65°C for formaldehyde cross-link reversal, see section 3.3.2 and 3.6) serves as reference for the feedback from the thermistor that is located next to the capillaries.

The described assembly allows stable temperature control for capillaries within a range of 3°C to 80°C (working range of the Peltier elements). Temperature fluctuations over 8 hours are less than 1°C. A temperature change from 4°C to 65 °C takes

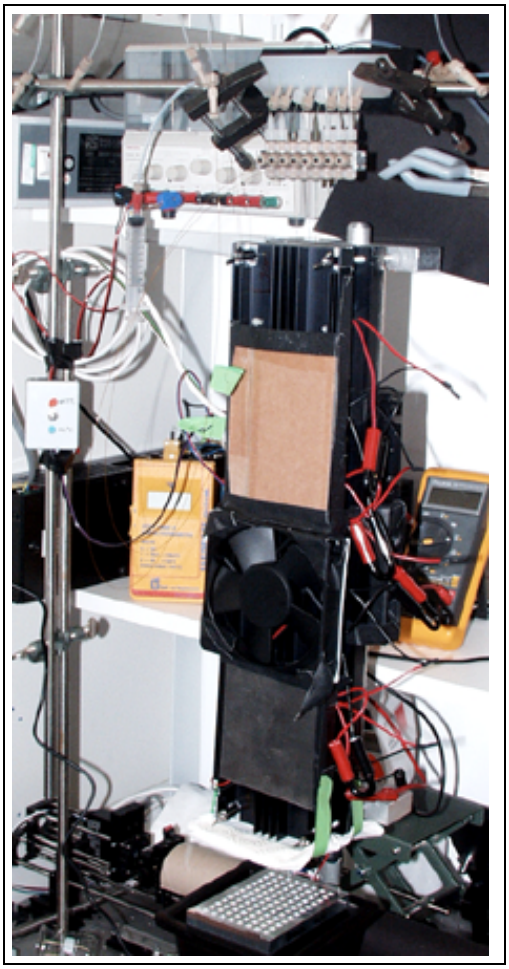

Figure 3.7: A photograph of the new Peltier array sandwich for capillary column heat control. Above the sandwich, the perspex manifold block and the injection micro-crosses can be seen. At the bottom of the picture, an aluminium block for cooling fraction collection tubes is easy to recognized. The temperature switch is at the very left of the picture

about 10 minutes, not passing a maximum of 65.5°C during the approach oscillations.

3.5 Coating and Modification of Silica Surfaces

Microfabrication techniques originate from the microelectronics industries. Thus, the range of available materials for microstructures was originally limited to the materials commonly used in this field, namely to silicon and glass, i.e., SiO_2.

Although new methods for fabrication of microstructures from plastic have emerged during the last years (see section 2.1.4) the presented work focusses on fused silica

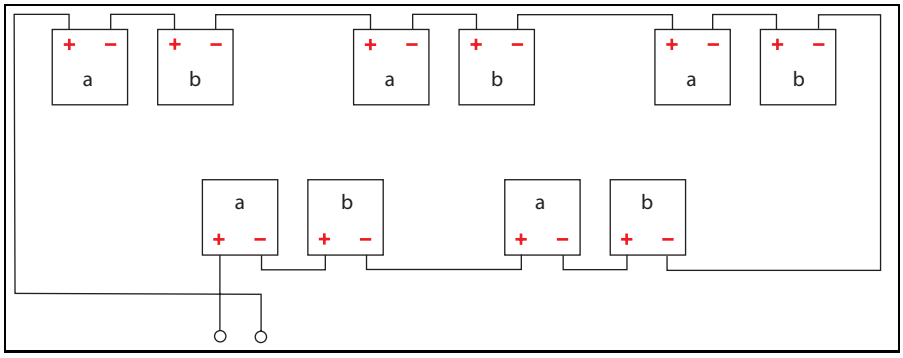

Figure 3.8: The arrangement of the Peltier cells connected in serial. Elements a were stacked on b. In this way, the outer one is cooling/heating the inner one to reduce the overall temperature gradient across the individual Peltier. This proved to be the best configuration for temperature stability and ramping times.

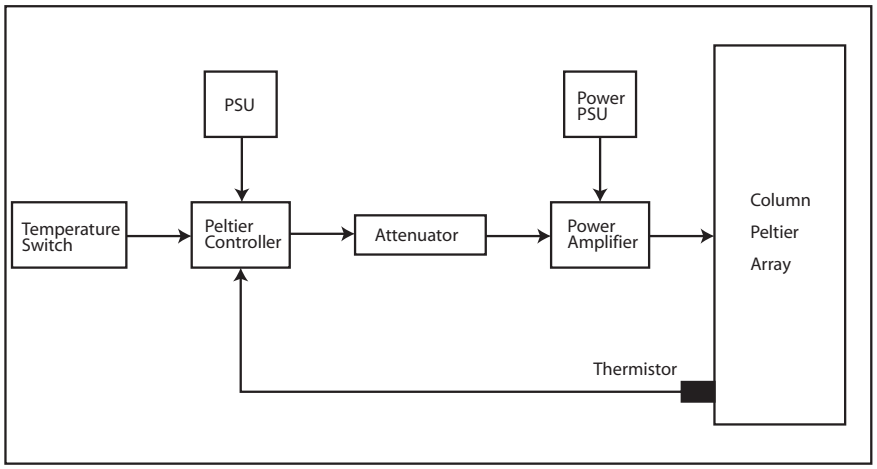

Figure 3.9: A schematic diagram of the peltier control by thermistor driven power-amplifiers. The "Control Module" from Wavelength Electronics gets input from the feedback thermistor and the temperature switch. Its output drives the power amplifier for the peltier elements via a signal attenuator.

glass capillaries serving as fluid guiding channels and solid substrate for antibody immobilization. The main reasons for this choice are the chemical inertness and optical transparency of fused silica glass as well as the commercial availability of suitable capillaries.

3.5.1 Coating Fused Silica Capillaries Homogeneously with Antibodies and Proteins

The coating of the glass channel walls involves the following steps: Cleaning, silanization, thermal curing of the silane layer, incubation of a bifunctional cross-linker and finally antibody/protein immobilization and Bovine Serum Albumin (BSA) blocking. Ideally, the resulting layer provides specific interaction with the sample passing through the channel (by the antibodies or other attached proteins) and at the same time saturates the surface with BSA and thereby inhibits any unwanted hence non-specific sample-wall interactions. The type of unspecific interaction of major concern for this work is unwanted adsorption of sample material to the channel walls. The particular coating method described in this section is derived from *Bhatia et al.* (1991), *Shriver-Lake et al.* (1997) and *Rowe et al.* (1999). The ideal coating resulting from this protocol is schematically shown in figure 3.10. It is homogeneous and exposes only the specific antigen binding groups of the antibody to the free channel volume. Free patches of glass surface are shielded and adsorption of molecules other than the specific antigen is suppressed by the inert BSA protein. Shielding potential free glass patches is essential for blocking unspecific adsorption since glass is inherently a highly charged surface and therefore strongly attracts charged molecules and polyelectrolytes such as proteins and DNA (see also section 2.1.4). Another cause for unspecific adsorption can be a mechanical inhomogeneity, i.e., a "blob" of the coating that traps molecules regardless of their chemical nature. This is avoided by a homogeneous and smooth coating.

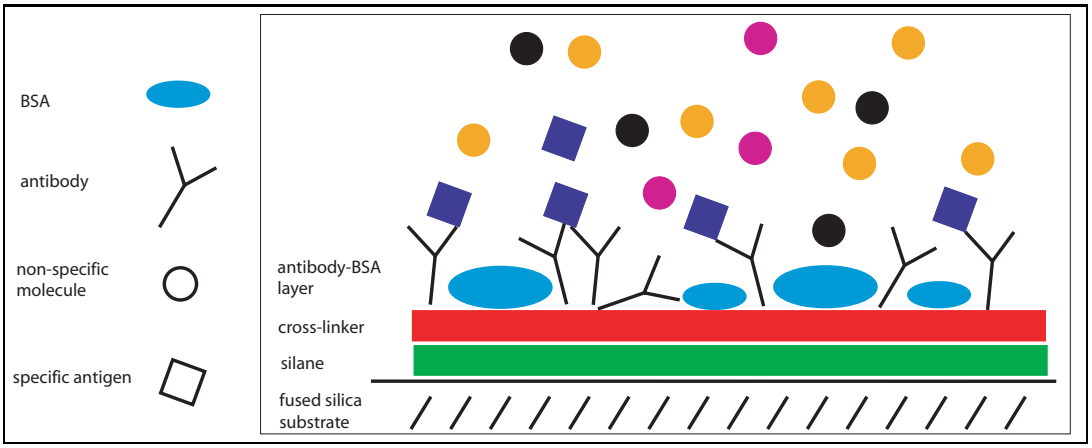

Figure 3.10: This scheme illustrates the ideal surface coating this work is aiming for: The only interaction of the coating with passing sample material is the specific binding of the antibodies and the antigen. All other potential interaction sites are shielded by the neutral protein BSA and therefore no other molecule than the one of interest (square) sticks to the surface.

Cleaning Protocol

Thorough cleaning of the glass substrate, prior to chemical modification, sets the basis for a homogeneous coating. The surface cleaning removes any organic contaminants and conditions the chemical state of the surface for the following treatment. Generally, cleaning with first basic, then acidic solutions that protonates the surface leads to a silanol-covered, hydrophilic surface required for efficient silanization. After thorough cleaning, the density of silanol groups on silica surfaces is $\approx 4.9 \times 10^{14}$ cm^{-2} (*Dong et al.*, 1998). The silanol groups are schematically shown in figure 3.14a.

The cleaning protocol for a 5 meter long capillary of 75 μm inner diameter is [1]:

1. Rinsing with 100% methanol : 1 N HCl (1:1, v:v) for 30 minutes at 5 bar
2. Rinsing with conc. H_2SO_4 ($> 97\%$) for 30 minutes at 5 bar
3. Rinsing with H_2O for 30 minutes at 5 bar
4. Drying with argon for 30 minutes at 5 bar

Cras et al. (1999) have extensively studied and compared various glass cleaning methods. They compared the above to other similar techniques (*Jönsson et al.* (1988) and section 3.5.3) that mostly involve very strong bases and aggressive acids but according to their data do not result in better coatings. Hence, for convenience and safety reasons the above protocol was chosen for this work.

Cross-linking Proteins (Covalently) to Silica Surfaces

To date, the main method for the covalent attachment of biological units, such as DNA and proteins, to silica surfaces has involved reaction of the surfaces with organofunctional silanes followed by the attachment of the biological molecule to the newly introduced functional group. A large number of procedures for the silanization of glass have been described and extensively reviewed in the literature (*Leyden* (1986), *Vandenberg et al.* (1991), *Lyubchenko et al.* (1996), *Halliwell and Cass* (2001)).

A silane is a silicon-organic molecule, with a functional group (usually an alkane, amino or thiol group) linked to a silicon atom and one, two or three methoxy groups (alternatively ethoxy groups) that spontaneously bind to silanol groups on silica surfaces at room temperature. Figure 3.11 shows a thiol functional silane ("mercaptosilane"). In theory, the reaction is relatively simple: The hydrolysis of the alkoxy

[1] A pressure of 5 bar in a 75 μm inner diameter capillary of 5 meter length corresponds to a flowrate of $1 \frac{\mu l}{sec}$, i.e. about 1 total volume every 22 seconds (section 2.1.3).

group yields hydroxyl groups that can covalently interact with the silanol surface (see figure 3.12a+b). The silane can be cleaved and the surface regenerated by the action of strong bases. However, the exact chemical reaction is still not fully understood (*Halliwell and Cass*, 2001).

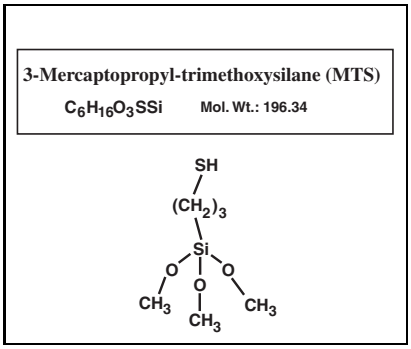

Figure 3.11: 3- Mercaptopropyl- trimethoxysilane (MTS)

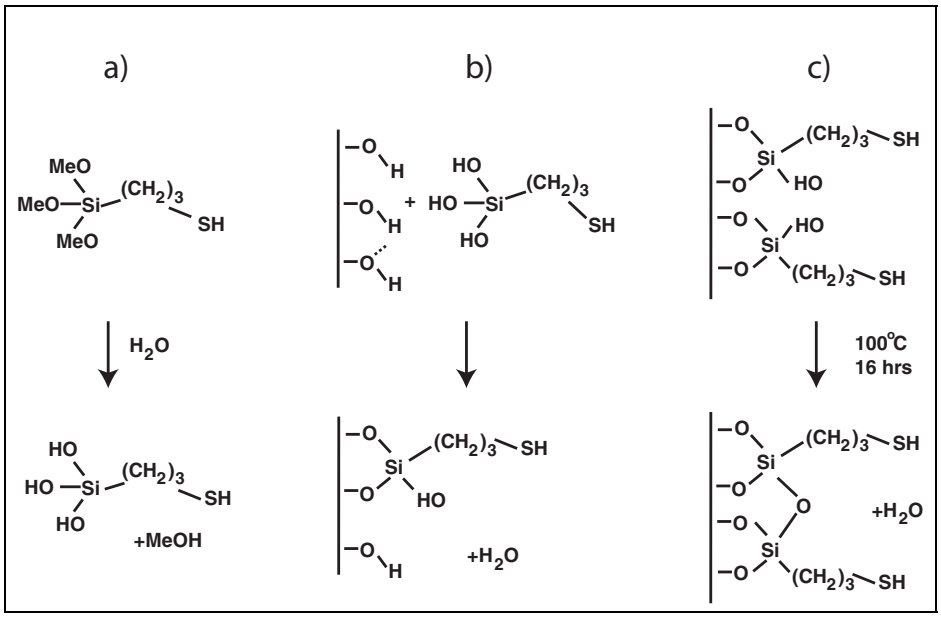

Figure 3.12: Silanization of Glass with MTS: The alkoxy groups of MTS are hydrolyzed to hydroxyl groups (a). This allows the silane to covalently condense to the oxide surface (b). Curing stabilizes the layer (c)

Since the hydrolyzed alkoxy groups of the silanes can also react amongst each other, polymerization of trialkoxysilanes can occur on the surface as well as in solution. This effect can lead to highly polymeric and heterogeneous surfaces, a potential disadvantage for applications that require molecularly smooth surfaces. To reduce the

formation of polymeric and inhomogeneous silane layers the main strategies are 1) to always use fresh silane and keep it under an inert gas (dry and oxygen free), 2) the limitation of alkoxysilane concentration upon surface modification, 3) the use of monoalkoxysilanes and 4) the use of anhydrous postsilanization "curing". The first two strategies are part of the parameter optimization and have thereby been incorporated in the protocols below that are derived from *Shriver-Lake et al.* (1997) and *Halliwell and Cass* (2001). As for the third strategy, monoalkoxysilanes are readily cleaved off the surface due to rapid hydrolysis and hence are no option if a stable coating layer is needed. The fourth strategy, i.e., the curing, is still discussed in the literature (for example *Ligler* (2001) versus *Halliwell and Cass* (2001)). "Curing" stands for the heating of the surface to $\approx 100°C$ in anhydrous and oxygen free conditions (under vacuum). This cross-links free silanol groups of surface bound silanes and stabilizes the bond of the silane with the silica surface (see figure 3.12c). However, the thiol group of mercapto-silanes as used in this work (see below) can easily oxidize and form inactive sulfonates. This oxidation is even faster when the temperature is increased. Therefore a good vacuum is required throughout the curing and the temperature must not exceed 100°C (*Ligler*, 2001). The coatings used for the experiments reported in chapter 4 have been done with curing since avoiding inhomogeneous surfaces is considered more important than the number of active binding sites on the surface.

In this work, the *3-Mercaptopropyl-trimethoxysilane* (MTS) molecule (see figure 3.11) has been chosen for protein attachment to glass. Its thiol functional group binds spontaneously to maleimide groups at room temperature which is exploited by the popular combination of MTS with the heterobifunctional cross-linker *N-gamma-maleimidobutylryloxy succinimide ester* (GMBS). The molecular structure of MTS and GMBS is illustrated in figures 3.11 and 3.13.

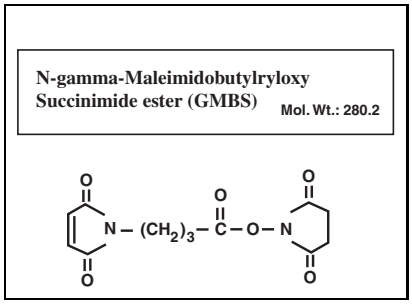

Figure 3.13: N-gamma-Maleimidobutylryloxy Succinimide ester (GMBS)

After thorough cleaning of the glass as described above, MTS is applied to the glass surface. After curing, the GMBS cross-linker is passed over the MTS layer and the maleimide group of the GMBS binds to the thiol group of MTS. Finally, the amino groups in lysine amino acids of antibodies (as well as any secondary amino

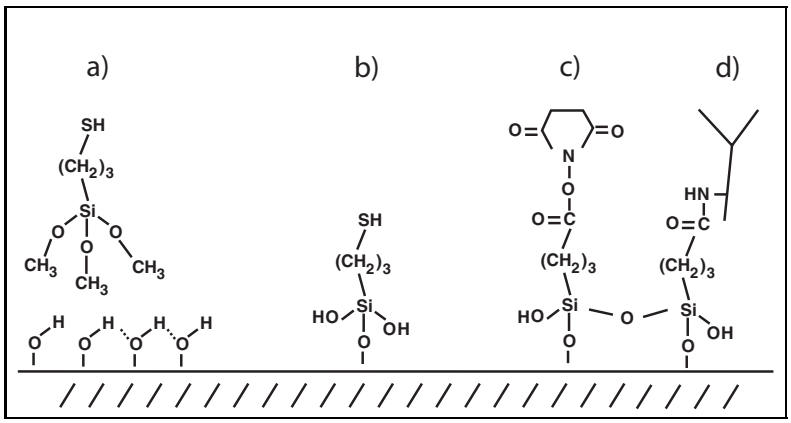

Figure 3.14: The 4 steps of the coating: The free MTS molecule (a), the silane attached to the surface (b), the cross-linker GMBS extended the functional arm of the silane (c) and the antibody bound to the NHS group of GMBS (d).

group of other proteins) react spontaneously with the succinimide ester group of GMBS. All the chemical bonds, illustrated in figure 3.14, form spontaneously at room temperature.

Protocol

The following detailed protocol for the surface coating has been applied to the capillaries for all the experiments presented in chapter 4. It is derived from *Shriver-Lake et al.* (1997) and *Bhatia et al.* (1991):

1. The capillary is flushed with a 2.5% solution of MTS in toluene at 5 bar for 1 hour.
2. Then the capillary is rinsed with 100% toluene for 30 minutes at 5 bar and then blown dry with argon at 5 bar for 30 minutes.
3. It follows an over-night (16 hours) curing at 100 °C in vacuum ($\leq$ 5 mbar).
4. Then the GMBS cross-linkers are dissolved in a minimum amount of dimethylformamide (DMF) and diluted to a 2mM solution with pure (100%) ethanol. The cross-linker solution is continuously pumped through the capillary at 5 bar for 1 hour at room temperature.
5. Now, the capillary is rinsed thoroughly with phosphate buffered saline (PBS) at pH 7.4 (5 bar for 10 minutes).
6. Immediately afterwards, the capillary is filled with 0.1 mg/ml to 0.5 mg/ml antibody in PBS and incubated for 1 hour at room temperature. Slow pumping of the antibody solution avoids antibody depletion zones in the inner capillary volume.

7. Then again, the capillary is rinsed thoroughly with PBS as in step 5.
8. Finally the capillary is flushed with 2% BSA in PBS pH 7.4 for 3 hours to block free unspecific binding sites on the surface.
9. After another quick rinse with PBS, the capillary is ready to be used for the CHIP assay.

Capillaries prepared in the described way were stored at 4°C, filled with PBS buffer, for a maximum of 5 days.

Column Capacity Estimation

To see if an immunoaffinity column coated that way has sufficient capacity for the requirements of a capillary based CHIP assay, the following estimation has been carried out:

The coating described in this section, using GMBS as a cross-linker, results ideally in an antibody density of $100 \pm 20 \ \frac{\text{ng}}{\text{cm}^2}$. From these 25% bind their specific antigen if it is provided in excess (*Shriver-Lake et al.*, 1997). A functionality of less than 100% is mainly due to the fact that NHS-functional cross-linkers bind to any amino group of the antibody amino acids (mainly Lysins), resulting in as many upside down orientated attached antibodies as correctly attached antibodies.

The molecular weight of an antibody is $\approx 150 \ \frac{\text{kg}}{\text{mol}}$.

That gives $(100 \ \frac{\text{ng}}{\text{cm}^2}) \times (150 \ \frac{\text{kg}}{\text{mol}})^{-1} \times (6 \times 10^{23} \ \frac{\text{antibodies}}{\text{mol}}) = 4 \times 10^{11} \ \frac{\text{antibodies}}{\text{cm}^2}$

The inner surface of a column of 60 cm length and 75 μm inner diameter is $\pi \times 75 \ \mu\text{m} \times 60 \text{ cm} = 1.41 \text{ cm}^2$.

Hence a column with such a coating has $0.25 \times (4 \times 10^{11} \ \frac{\text{antibodies}}{\text{cm}^2}) \times (1.41 \text{ cm}^2)$

$$= 1.41 \times 10^{11} \text{ active binding sites} \tag{3.2}$$

on its length of 60 cm.

3.5.2 Alternative Coatings

The following alternative coatings were tested for applicability to CHIP assays in fused silica microchannels. As described and discussed in section 2.1.5 and chapters 4 and 5, the predominant problem with CHIP assays in capillaries is the specificity of the separation, i.e. the background levels of molecules non-specifically adsorbed to

the involved surfaces. Therefore, the coatings described in this section were tested with a particular focus on this issue.

Protein A

Protein A is a 64 kD bacterial surface protein derived from the cell wall of *Staphylococcus aureus*. It contains four Fc specific binding domains for IgG antibodies (see section 2.2.2). This selective affinity for Fc regions of many mammalian immunoglobulins leaves the Fab region free for antigen binding. Thus, protein A can be used for immobilizing antibodies on solid substrates (with immobilized IgGs highly functional due to correct orientation). In fact, for certain applications, the immobilization of IgG molecules to solid substrates via protein A results in better antigen binding (*Anderson et al.*, 1997). But protein A does not bind antibodies covalently, making the coating rather unstable to changing and harsh buffer conditions. For applications where permanent attachment of antibodies is required, protein A is not the optimal choice. Protein A as a means of attaching antibodies to solid phase matrices is reviewed in *Nisnevitch and Firer* (2001) together with various alternative techniques.

Also, protein A can be used directly to purify antibodies from solution. The original CHIP assay protocol (section 2.3.3) relies on this to extract anti-GAF antibodies from chromatin.

In this work, capillaries were coated with protein A by the same chemistry as antibodies (section 3.5.1). These capillary-columns were run in parallel with antibody-coated columns and analyzed in the same way. The results are described in section 4.6.

Polyethylene Glycol (PEG)

Polyethylene glycol is known to effectively shield surfaces against adsorption of biomolecules (*Österberg et al.* (1995), *Zhang et al.* (1998), *Zhang et al.* (2001), *Piehler et al.* (1996), *Piehler et al.* (2000) and *Alcantar et al.* (2000)). To compare shielding properties of a PEG layer on glass walls to a BSA layer, PEG-silane was grafted to the inner walls of capillaries. Figure 3.15 shows the particular compound that was purchased from Shearwater Corporation, USA.

The coating procedure involves the same cleaning as GMBS-mediated antibody attachment. Then, a 5% solution of PEG-silane in anhydrous toluene was pumped through the capillaries for one hour, followed by a 30 minutes rinse with pure toluene. Before curing the coating at 100°C in vacuum for 16 hours, the capillary was blown dry with argon. The capillary was then stored filled with PBS buffer at 4°C for up to 5 days. Results are presented in section 4.6.

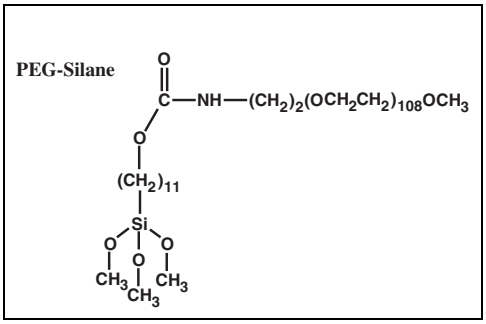

Figure 3.15: A PEG-silane with a molecular weight of ca. 5000 Dalton, from Shearwater Corporation, USA.

3.5.3 Photo-patterned Surface Coating

In the field of biosensor design there has been increasing interest in selective immobilization of macromolecules and proteins — and especially antibodies — to solid substrates in discrete patterns (see, for example, *Sundberg et al.* (1995), *Fodor et al.* (1991) and *Pritchard et al.* (1995)). The idea behind is to immobilize an array of many different types of molecules on one substrate. However, non-specific binding or physisorption is still a bigger problem than it is for a single step immobilization of only one molecular species (*Pritchard et al.* (1995) and *Conrad et al.* (1997)).

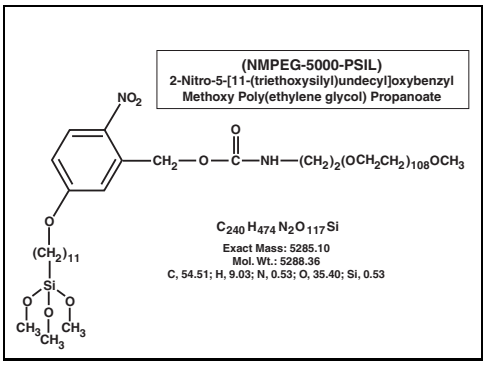

Figure 3.16: The NMPEG-5000-PSIL molecule, synthesized by David Conrad, NRL Washington, USA.

In an effort to solve that problem, *Conrad et al.* (1997) synthesized and characterized a photoactivatable PEG-silane, the "NMPEG-5000-PSIL" molecule shown in figure 3.16 (*Conrad et al.*, 1998). This compound produces an amine reactive group upon UV irradiation at ≈ 310 nm. Irradiation cleaves off the PEG polymer and leaves an activated surface bound aldehyde group that forms a stable covalent bond with antibody amino groups (*Conrad et al.*, 1997). Sodium cyanoborohydrate has to be added to the buffer to reduce the intermediate unstable bond ("Schiff bases", *Conrad*

et al. (1997) and references cited therein). The principle of this coating technique is shown in figure 3.17. The combination of the effective shielding of non-specific adsorption by a PEG layer with the covalent attachment makes this a very attractive method for designing multianalyte detection devices based on antibody arrays.

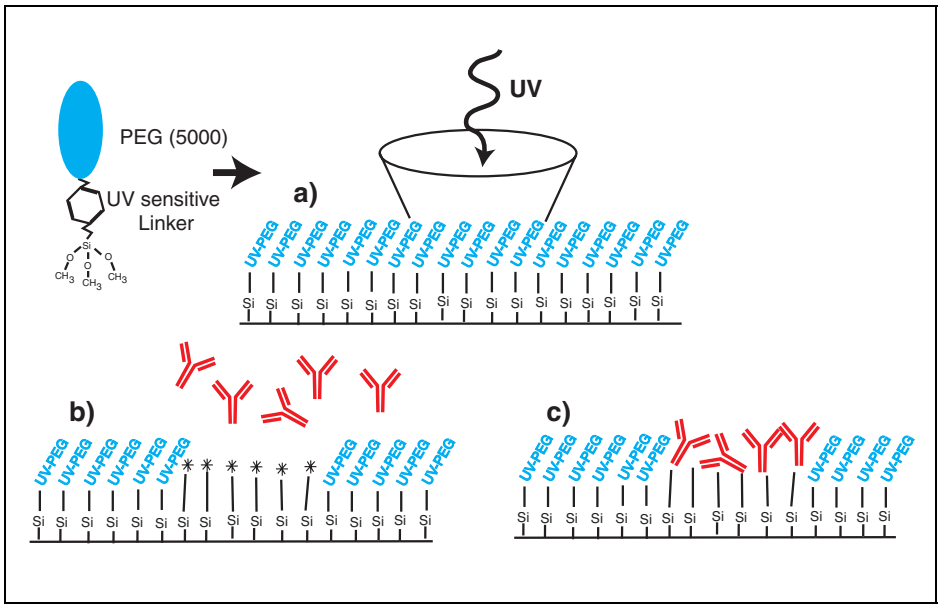

Figure 3.17: This figure schematically explains the process of creating covalently attached antibody patterns on glass using the NMPEG-5000-PSIL molecule. The remaining surface is kept inert by the PEG layer.

To evaluate the value and applicability of this technique for the purposes of a capillary based multianalyte CHIP assay (section 3.6), test coatings were carried out on coverslips. These experiments are presented in section 4.1.

The NMPEG-5000-PSIL molecule was provided by David Conrad from the Naval Research Laboratory in Washington. The compound was always handled in a dry ($\leq 15\%$ humidity) atmosphere with low oxygen content ($\leq 1\%$ O_2).

Protocol

The patterned surface coating with antibodies is prepared as follows:

The coverslips are cleaned according to a procedure involving "Piranha" solution as described in *Seehofer* (1997) and *Jönsson et al.* (1988):

1. Rinsing with 1M KOH for 10 minutes at 5 bar
2. Then rinse with water for 5 minutes at 5 bar

3. Rinsing with "Piranha Solution"[2] for 30 minutes at 5 bar.
4. Rinse thoroughly with water (> 15 minutes at 5 bar)
5. Blow dry with argon for 30 minutes at 5 bar

Then, the homogeneous layer of the photo-cleavable PEG-silane is applied by:

1. incubating 0.5 $\frac{\text{mg}}{\text{ml}}$ NMPEG-5000-PSIL in acetate buffer 0.1 M, pH 4.5 for 1 hour.
2. After rinsing thoroughly with acetate buffer, changing the wash buffer at least three times, the coverslips are cured in acetate buffer at 70°C for 16 hours (over night).
3. After curing they are thoroughly rinsed with 100% ethanol and stored in 100% ethanol for up to 2 weeks (several months are possible according to David Conrad (personal communication)).
4. To create a pattern of immobilized antibodies, the coverslips are illuminated with a microscope-coupled nitrogen laser (P.A.L.M. Microlaser Technologies GmbH, Germany).
5. It follows a quick PBS buffer rinse.
6. Then the coverslips are incubated with the antibody solution (0.5 to 1 $\frac{\text{mg}}{\text{ml}}$ fluorescently labeled antibody with 200 $\frac{\mu\text{g}}{\text{ml}}$ $NaBH_3CN$ in PBS buffer for 90 minutes.
7. Now again, the coverslips are briefly rinsed with PBS buffer before exposed to a 2% BSA solution for saturation of any remaining free binding sites for 60 minutes.
8. After another brief PBS wash, the surfaces are incubated with the fluorescently labeled antigen (200 $\frac{\mu\text{g}}{\text{ml}}$) for 1 hour.

All antibodies are labeled with Alexa dyes from Molecular Probes Europe. This is essential for further microscopy analysis since these are the only dyes that keep their activity after an incubation with the very strong reducing agent sodium cyanoborohydrate ($NaBH_3CN$).

The coverslips are analyzed by confocal fluorescence microscopy (see section 3.8).

3.6 CHIP Assay in Fused Silica Capillaries

There are two principal ways of transferring the antibody-functionalized surface required in CHIP assays (see chapter 2.3) into micrometer-sized channels to build a micro immuno-affinity column:

[2] "Piranha Solution" is 100% sulfuric acid : H_2O_2, (4:1, v:v)

One is to inject functionalized microparticles (beads) in a microchannel and keep them in place by either a frit-structure or other forces, e.g, paramagnetic beads with a strong magnet. In this case a homogeneous passivation of the channel walls is required to prevent unspecific adsorption (see section 3.5.2).

The second possibility is to functionalize the inner walls of the microchannel directly with a homogeneous antibody-layer and reduce unspecific adsorption by subsequent saturation of the remaining surface with a neutral protein (BSA, casein or milk powder).

In order to keep the hydrodynamic aspects simple and to avoid any problems with chromatin clogging in the channel the second option was chosen for this work. This also keeps the experimental setup more simple and flexible for potential integration in other microfluidic systems. The results of the following experiment which investigates the feasibility of a capillary-based low-volume immunopurification of GAF from *Drosophila* chromatin are presented in chapter 4.

The goal, as discussed in section 2.3.2 and 3.3.2, was to demonstrate the enrichment of hsp26 fragments in the eluates from the GAF chip experiment. This would confirm that this region on the *Drosophila* genome is indeed a specific binding target for GAF *in vivo*. Also, it would prove that the experimental format of a CHIP in capillaries is performing well and that the advantages of micro-scale experiments (section 2.1) can be exploited for biological research in the field of chromatin remodeling and transcription regulation (section 2.3.1).

Towards this end, the inner wall of fused silica capillaries was completely and homogeneously coated with anti-rabbit antibodies. After functionalization they were incubated with Bovine Serum Albumin or milk powder to saturate remaining free binding sites to prevent non-specific adsorption that could cause background problems in the analysis (see section 3.5.1).

Formaldehyde cross-linked and mechanically sheared chromatin was prepared and incubated with anti-GAF antibody as described in section 2.3.3 and 3.3.2.

Exactly the same reagents as used for successful large scale CHIP assays were employed (see section 3.3.2 and *Gilfillan* (2000)).

The sample was then pumped through the capillary where the complexes of rabbit-anti-GAF antibody and GAF (with associated and fixed DNA fragments) can be recognized and bound by the anti-rabbit antibodies on the channel walls. After "loading" the capillary walls (acting as stationary phase for the immunochromatographic separation, see section 2.2.2) the column was flushed thoroughly with buffer. The detergent modified RIPA buffer and the high salt contents used for this purpose have already been discussed in section 3.3.2. After washing, the column was heated to 65°C in Tris buffer to reverse the formaldehyde cross-links (section 3.3.2 and *Solomon*

and Varshavsky (1985) and *Orlando et al.* (1997)).

Now the DNA fragments are detached from their associated proteins and were eluted from the column and detected and quantified by PCR.

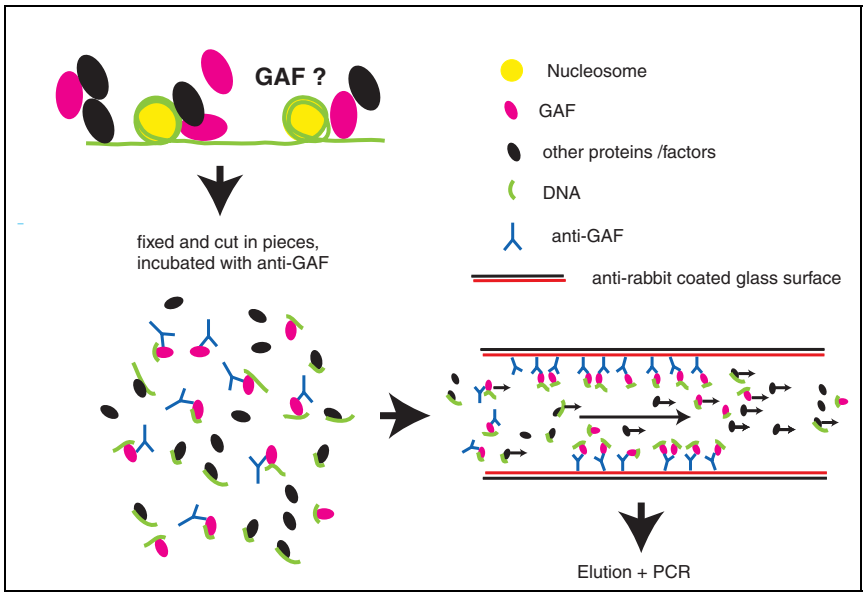

Figure 3.18: Schematic overview on the CHIP experiment in capillaries.

Figure 3.18 illustrates the idea of this experiment. An ideal CHIP experiment with a sufficiently specific and sensitive immunoaffinity column would lead to a result similar to the one sketched in figure 3.19. The aim is to demonstrate an enrichment of the DNA fragment associated to GAF ("hsp26") relative to a control sample where the ani-GAF antibody was left out and hence specific enrichment is not possible (see protocol below, step 3). An additional control was included by surveying contingent enrichment of a DNA fragment that should not be specifically accumulated by the column. The coding sequence for the TOPOII gene in *Drosophila* does not include GAF-binding regions (*Gilfillan*, 2000) and consequently cannot be fished with anti-GAF antibodies. Hence any detected fragment from that gene in the CHIP eluates accounts for non-specifically adsorbed material on the column and therefore is a good control for the specificity of the GAF immunopurification.

Parameters that will influence the outcome of these experiments are

- the pre-coating and cleaning method
- the concentration of antibody solution used in the coating step
- the capillary length (i.e. the active volume)

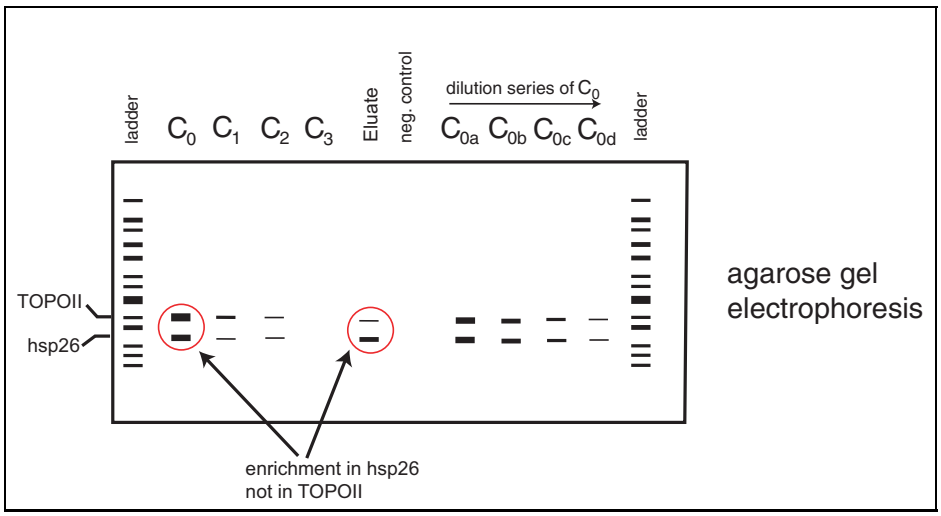

Figure 3.19: The ideal result of a CHIP assay: The figure shows a schematic agarose gel image (see section 2.4.2). Lane C_0 shows the PCR product of the sample that has been injected into the column. C_1 to C_3 show PCR products from samples that have been collected from the washing steps. The concentrations go down as not bound material gets washed out from the column. Changing to elution conditions (65°C) washes the hsp26 fragments out, increasing their concentration in the collected samples while the non-specific fragments are not enriched. An experiment with no anti-GAF antibody added to the chromatin (negative control) should not show this enrichment. The dilution series of C_0 is done in steps of $1:10$. The total concentration depends on C_0, discussed in section 3.3.1. The "ladder" is a standard mixture of DNA fragments of known size and therefore can be used as a scale to identify sample fragments.

- the concentration of chromatin pumped through the column
- the incubation flow rate / the incubation time in case of stopped flow
- number of washing steps / type of washing buffer

Protocol

To start with, a reduction of sample material from 100 μl to 3 μl was implemented. This kept the preparative handling of the samples in the range where they could be easily manipulated with standard laboratory pipettes. Also, the amount of target molecules stayed in a range that did not yet challenge PCR detection sensitivity.

The protocol for chromatin IP in capillaries is:

1. Coat a glass capillary with antibodies as described in section 3.5.1. Take capillaries with an inner Diameter of 75 μm, i.e. a volume of about 3 μl in a 60 cm column (4.4 μl/m). For the control columns, leave out the antibody and only incubate 3% BSA.

2. Adjust a 25 μl aliquot of chromatin to RIPA buffer conditions by adding 5 μl of each of the following: 10% Triton-X-100, 1% Na-deoxycholate, 1% SDS, 1.4 M NaCl. Then 2.5 μl of 0.1 M Tris pH 8.0 and 10 mM EDTA.

3. Split the resulting 50 μl in 2×25 μl (anti-GAF + and −, as control). To one of them (+ sample) add 0.5 μl of the rabbit-anti-GAF antibody. The other serves as a control (− sample). Incubate both rotating at 4 °C over night. The following steps are applied to both samples identically.

4. Dilute the chromatin 1 : 10 in RIPA.

5. Mount the columns on the fluid control manifold setup (see section 3.4.2), pre-fill them with RIPA buffer and cool them to 4°C.

6. Inject 3 μl of the chromatin 1 : 10 into each column by advancing the sample plug by 0.5 μl every 10 minutes, resulting in a total incubation time of 1 hour. The columns are cooled to 4°C during that incubation step.

7. After incubation, still at 4°C, wash the columns with

   - 125 μl of RIPA per column (50× column volume)
   - 125 μl of 500 mM LiCl buffer (500 mM, 10 mM Tris pH 8.0, 1 mM EDTA, 0.5% NP-40, 0.5% Na-deoxycholate)
   - 125 μl of 10 mM Tris pH 8.0

8. Heat the columns to 65°C for 6 hours to reverse cross-links (they're still filled with Tris buffer from the last wash step).

9. After 6 hours take 3 successive elution aliquots of 10 μl per column by pumping 3×10 μl of Tris buffer per column.

10. From these 10 μl eluates, take $1 - 4$ μl as a template for each PCR reaction and run the products on a 2% agarose gel electrophoresis (as described in section 3.7).

3.7 PCR Detection of the Target Fragments

Section 3.7.1 describes the design of the PCR primers and the adjustment of PCR parameters for the chosen target fragments. In section 3.7.2 the protocol for the agarose gel electrophoresis is given and in section 3.7.3 the details on the multiplex PCR carried out in this work are listed.

3.7.1 The Target Fragments - Multiplex PCR

For the PCR detection of hsp26 fragments (see sections 3.3.2 and 3.6) in the eluates from immunoaffinity columns or beads (chapter 4) the following primers have been designed. For the hsp26 fragment:

GAGA-Lower (G5L): 5'-CGTCGCCCAGTTCAAGCCCAGTG-3', tm=57.7
GAGA-Upper (G5U): 5'-CGCCTTGTAGCCATCGGGAACCT-3', tm=56.3

They flank a 151 bp amplicon.

A second primer pair was designed to amplify a 240 bp fragment from the region coding for the TOPOII gene. They were always added as a negative control (see section 3.6). The TOPO-primers are:

TOPO-NLower: 5'-GCAGGGGATCAATCTCAAGACC-3', tm=55.0
TOPO-NUpper: 5'-TTTTGGCTCCTTGGGCTCTTTG-3', tm=54.8

The primers have been purchased from Biospring, Frankfurt, Germany. The sequence of the amplicons as well as information on the primers used in this work are given in appendix C.

The oligonucleotide sequences have been chosen with the help of a software for primer design ("Geneskipper", developed at EMBL). Given the sequence of the target amplicon, this software calculates the melting temperatures and checks for possible secondary binding of the primer. The melting temperature T_m is the temperature where half of the primer oligos are bound to target DNA strands under reference conditions. The longer the primer, the higher T_m. Since the nucleotide-pairs G-C and A-T have different binding energies the melting temperature of a primer also depends on its sequence. The melting temperatures of a set of primers should be similar to ensure equal annealing and thus equal amplification performance. Secondary binding is unwanted annealing of the primer to sites on the DNA target other than the target priming site.

Both primer pairs were added to the same reaction volume ("multiplex-PCR"). Adding two (or more) primer-pairs to the PCR reaction results in the amplification of several products in a single reaction. Care has to be taken that sufficient resources (dNTPs, polymerase enzyme) are available to ensure that the amplification of a more numerous fragment does not deplete the resources for the reaction and suppresses the amplification of the other fragment (compare to section 2.4.3).

After the software design, optimal reaction conditions have to be determined. The

empirical optimization of the PCR protocol for the amplification of the two target sequences "hsp26" and "TOPOII" from sheared and fixed *Drosophila* chromatin, has involved the following parameters:

Primer:

6 primer pairs have been compared to find a set for both fragments that amplify comparably well from *Drosophila* genomic DNA. Both genes, hsp26 and TOPOII are single copy genes and therefore a multiplex PCR from genomic DNA should produce the same amounts of each amplicon. Figure 3.20 shows a combined search for the best set of primers and buffer (comment on the buffer: see below).

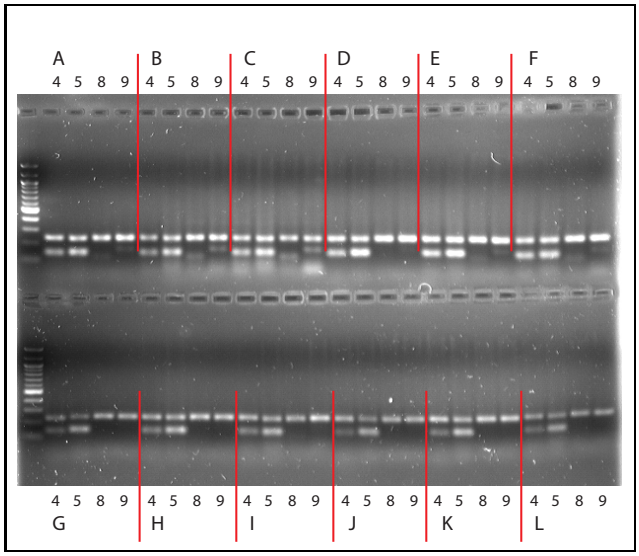

Figure 3.20: Screen for the best primer-buffer-combination. Labels 4, 5, 8 and 9 stand for different primer sets. Labels A to L stand for 12 different PCR buffer pre-mixes from the 'FailSafe"^{TM} PCR System from Epicentre, USA. The primer set that gives the strongest double-band (i.e. amplifies TOPO and hsp26 fragments equally well) is set 5. Buffers B and E perform both very good. Buffer B has been chosen for further experiments.

The 4 primer sets (no. 4, 5, 8, 9, each set contains a pair of primers for the TOPO fragments and a pair for the hsp26 fragment) are the result of a pre-selection. The other 2 primer sets that have been tested give no significant signal at all and are not included in the figure 3.20. Primer set 5 has been chosen for the CHIP experiments in this work since it shows the strongest double band (i.e. amplifies TOPO and hsp26 fragments equally well).

Cycle number:

In order to obtain a visible band on an ethidium bromide stained agarose gel from less than 100 template hsp26 fragments from chromatin ($10^{-4}\times$ dilution of the chromatin starting material, see section 3.3.1) 35 cycles were necessary.

Annealing temperature:

The best annealing temperature is usually about 5°C below T_m. The lower the annealing temperature, the faster the primers anneal, resulting in higher reaction yield. The higher the annealing temperature, the less non-specific annealing occurs, resulting in more specific amplification. The variation of the annealing temperature between 50°C and 60°C gave best results at 58°C.

Cycle times:

Duration of the individual steps within one PCR cycle is another crucial parameter. Most polymerases synthesize $\approx$ 1 kilobase per minute. And the longer a double stranded DNA fragment, the longer it takes to denature it at 95°C. Thus, the cycling protocol needs to be optimized. For this work, the extension time and the duration of the first denaturing step were evaluated.
The resulting protocol is:

1. Heating to 95°C for 5 minutes to make sure all double stranded DNA is denatured.
2. 35 cycles of
   - 20 seconds at 95°C (denaturing)
   - 30 seconds at 58°C (annealing)
   - 30 seconds at 72°C (extension)
3. 3 minutes at 72°C (for final extension of any unfinished double strand.
4. Reaction stop by cooling the tubes to 4°C

Buffer mixes:

Buffer conditions are essential for PCR amplification. The polymerase enzyme works best if for example salt concentrations are optimized. Other reaction buffer additives

influence reaction performance. To avoid unnecessary efforts, a commercial PCR buffer screening set from Epicentre, USA ("FailSafe"^{TM} PCR System, see below) was used to screen 12 different buffer conditions. One of the buffers (buffer "B") has shown the best results in the PCR and has therefore been used for the experiments (see figure 3.20.

For the reaction buffer and polymerase, the "FailSafe"^{TM} PCR System from Epicentre, USA has been used. It provides an enzyme premix with 2.5 Units/μl [3] and a set of 12 different 2× buffer premixes. The FailSafe^{TM} PCR enzyme mix is a blend containing a highly processive $5' \rightarrow 3'$ polymerase and a $3' \rightarrow 5'$ proofreading enzyme for high fidelity sequence replication. The FailSafe PCR 2× PreMix contains 100 mM $Tris-HCl$ (pH 8.3, 22°C), 100 mM KCl and 400 μM of each dNTP. The concentration of $MgCl_2$ as well as of the "FailSafe PCR Enhancer" is not given.

PCR reactions were done in a 50 μl volume. Each reaction mix consisted of 25 μl FailSafe PCR 2× PreMix "B", 1 μl of each of the 4 primers (400 nM each), 0.5 μl of the FailSafe PCR Enzyme Mix (1.25 Units) and between 1 and 4 μl template material. The volume was finally filled up to 50 μl with double distilled and sterilized water.

The PCR reactions were run on a 96 well Peltier thermocycler from MJ Research (Gradient Cycler PTC-225).

Attention has also to be payed when quantitating the PCR products from a multiplex PCR by comparing the intensities of agarose gel electrophoresis bands. Since the two amplicons compete for resources and amplification efficiency depends on the amplicon sequence, the reaction kinetics have to be taken into account. This is also discussed in section 2.4.3.

3.7.2 Agarose Gel Electrophoresis

PCR products were electrophoretically separated on agarose gels after the following protocol:

1. Boil 2% agarose in TAE buffer (see section 3.1) was in a microwave until the solution becomes clear.
2. Pour the liquid gel in a PMMA gel tray (made in house at EMBL). Let the gel polymerize. Then fill the tray with TAE buffer.
3. Mixed 10 μl from the PCR reaction volume with 2 μl of loading dye (50% ficoll buffer with a grain of orange G dye, see *Sambrook et al.* (1989) page 6.12).

[3] Unit definition: One unit of polymerase enzyme premix converts 10 nmoles of deoxyribonucleotide triphosphates in to acid-insoluble material in 30 minutes at 74°C using standard assay conditions.

4. Pipet 5 to 10 μl of this in the loading wells on one side of the gel.

5. Apply 50 volts for about 1 hour (until migration front reaches the other end of the gel).

6. Soak the agarose gel in ethidium bromide bromide solution (300 μl ethidium bromide bromide in about 300 ml of distilled water) for about 20 minutes and then destain in a 4 liter water tray on a rocking table (20 to 30 minutes).

7. Finally, place the gel in a UV transilluminator (AlphaDigiDoc^{TM} from Alpha Innotech Corporation).

8. Take images with the connected CCD camera (8 bit from Alpha Innotech Corporation, model number 8710-81001, typical aperture 5.6, exposure time 1 minute. These parameters depend very much on DNA band intensities).

A comprehensive and practical introduction to agarose gel electrophoresis is given in *Sambrook et al.* (1989), chapter 6.

3.7.3 Real Time PCR

For better quantitation of the experiments in chapter 4, real time PCR (introduced in section 2.4.3) analysis has been carried out.

All real-time PCR reactions for this work have been run on an ABI Prism ^{R} 7000 Sequence Detection System from Applied Biosystems (ABI, a PE Biosystems company). The entire process of calculating C_Ts, preparing a standard curve, and determining starting copy number is performed by the software.

The fluorescent probes were designed with the "Geneskipper" software from EMBL in the same way and according to the same general criteria as the primers (see above). In addition, there are a few particular criteria for the design of TaqMan^{R} probes (see for example *Giulietti et al.* (2001)):

- Following the recommendations from ABI, the ideal melting temperature T_m of the probes should be $\approx$ 10%grd above the melting temperatures of the primers. To prevent non-specific binding and dimer-formation between the probes and the primers, a compromise was found with T_m of the probes $\approx$ 5%°Cabove T_m of the primers.

- There must not be a G at the 5' end of the probe. This is the end where the reporter dye is attached and a G in the first position would quench the fluorescence permanently due to its optical properties.

- The probe should contain more G than C bases (*Giulietti et al.*, 2001).

As reporter dyes at the 5' end of the oligomer, VIC (™ by PE Biosystems) and 6FAM (6-carboxyfluorescein) were chosen. The quencher dye was TAMRA (6-carboxytetramethylrhodamine) for both probes.

The probes are:

TaqMan probe "topo TaqMan":
VIC-5'-TCC CAG ATC CCG ATG GAG AAC CCG T-3', tm=60.7

TaqMan probe "hsp26 TaqMan":
6FAM-5'-CAT GGT CGT CCT GGC GTT CCT CA-3', tm=62.0

Primer TOPO-L-Taq, replacing TOPO-NL:
5'-TTA AGT CAA TGG GAG GCG GA-3', tm=54.8

The probes positions on the amplicon sequence are given in appendix C.

3.8 Laser Scanning Confocal Microscopy

Confocal microscopy is a technique that primarily offers the possibility of removing the out of focus background from fluorescence microscopy images from thick specimen. It also has increased optical resolution compared to conventional epifluorescence microscopes. Another powerful application of confocal microscopy is the reconstruction of a 3-dimensional image from a series of primary images taken at different focal planes of a thick specimen (such as e.g. cells). In modern confocal microscopes, lasers are used for fluorescence excitation. Laser Scanning Confocal Microscopy (LSCM) is an established tool for obtaining high resolution images and 3-D reconstructions of fluorescent specimen.

The basics of confocal microscopy were developed by *Minsky* (1961). *Wilson* (1990) gives an extensive technical and historical introduction in the method. An application-oriented introduction to confocal microscopy in biological research is given by *Stevens et al.* (1994). For quick information, the URL *http://micro.magnet.fsu.edu/primer/resources/confocal.html* can be recommended.

3.8.1 What is Laser Scanning Confocal Microscopy?

In LSCM, an expanded laser light beam is focussed by an objective lens onto a small spot of a fluorescent specimen. Through a x-y deflection mechanism this beam can be scanned over the specimen. The mixture of reflected light and emitted fluorescent light is captured by the same objective and is focused onto a photodetector (photomultiplier) via a dichroic mirror (beam splitter). The reflected light is deviated by the dichroic mirror while the emitted fluorescent light passes through and reaches the photomultiplier. A confocal aperture (pinhole) is placed in front of the photodetector, such that the fluorescent light from points on the specimen that are not within the focal plane (the so called out-of-focus light) will be blocked by the pinhole. In this way, out-of-focus information from above and below the focal plane is greatly reduced. This becomes especially important when dealing with thick specimens. A simple arrangement of a LSCM illustrating the confocal principle is shown in figure 3.21.

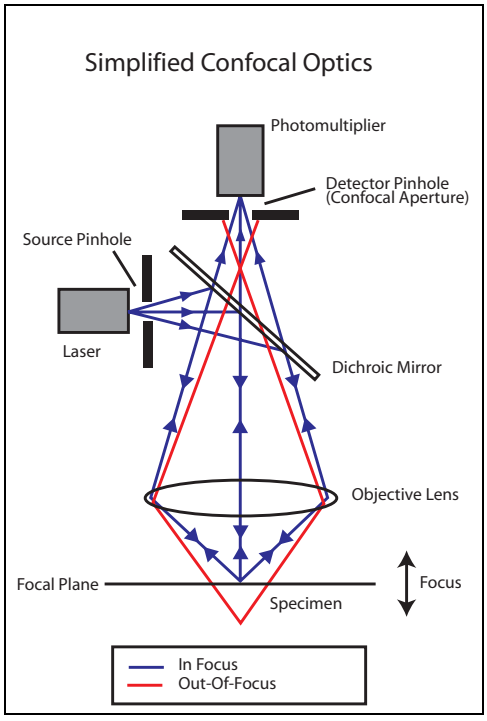

Figure 3.21: A simplified presentation of the confocal principle in LSCM.

A 2-D image of the specimen is generated by performing a raster sweep of the specimen at the focal plane. This pixel-based image is displayed on a computer monitor attached to the microscope. The relative intensity of the fluorescent light, emitted from the illuminated spot, corresponds to the intensity of the resulting pixel

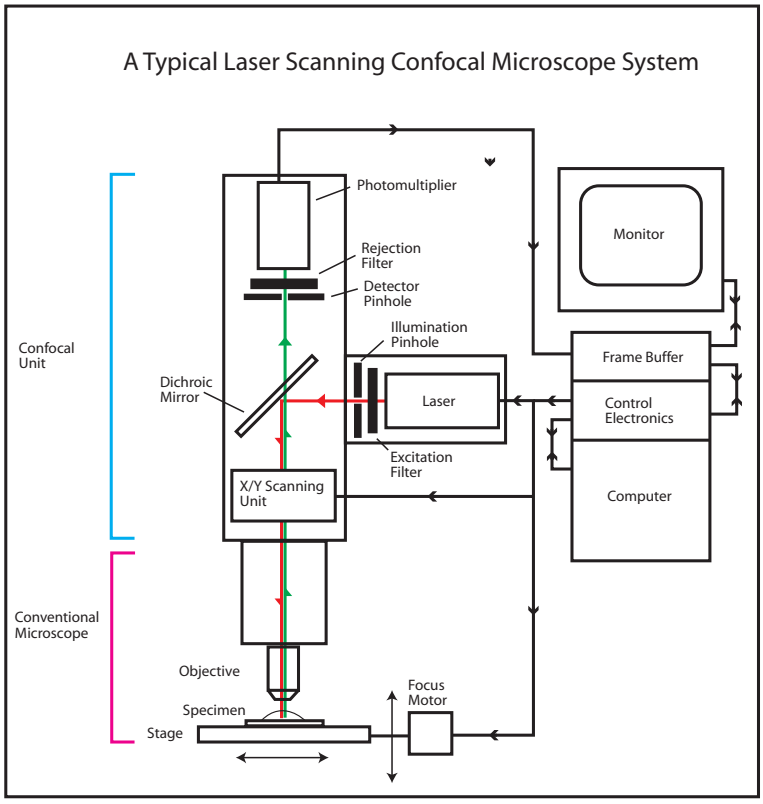

Figure 3.22: A general setup of a LSCM system.

in the image (typically 8-bit greyscale). The plane of focus (Z-plane) is selected by a computer-controlled fine-stepping motor which moves the microscope stage up and down. A 3-D reconstruction of a specimen can be generated by stacking 2-D optical sections collected in series.

The general setup of an LSCM system is shown in figure 3.22. It should be noted that most laser scanning confocal microscopes consist of a confocal unit attached to a conventional fluorescence microscope.

3.8.2 Fluorescence Imaging of the Labeled Glass Coatings

In the presented work, laser scanning confocal fluorescene microscopy was employed to image fluorescently labeled antibodies which were covalently attached to glass surfaces. Simultaneously, the adsorption of specific antigen or non-specific material to these glass surfaces was monitored. The main reason to use LSCM for control experiments in this work is that confocal pixel-oriented image acquisition is the only possibility to map the 3-dimensional curved inner surface of a fused silica glass capil-

lary (see sections 4.1 and 4.2). Also, the high optical resolution of a confocal system allows to observe very small features (i.e. possible defects) of the antibody-coatings.

For the detection of fluorescently labeled surface coatings as well as for the detection of immobilized antigen on the antibody coated surfaces a Zeiss LSM 510 confocal microscope from the Advanced Light Microscopy Facility (ALMF) at EMBL was used.

Chapter 4

Experiments

This chapter describes the experiments that have been carried out to investigate the feasibility of a chromatin immunoprecipitation experiment from *Drosophila Melanogaster* in micrometer-scaled channels.

The sections of this chapter follow the logical path of modifying an existing method, starting with the evaluation of the basic glass coating chemistry and then moving step by step from the protein A agarose beads to the final goal of a CHIP assay in antibody-coated glass capillaries. Section 4.1 presents the qualitative results that were obtained from coating antibodies on coverslips in photo-patterned structures. Section 4.2 discusses the coating quality from a semi-quantitative fluorescence image analysis of homogeneously antibody-coated capillaries. Section 4.3 gives the PCR analysis data from eluates of a "classical" CHIP experiment with protein A agarose beads (see section 2.3.3) carried out by Gregor Gilfillan at the University of Munich. (The eluates were re-analyzed for the presented work.) Section 4.4 describes the results from a CHIP assay experiment with paramagnetic beads in reaction tubes (see section 3.3.2). The results of an immunoprecipitation in capillaries to purify a biotinylated DNA fragment from non-biotinylated fragments are given in section 4.5. For this purpose, anti-biotin antibodies were attached to the capillary-column. This experiment verifies the functionality of the fluidic setup with a very simple separation task. The following section 4.6 discusses the CHIP assay experiments in capillaries as described in section 3.6.

4.1 Experiment 1 - Covalently Immobilized Antibody Patterns on Glass

In this section, the photo-patterned attachment of fluorescently labeled antibodies, as discussed in section 3.5.3, is presented. The substrates were coverslips for cell culture applications (CELLocate, Eppendorf, Germany). They were prepared as described in section 3.5.3.

The antibody concentration for attachment was 0.5 and 1 $\frac{mg}{ml}$ fluorescently labeled rabbit anti-goat antibody (#9, see section 3.1) in PBS buffer. As a control, BSA is added to one sample instead of the antibody #9. The antigen was a goat anti-mouse antibody (#8) that is specifically recognized by the first, surface-bound antibody. As a control, one coverslip was incubated with a rabbit anti-mouse antibody (#6, see section 4.1).

The images were acquired by confocal microscopy (section 3.8).

The results clearly show that there is very little unspecific binding and the little ring-shaped patches show functional antibodies that specifically recognize the target they are designed for.

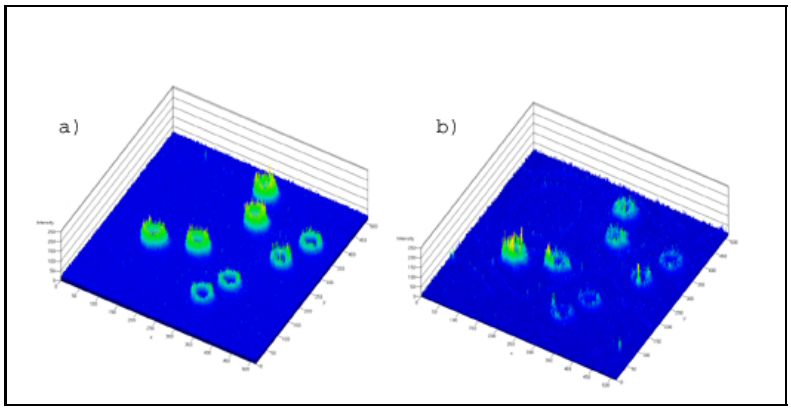

Figure 4.1: Left: 0.5 $\frac{mg}{ml}$ immobilized rabbit-anti-goat antibody, right: specific antigen, goat-anti-rabbit antibody

The following gives an overview on the analysis of five representative coverslips. In the figures 4.1, 4.2, 4.3, 4.4 and 4.5, the left intensity plot (a) shows the fluorescence signal in the green detection channel. In green, the Alexa 488 labeled antibody that was attached to the glass surface is detected. Figure 4.4 shows the control where no antibody was attached to the glass. The right plot (b) shows the fluorescence signal of the red channel (which detects the specific and non-specific probes labeled with Alexa 546).

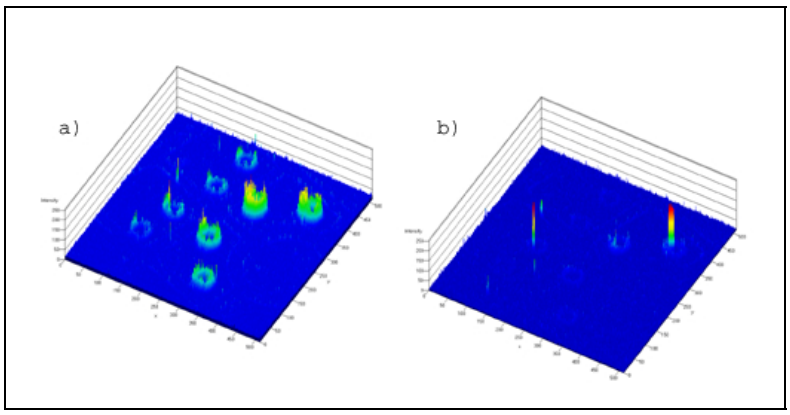

Figure 4.2: Left: 0.1 $\frac{\text{mg}}{\text{ml}}$ immobilized rabbit-anti-goat antibody, right: specific antigen, goat-anti-rabbit antibody

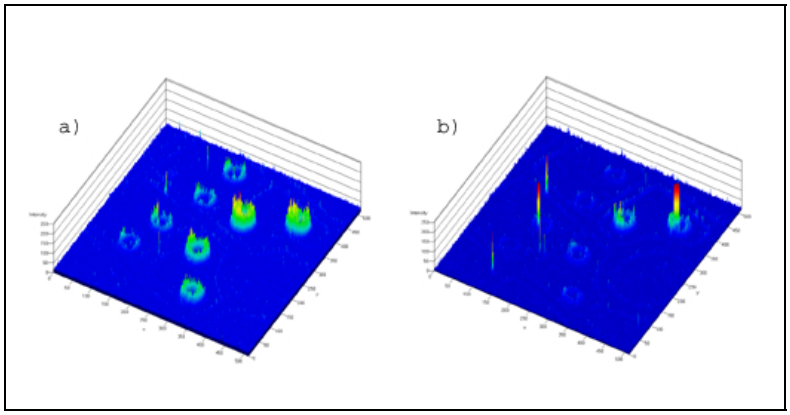

Figure 4.3: Same as figure 4.2, but red excitation laser turned up → more signal.

Figure	attached	conc.	probe		green laser	red laser
4.1	ab#9	0.5 $\frac{\text{mg}}{\text{ml}}$	ab#8	specific	fix	fix
4.2	ab#9	0.1 $\frac{\text{mg}}{\text{ml}}$	ab#8	specific	fix	fix
4.3	ab#9	0.1 $\frac{\text{mg}}{\text{ml}}$	ab#8	specific	fix	turned up
4.4	BSA	0.5 $\frac{\text{mg}}{\text{ml}}$	ab#8	—	fix	fix
4.5	ab#9	0.5 $\frac{\text{mg}}{\text{ml}}$	ab#6	non-specific	fix	fix

Antibody #9 (ab#9) specifically recognizes ab#8, but not ab#6. ab#8 and ab#6 are both labeled with the same dye (Alexa 546) and always applied in the same concentration (0.2 $\frac{\text{mg}}{\text{ml}}$ in PBS). For antibody and dye specifications see section 3.1.1.

From these pictures, although not quantitatively analyzed, the contrast between

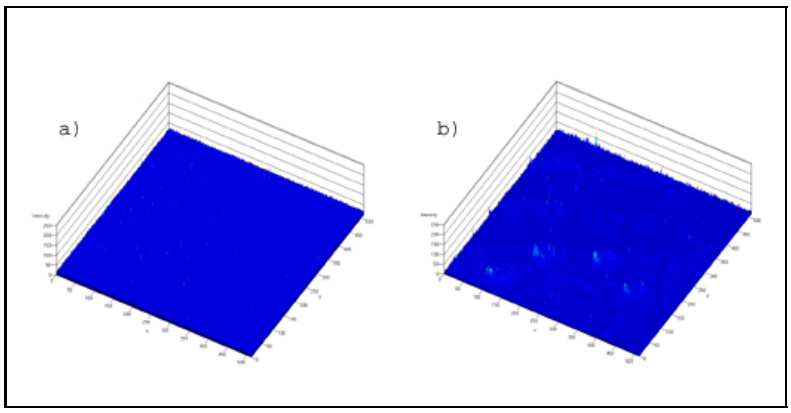

Figure 4.4: Left: 0.5 $\frac{\text{mg}}{\text{ml}}$ immobilized BSA, right: specific antigen, goat-anti-rabbit antibody

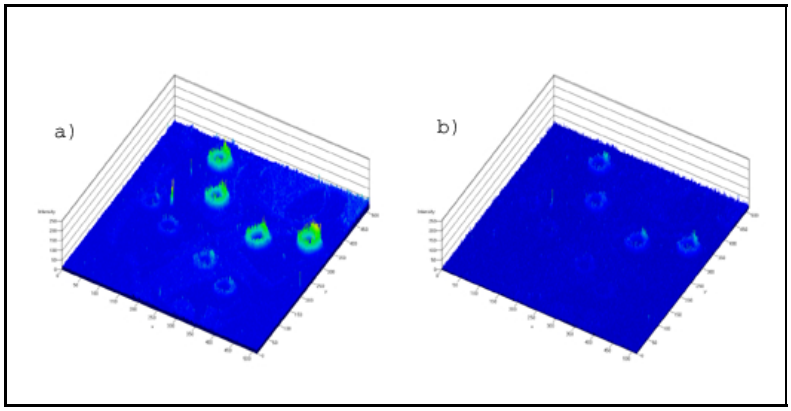

Figure 4.5: Left: 0.5 $\frac{\text{mg}}{\text{ml}}$ immobilized rabbit-anti-goat antibody, right: non-specific antigen, rabbit-anti-mouse antibody

the specific patterns and the rest of the surface is remarkable. This indicates that non-specific binding is effectively prevented by the PEG layer (see section 3.5.3).

As can be seen in the figures, the sample substrates have been UV-irradiated on 8 circular patches. 4 of them form a half-circle and the other 4 are positioned in a straight line. The 4 rings arranged in a half-circle have been irradiated with 20% higher laser power compared to the 4 straight circles. They show stronger specific signal. At the same time though, they also clearly show higher signal from the non-specific probe. This is likely to be due to coating damage from the laser.

After this successful evaluation of the coating technique developed by *Conrad et al.* (1997), further work was concentrated on the homogeneous coatings described in section 3.5.1. Yielding much larger active antibody surfaces, they were considered more useful for the initial proof of concept of a CHIP assay in capillaries where detection limits are a major issue (see section 3.3.1 and 4.6).

4.2 Experiment 2 - Confocal Fluorescence Imaging of the Covalently Immobilized Antibodies in Capillaries

The geometrical constraints of the round fluid-guiding channel in a capillary complicate the surface examination, i.e. the analysis of the applied coating. Most suitable surface analytical techniques for biomolecular surface modifications such as for example surface plasmon resonance (SPR, recently reviewed by *Green et al.* (2000)), scanning probe microscopy (SPM, see for example *Garrison and Ratner* (1997)), reflectometric interference spectroscopy (RIfS, *Gauglitz et al.* (1993)) and other optical methods (reviewed by *Brecht and Gauglitz* (1995)), require flat samples.

A simple and common method for monitoring specific and non-specific binding that is sufficiently flexible in terms of accessibility of the surfaces is fluorescence microscopy (see e.g. (*Alcantar et al.*, 2000)). In this work confocal scanning microscopy (see section 3.8) was chosen to image the density of antibodies and specific as well as non-specific probe molecules (in this case also antibody proteins) on the inner walls of 75 μm ID fused silica capillaries.

To test the homogeneous attachment of antibodies to the capillary walls as described in section 3.5.1, fluorescence intensity measurements of immobilized labeled antibodies were carried out.

Two experiments were performed, one for analysis of antibody attachment based on non-cured silane layers (curing is discussed in section 3.5.1) and one involving cured silane layers. The coating was done according to the protocol described in section 3.5.1.

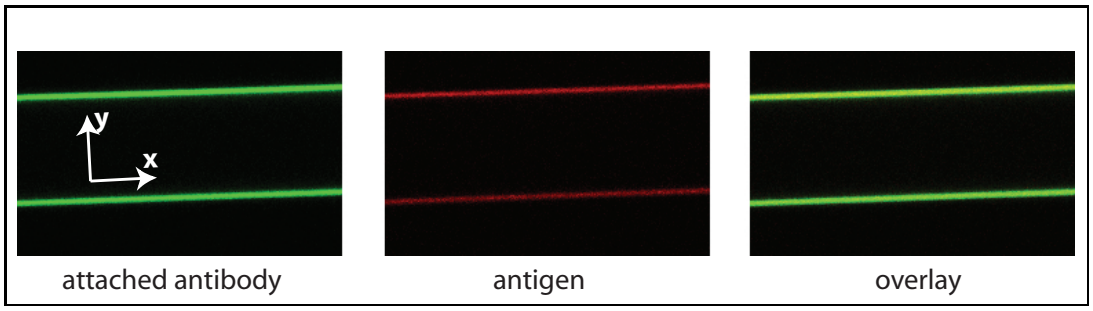

Figure 4.6: Fluorescence image of the cross-section of a capillary that was coated with labeled antibodies. The attached antibody (Alexa 488) is shown in green and the antigen (Alexa 546) in red. The overlay shows the co-localization of antibody and antigen.

The antibodies attached to the glass were antibodies #11. This is a goat-anti-rabbit antibody labeled with Alexa 488 (see section 3.1).

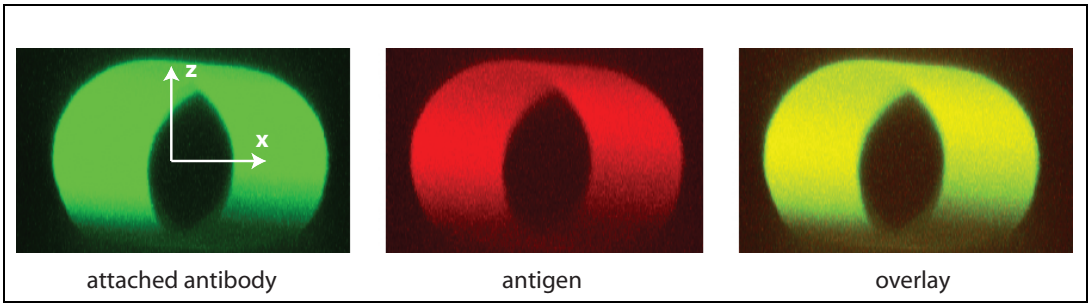

Figure 4.7: 3D reconstruction of the inner capillary surface coating based on images as shown in figure 4.6. The fact that the surface is not mapped on the full circumference is not due to missing fluorescent coating at the bottom. The missing signal is caused by optical refraction of the excitation and emission light at the capillary surface (outer and inner). The presented capillary shows a smooth coating all around the channel wall as was verified by rotating the capillary on the microscope stage.

Before placing the samples on the object table of the confocal microscope (Zeiss LSM 510, see section 3.8), the polyimide coating on the outside of the fused silica capillaries was etched off with concentrated nitric acid on the length of $\approx$ 5 mm. The obtained transparent window was rinsed with water and polished with ethanol (see *Lindberg and Roeraade* (1998)).

On the microscope, a stack of images from each sample was taken. Figure 4.6 shows an example of one slice of the image-stack, approximately from the "equatorial" plane of a capillary. The two channels are displayed separately and an overlay is displayed to show co-localization of the signals. Figure 4.7 shows a 3D-projection of the whole image stack, giving an impression of the quality and homogeneity of the surface coating within the limits of the optical resolution of the confocal microscope. The fact that the projection does not show the full round of the channel wall (bottom part of the projections in figure 4.7) is due to the refraction of the laser light on the round capillary walls (inner and outer walls) and does not represent coating defects. This was verified by rotating the capillary under the microscope.

The software of the Zeiss LSM 510 microscope includes a tool to extract pixel intensities along a selected line and to save the data in a table. A screen-print of this function is shown in figure 4.8. Fluorescence pixel intensities were taken from 7 slices around the equatorial plane ($1 \pm 3 = 7$ planes) and averaged. The averages include at least 2800 data points from the same capillary wall. To compare these data between individual capillaries it has to be stressed that the microscope settings (and especially the laser intensities) were kept constant throughout all measurements. Also, the specific antigen and the non-specific probe molecule were labeled with the same dye and were applied in the same concentrations to give comparable signals.

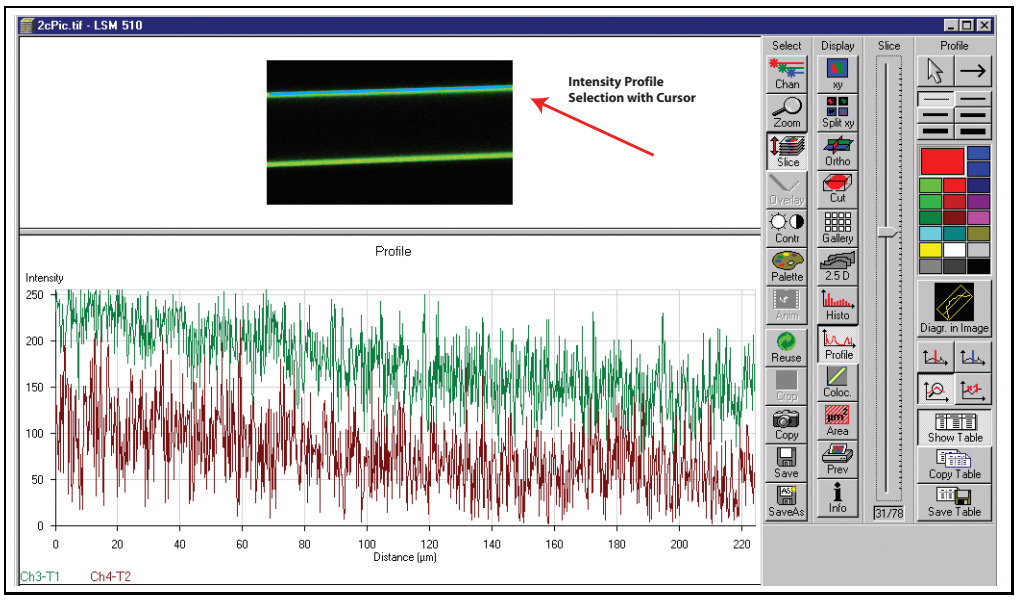

Figure 4.8: The software extraction of pixel intensities (LSM 510, Zeiss, Jena).

a) A Not Cured Silane Layer

Capillaries were prepared according to the protocol given in 3.5.1. The antibody that was attached to the glass (antibody #11, see section 3.1) was applied in 0.1 mg/ml concentration according to the protocol. After coating, a solution of 0.1 mg/ml antibody #6 (used as specific antigen, see section 3.1) was pumped through one capillary for 1 hour. A second capillary was incubated with 0.1 mg/ml antibody #8 (non-specific for antibody #11) for the same time. A third capillary was prepared with no antibody but only BSA attached to the wall as a control (2% BSA in PBS instead of the antibody solution). This capillary was also flushed with 0.1 mg/ml antibody #8 for 1 hour. Finally all 3 capillaries were rinsed with PBS buffer.

Figure 4.9 shows the average values (calculated as described above) of specific versus non-specific signal. The data show significantly more specific binding than non-specific adsorption. The specific signal is 145.8 ± 46.4 (in arbitrary units). The non-specific signal is 37.5 ± 29.7. The control signal is 22.1 ± 23.9 showing that the non-specific binding does not depend on the particular molecular species attached to the glass wall.

However, in the projection presentation of the data it is clearly visible that the non-specific adsorption of molecules is caused to a considerable proportion by coating defects. The signal in the red channel in figure 4.10 shows the non-specific signal in a capillary with such defective coating. The overlay reveals that non-specific adsorption is concentrated on the areas where also inhomogeneities in the signal of the attached

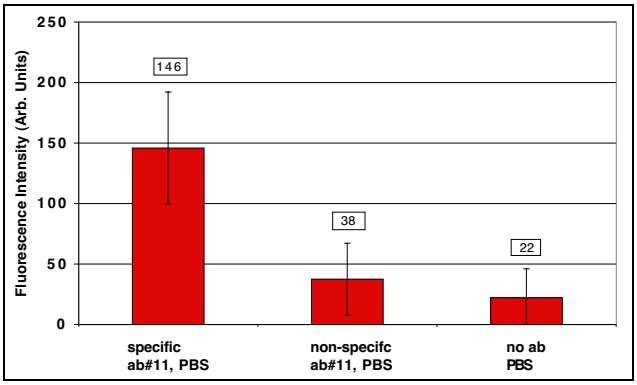

Figure 4.9: Specific and non-specific binding to antibody coated capillary walls. The silane layer in this experiment was not cured. Significantly more specific binding (left) compared to non-specific binding (middle and right) is evident.

antibody are visible.

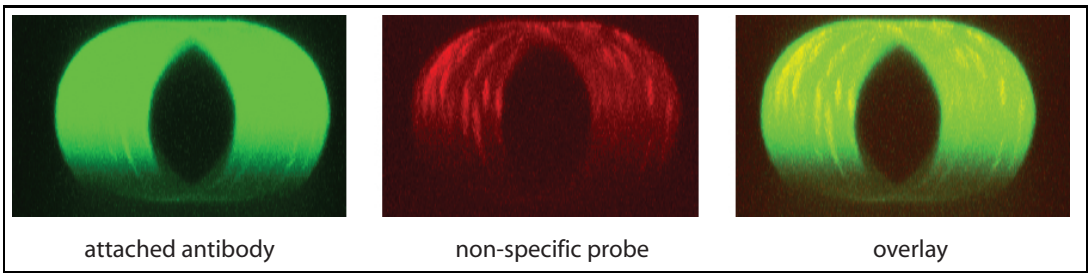

Figure 4.10: An example for coating defects causing non-specific binding. The red channel (middle) shows patches of non-specific signal. The overlay reveals that they are co-localized with the inhomogeneities in the antibody layer.

According to the discussion in the literature (see section 3.5.1) these inhomogeneous layers should get improved by including a temperature curing step in the silanization step.

b) A Cured Silane Layer

Capillaries were again prepared according to the protocol given in 3.5.1. This time the silane layer that forms the basis of the coating was cured according to the protocol in section 3.5.1.

Antibodies #11 and #12 were applied in 0.5 mg/ml concentration. BSA was applied in a 3% solution in PBS. After coating, solutions of 0.1 mg/ml antibody #6 (specific antigen) and 0.1 mg/ml antibody #8 (non-specific for antibody #11) were pumped through the capillaries for 1 hour. Finally, the capillaries were rinsed with RIPA buffer

to ensure the same treatment as during the CHIP assays in capillaries (section 3.6 and 4.6). PBS washing was applied to a subset of the capillaries for comparison.

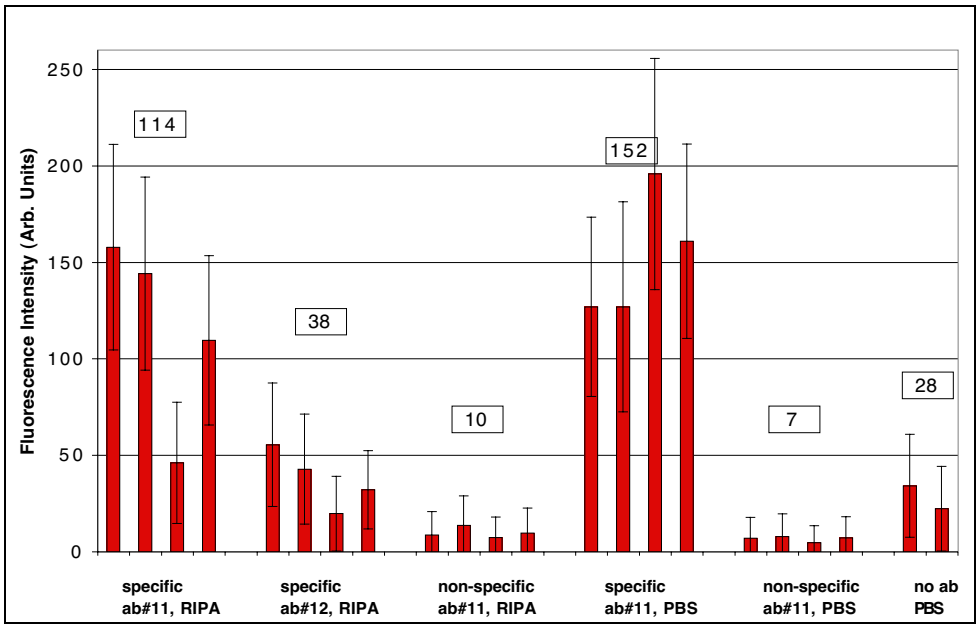

Figure 4.11: The 4 bars in each group stand for 4 independent capillaries per group. The overall averages are given in the boxes next to each group.

In figure 4.11 the average fluorescence intensities of specific and non-specific probes are presented. Antibody #11 -coated capillaries show more specific binding than antibody #12-coated capillaries. The specific signal is 114 ± 50 (for the RIPA washed capillaries, in arbitrary units). The non-specific signal for the RIPA washed capillaries is 10 ± 10. For PBS washed capillaries the respective values are 152 ± 50 (specific) and 7 ± 6 (non-specific). Also, antibody-coated capillaries show less non-specific binding than capillaries where the attached antibody was replaced by BSA. Non-specific binding as well as specific binding also depend to some extend on the washing buffer.

Furthermore, figure 4.12 shows that the cured silane layer, in combination with higher antibody concentrations in the incubation step for attachment (0.5 mg/ml instead of 0.1 mg/ml), results in less inhomogeneities than the not cured silane layer. The 3 images from 3 different capillaries show only few speckles of non-specific signal. The sharp contours of the bright spots in the two left images suggest that these defects come rather from scratches in the glass than from poor coating quality.

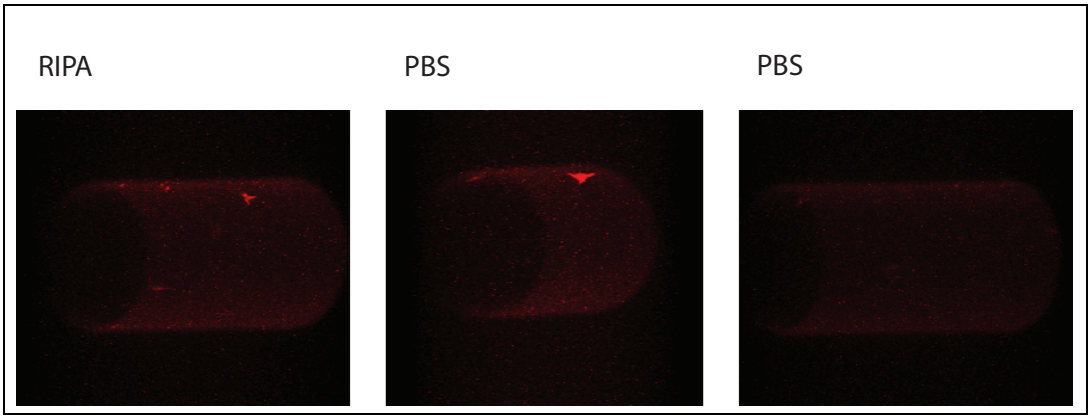

Figure 4.12: Fluorescence signal of non-specifically adsorbed material on capillary walls with covalently attached antibodies. The silanization of the glass surfaces involved curing (see section 3.5.1). There was no significant influence of the used wash-buffer (PBS or RIPA).

4.3 Experiment 3 - CHIP with Protein A Agarose Beads in Reaction Tubes

A large-scale CHIP assay according to the original protocol published by *Cavalli et al.* (1999) (see section 2.3.3) was carried out by Dr. Gregor Gilfillan (University of Munich) and the eluted DNA was re-analyzed by the author using the PCR protocols described in section 3.7.

There were 4 samples: 2 independent immunoprecipitation (IP) experiments (1 and 2) and each with a negative control (where the anti-GAF antibody was left out in the chromatin preparation, see section 2.3.3 and 3.3.2). Hence, there were 4 PCR reactions: 1+, 1−, 2+ and 2−.

From a successful experiment, i.e. enrichment of hsp26 fragments but not of the control TOPO fragments (see section 3.3.2 and 3.7.1), one would expect more hsp26 PCR product in the "+" samples compared to the "−" samples, while the TOPO product should show no enrichment.

PCR and Agarose Gel Electrophoresis

From each of the 4 samples 1 μl was taken and added as template to a 50 μl PCR reaction as described in section 3.7.1. The products were separated on an agarose gel (see also section 3.7.2) which is shown in figure 4.13. The running direction (R) of the gels (in all figures presented in this work) is always top-to-bottom.

The first lane shows the DNA weight marker ("ladder") that indicates where which

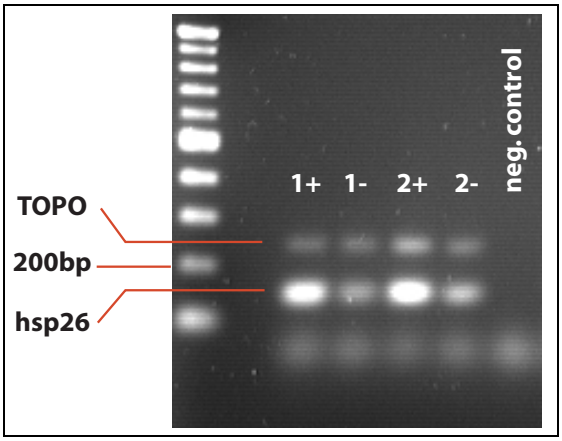

Figure 4.13: PCR products from protein A agarose bead-CHIP eluates, separated by agarose gel electrophoresis. The hsp26 fragment is significantly enriched in the "+" samples compared to the "−" samples. TOPO shows no enrichment.

DNA fragment size can be expected on the gel. The band with 200 basepair (bp) long fragments is labeled, and relative to this the bands of the target hsp26 fragment and the control TOPO fragment (151 bp and 240 bp in size, respectively) were identified. On the right of the 4 sample lanes, a negative control was added, i.e. a PCR reaction to which no template was added and therefore no product is expected.

From comparing the intensities of the bands it is evident that both IP experiments show enrichment of hsp26. The control fragment TOPO is not enriched. A more quantitative analysis is presented in the following.

Semiquantitative Analysis with NIH Image Software

The pixel intensities from the agarose gel image were analyzed with the "Gel Plotting" macro of the *NIH Image*[1] image analysis software.

Figure 4.14 shows the intensities of the individual bands as obtained from *NIH image* software. The intensity numbers correspond to the area under the plot curves. The plots are obtained by averaging the pixel intensities along the direction perpendicular to the running direction of the gel and then plotting them along the running direction. An enrichment of ≈ 5 fold (IP number 1) and ≈ 5.5 fold (IP number 2) in hsp26 is found. It is important to note that this is a minimum value of the relative enrichment. This is due to the fact that the strong bands in figure 4.13 are "saturated". The

[1]NIH Image is a public domain image processing and analysis program for the Macintosh. It was developed at the Research Services Branch (RSB) of the National Institute of Mental Health (NIMH), part of the National Institutes of Health (NIH). See http://rsb.info.nih.gov/nih-image/about.html

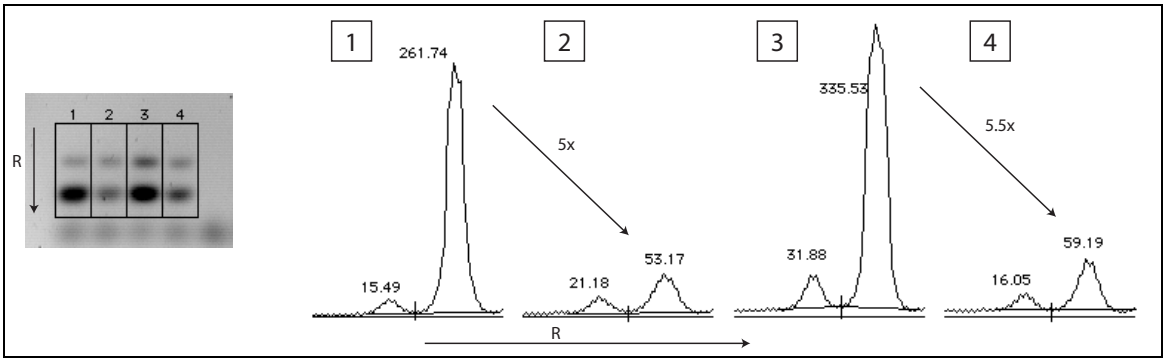

Figure 4.14: Band intensity analysis of PCR products on an ethidium bromide stained agarose gel ("Gel Plotting" macro from *NIH Image* software).

intensities have the value of 255 on a wide range of the band indicating saturation of the 8 bit CCD chip in the camera. The real intensity value, passing out of the detectable range, would reveal a higher or at least the same enrichment. Instead of upgrading the camera to 16 bit, the step to real time PCR was chosen to improve these data. They are presented in the following paragraph.

Real Time PCR Results

A real time PCR amplification of the CHIP eluates from all 4 IP experiments discussed in this section was performed on an ABI Prism 7000 Sequence Detection System. The experiment is explained in section 3.7.3. 1 μl template was added to each reaction.

The results are summarized in figure 4.15. They confirm the semi-quantitative agarose gel analysis. But it is clear that saturation of the gel images (and possibly plateau phase effects of the PCR, see section 2.4.3) have covered the real numbers of starting material.

Real time PCR analysis reveals a 9.5 fold enrichment in experiment IP 1 and 5 fold in experiment IP 2 of the "classical" CHIP with protein A agarose beads. There is no significant enrichment of the non-specific control TOPO fragments. The signal-to-noise ratio (specific hsp26 to non-specific TOPO signal) takes values between 4 and 7.

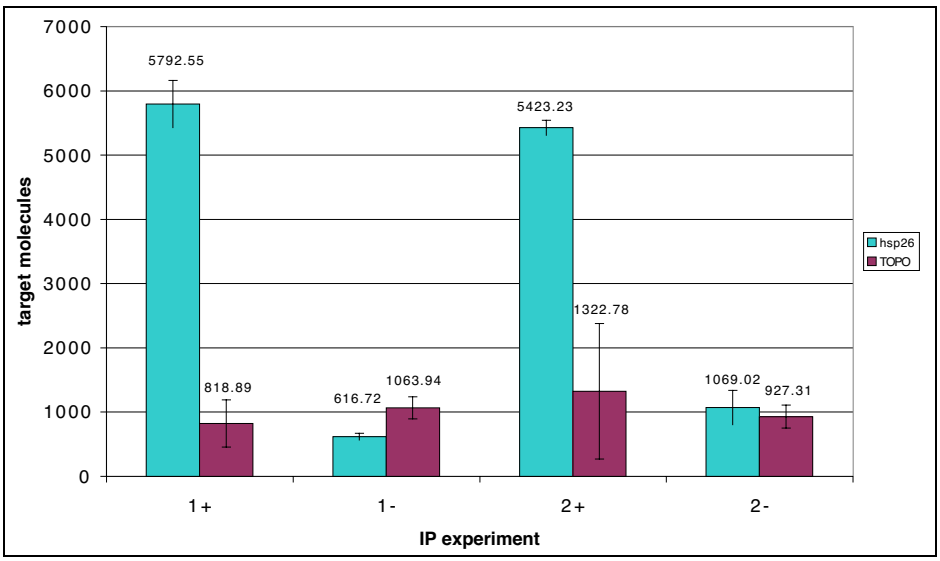

Figure 4.15: Real time PCR analysis of the large-scale CHIP with protein A agarose beads. Enrichment of hsp26 in IP 1+ versus 1− (9.5 fold) and 2+ versus 2− (5 fold). TOPO enrichment is not significant. Signal to background (specific to non-specific) ratios are 4 to 7. Values are averages from 3 identical real time PCR reactions. Error bars are standard deviations.

4.4 Experiment 4 - CHIP with Magnetic Beads in Reaction Tubes

The "classical" CHIP assay with protein A agarose beads presented in the previous section was repeated with paramagnetic "Dynabeads" as specified in detail in section 3.3.2. This experiment was required to verify that minor modifications to the protocol did not adversely affect IP performance. Modifications from the originally published CHIP protocol (appendix B) were: The protein A pre-cleaning step of the chromatin sample prior to anti-GAF incubation and proteinase K treatment of the IP eluate before formaldehyde cross-link reversal were left out for practical reasons (compare protocols in appendix B and in section 3.3.2). Also, this was the first CHIP assay with the same buffers and samples from the same chromatin preparation as was used for the later capillary experiments. Thus, the experiment presented in this section served a positive control experiment for these later experiments.

6 assays were carried out: 3 independent immunoprecipitation (IP) experiments (1, 2 and 3). Each of these 3 was done with a negative control in parallel (where the anti-GAF antibody was left out in the chromatin preparation, see section 2.3.3 and 3.3.2). IP 1 was done with protein A coated Dynabeads, IP 2 with sheep-anti-rabbit coated Dynabeads and IP 3 as a control with streptavidin coated Dynabeads (the protein streptavidin has no affinity for rabbit-anti-GAF antibodies and therefore no

specific enrichment of hsp26 fragments is expected from this IP experiment). Hence, altogether there were 6 PCR reactions from IP samples: 1+, 1−, 2+, 2−, 3+ and 3−. Starting chromatin has a maximum target sequence concentration of 2×10^6 per microliter ("C_0", see section 3.3.1). A 1 : 10 dilution of this in RIPA buffer was used as IP starting material ($C_0 \times 10^{-1}$). As a reference for PCR, a dilution series of the starting chromatin material was prepared by successive further 1 : 10-dilution. The lanes labeled 4 to 9 in figure 4.16 are PCR products from this dilution series: $C_0 \times 10^{-1}$ (lane 4) to $C_0 \times 10^{-6}$ (lane 9) respectively.

Again, from a successful IP experiment, one would expect more hsp26 PCR product in the "+" samples compared to the "−" samples. TOPO product should not show any enrichment.

PCR and Agarose Gel Electrophoresis

From each of the 6 samples 4 μl were taken and added as template to a 50 μl PCR reaction as described in section 3.7.1. 10 μl of each reaction product were loaded on an 2% agarose gel. Figure 4.16 shows the resulting image from the gel electrophoresis of the PCR products (see also section 3.7.2).

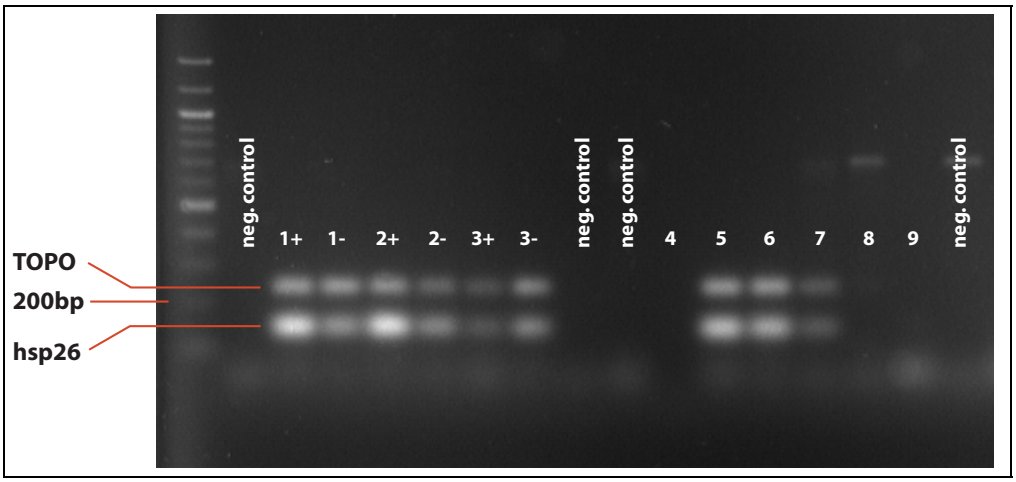

Figure 4.16: PCR from CHIP with paramagnetic beads. 1: protein A beads, 2: sheep-anti-rabbit coated beads, 3: streptavidin coated beads (control), 4-9: dilution of starting material in 1:10 steps. The clearly visible bands in lane 7 represent the product from less than 800 template molecules.

The first lane shows the DNA ladder of which the band with the 200 basepair (bp) long fragment is labeled. The bands of the target hsp26 fragment and the control TOPO fragment (151 bp and 240 bp in size, respectively) are also marked on the left side of the figure. Negative controls (no template) are indicated and the dilution series is labeled with numbers 4 to 9 (see above).

From comparing the intensities of the bands it is evident that both IP experiments, number 1 and 2, show enrichment of hsp26 in the "+" sample compared to the "−" sample. The control fragment TOPO is not significantly enriched. As expected, IP number 3 also does not show enrichment. From the still clearly visible bands in lane 7, it can be seen, that samples containing 800 template molecules can be reliably detected by ethidium bromide stained agarose gels.

A semi-quantitative analysis is presented in the following.

Semiquantitative Analysis with NIH Image Software

The pixel intensities from the agarose gel image were analyzed with the "Gel Plotting" macro of the *NIH Image* image analysis software as described in section 4.3.

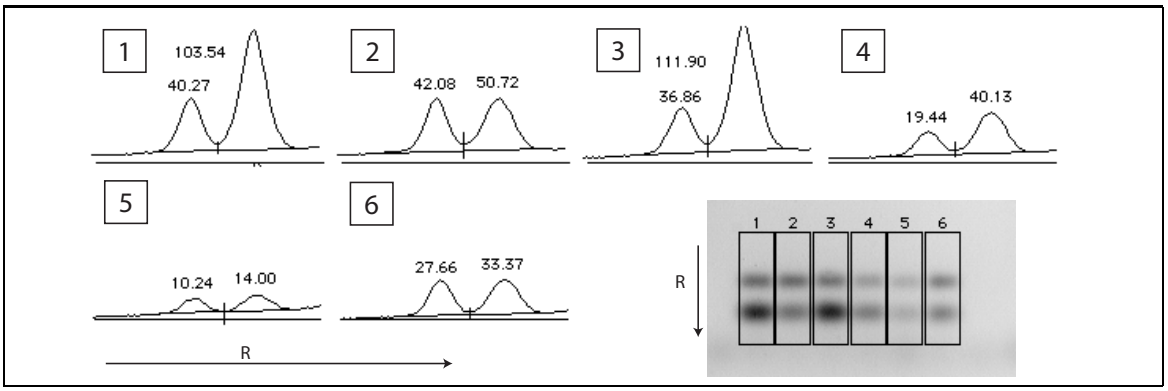

Figure 4.17: Band intensity analysis of PCR products on an ethidium bromide stained agarose gel ("Gel Plotting" macro from *NIH Image* software). The intensity plots of the bands along the running direction of the gel ("R") are labeled with the value of the surface area under the curves. The first of the two peaks corresponds to the TOPO-band and the second to the hsp26-band. Lane 1 versus 2 (IP 1+ versus 1−) shows ≈ 2 fold enrichment in hsp26 and Lane 3 versus 4 (IP 2+ versus 2−) shows ≈ 2.8 fold enrichment in hsp26. Lane 5 versus 6 does not show enrichment (as expected) but rather a decrease in hsp26 band intensity which could originate from PCR performance variation or from fluctuations in non-specific adsorption of sample material to the beads. Note: Numbering is different from figure 4.16.

Figure 4.17 shows the intensities of the individual bands as obtained from *NIH Image* software. Numbering is different from the numbering in figure 4.16 since only a subset of lanes was analyzed. The intensity numbers are obtained as described in section 4.3. An enrichment of ≈ 2 fold (IP number 1, lane 1 versus 2 in figure 4.17) and ≈ 2.8 fold (IP number 2, lane 3 versus 4 in figure 4.17) in hsp26 is found. The control IP (number 3) does not show enrichment but a decrease in signal of ≈ 2 fold (IP number 3, lane 5 versus 6 in figure 4.17). Since there was no target-specific coating on the beads in IP 3, this accounts for fluctuations in IP efficiency as well as

variable PCR performance. As discussed in the previous section, these numbers are crude estimates for relative enrichment.

Real time PCR was performed for more quantitative analysis and is presented in the following paragraph.

Real Time PCR Results

A real time PCR amplification of the CHIP eluates from all 6 IP samples discussed in this section was performed. Details on the reaction are explained in section 3.7.3. Simplex (as opposed to multiplex) PCR was carried out, i.e. hsp26 and TOPO fragments were analyzed in separate reactions. This was done in order to exclude any effects caused by competition of the two independent fragment amplifications for reaction resources. 1 μl template was added to each reaction.

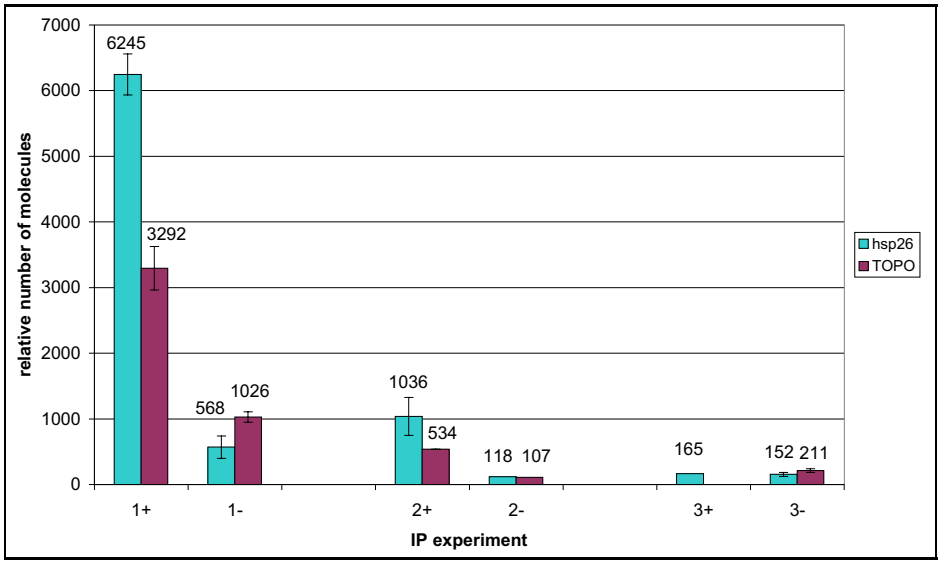

Figure 4.18: Results from real time PCR analysis of a large-scale CHIP with Dynabeads. hsp26 is enriched 11 fold in IP 1 and 8.7 fold in IP 2. IP 3 (non-specific, streptavidin coated beads) does not show any enrichment. This real time PCR analysis shows that TOPO is also enriched with protein A beads (IP 1) and anti-rabbit coated beads in IP 2 which contradicts the agarose gel electrophoresis analysis in the previous paragraph. Values in this diagram are mean values over three identical real time PCR experiments. Error bars represent the standard deviation.

The results summarized in figure 4.18 confirm the semi-quantitative agarose gel analysis. IP 1 shows a 10.7 fold enrichment in hsp26 (+ versus −). In IP 2, hsp26 is enriched 8.7 fold while there is no hsp 26 enrichment in IP 3. TOPO enrichment with both specific beads, IP 1 and IP 2, is ≈ 5 fold, which is in contradiction to the gel electrophoresis analysis (figure 4.17). This contradiction could be due to a calibration

error of the ABI Prism 7000 system. Target quantitation is performed by comparing fluorescence intensities to a dilution series of known target concentrations (see section 2.4.3). In the case of these experiments, IP starting material is successively diluted 1 : 10 in TE buffer (see for example figure 4.16) and 3 of these are dilutions are taken as template material for reference reactions (3 series of 3 data-points, for statistical reasons). In this particular real time PCR run, standard deviations of the reference values taken for calibration were indeed quite large. Optical inspection of the calibration curves was carried out and the calibration was considered sufficiently good. Obviously, care has to be taken when only low target molecule numbers are involved as is the case for this experiment. Due to lack of IP eluate material this PCR run could not be repeated.

4.5 Experiment 5 - Fishing Biotinylated DNA with Anti-Biotin Antibodies

To prove the functionality of the fluidic setup and the coating, the following immunoseparation experiment was carried out:

Biotinylated hsp26 fragments and control TOPO fragments (from the hsp26 promoter region (160 bp) and the TOPO encoding region (220bp), as described in section 3.7.1) were produced in large amounts by a preparative PCR: The target fragments were PCR amplified from genomic DNA (from *Drosophila Melanogaster*) using biotinylated primers for the hsp26 fragment. This produces a sample that contains biotinylated hsp26 fragments (each fragment has a primer built in at its end) and not biotinylated TOPO fragments in approximately equal amounts. PCR reaction conditions were the same as for the analytical PCR reaction of CHIP eluates (section 3.7.1).

2 preparative reactions were carried out, one with biotinylated GAGA-Lower and GAGA-Upper primers ("+" sample), and one with normal not biotinylated primers (for the "−" control in the following immunoprecipitation).

The concentration of the PCR products that served as starting material for the following immunoprecipitation were determined by PicoGreen^{TM} fluorescence spectrometry with a Fusion^{TM} Universal Microplate Analyzer from Packard Bioscience. The concentrations were 30 ± 3 ng/μl for both, the "+" and the "−" sample. This corresponds to $C_4 \approx 3 \times 10^{10}$ molecules of double stranded DNA fragments per microliter ("C_4" is experiment-determined nomenclature).

Anti-biotin antibodies from Sigma (antibody (ab) #15, section 3.1) were attached to capillary walls following the protocol in section 3.6, including extensive saturation

with BSA. 8 capillary columns were mounted to the fluidics manifold described in section 3.4.2. 2 were coated only with BSA and the others were coated with anti-biotin antibodies. The following tabular gives an overview on the 8 capillaries:

column #	1	2	3	4	5	6	7	8
Coating	BSA	ab#15	ab#15	ab#15	BSA	ab#15	ab#15	ab#15
injected conc.	$C_4/10$	$C_4/10$	$C_4/100$	$C_4/1000$	$C_4/10$	$C_4/10$	$C_4/100$	$C_4/1000$
injected molec.	10^{10}	10^{10}	10^9	10^8	10^{10}	10^{10}	10^9	10^8
biotin	+	+	+	+	−	−	−	−

3μl from a 1 : 10 dilution of C_4 in TE buffer were injected into the columns and incubated for 1 hour (advancing the sample plug by 0.5 μl every 10 minutes, resulting in a total incubation time of 1 hour). The columns were cooled to 4°C during that incubation step. Then, still at 4°C, the columns were extensively washed with

- 125 μl of RIPA per column (50× column volume)
- 125 μl of 500 mM LiCl buffer
- 125 μl of 10 mM Tris pH 8.0

This corresponds to over 28 times the column volume for each of the three washing steps (capillary volume: 4.4 μl per 60 cm). For the washing buffers see the protocol in section 3.6, step 7. After washing, the antibody-antigen interaction was broken by flushing with a glycin buffer pH 2.5 (which is a common elution buffer for immunoaffinity chromatography (*Harlow and Lane*, 1988), see section 3.1.2).

Fractions were taken every 10 μl from each column.

Fraction 1:	before sample injection	Fraction 5:	2nd eluate
Fraction 2:	after sample injection	Fraction 6:	3rd eluate
Fraction 3:	during washing	Fraction 7:	4th eluate
Fraction 4:	1st eluate	Fraction 8:	5th eluate

From each sample, 1 μl was taken as template for the PCR detection reaction that was then analyzed in the same way as described in the previous sections.

Figure 4.19 shows the agarose gel electrophoresis analysis of the columns 1, 2, 5 and 6 and figure 4.20 summarizes the real time PCR results of the eluates from these columns.

The results of the agarose gel electrophoresis analysis of the columns 3, 4, 7 and 8 are presented in figure 4.21 followed by the corresponding real time PCR values in figure 4.22.

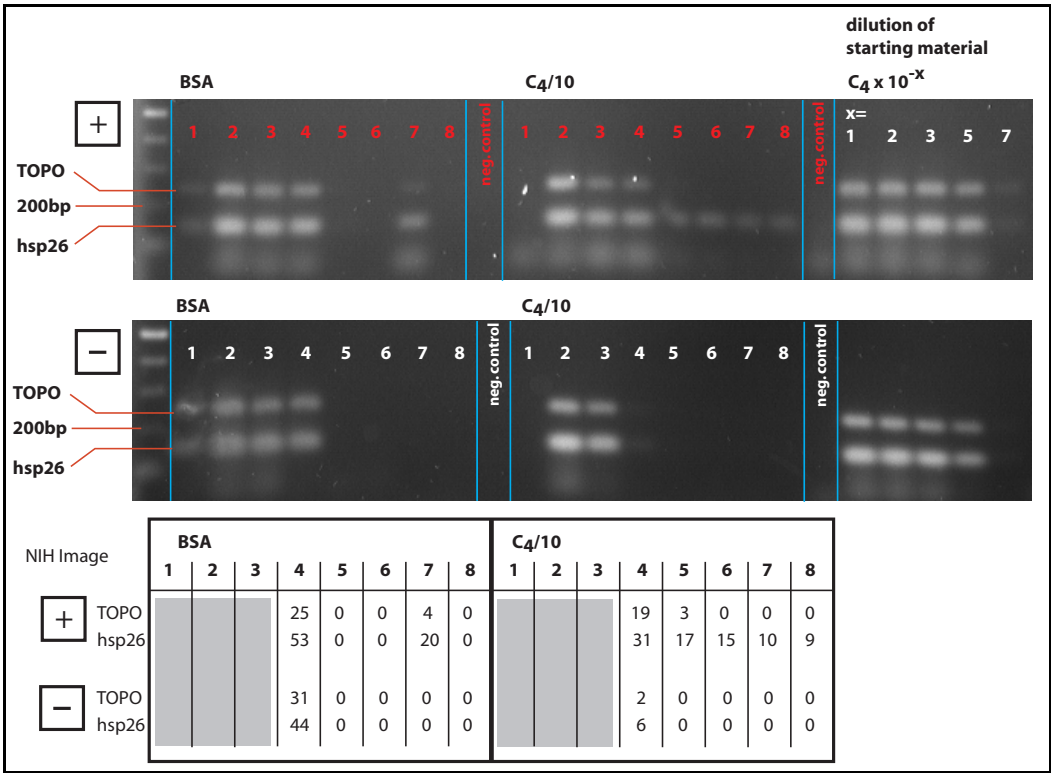

Figure 4.19: Agarose gel electrophoresis analysis of an IP of biotinylated hsp26 from a DNA mixture. Eluate analysis from the 4 columns 1, 2, 5 and 6 are presented. Starting material was 3 μl of $C_4/10$, corresponding to 9×10^{10} target molecules in the sample plug. The numbered lanes on the gel correspond to the fraction numbers (elution starts in lane 4). The bottom part of the figure shows the results from the *NIH Image* analysis. The numbers were obtained exactly as in the previous sections (4.3 and 4.4). They show clear enrichment of the hsp26 fragment in the "+" columns relative to the "−" columns. PCR products of a dilution series of $C_4/10$ directly used as PCR template can be seen on the right of every gel. It indicates that PCR products from a 10^{-5} fold dilution of C_4 (i.e. $\approx 10^4$ molecules per microliter) can still be seen on the gel. The BSA saturated column (the left half of the figure) shows some signal in the "+" column in lane 7, but no systematic enrichment. This can be regarded as background.

		BSA				C4/10			
	lane	4	5	6	7	4	5	6	7
Plus	TOPO	112050	343	0	21172	20765	0	0	0
	hsp26	151412	753	214	13769	445015	20234	4639	16086
Minus	TOPO	64336	135	4	0	990	0	0	0
	hsp26	89375	449	278	211	2137	260	313	165

Figure 4.20: Results from the real time PCR analysis for columns 1, 2, 5 and 6. They correspond to the results presented in figure 4.19. The numbers are target molecule numbers in 1 μl eluate. The high numbers in lane 4 can be explained by some minor overlap of washing an elution. There is strong enrichment of hsp26 fragments in the "+" columns relative to the "−" columns (factor 10 to 50). This is consistent with the *NIH Image* analysis numbers in figure 4.19.

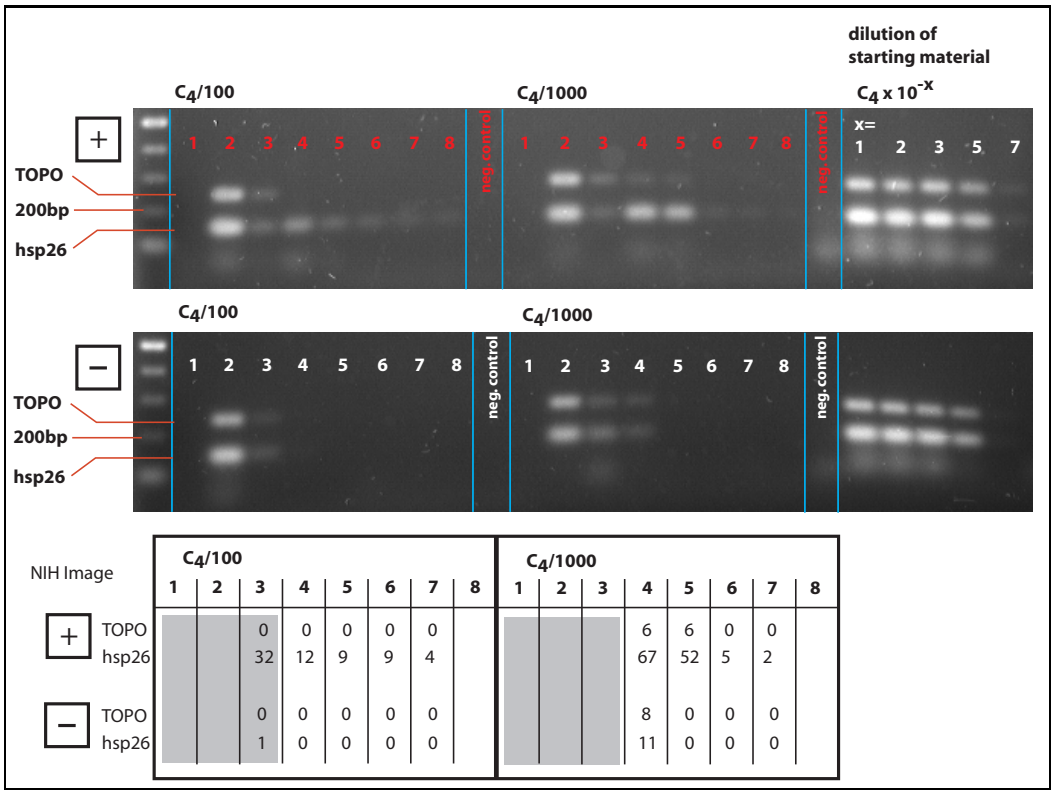

Figure 4.21: Agarose gel electrophoresis analysis of the IP columns number 3, 4, 7 an 8. The figure is analogous to figure 4.19. The hsp26 enrichment in these samples is as good as in figure 4.19. The smaller numbers can be explained by the lower target concentration in the injected sample plug ($C_4/100$ and $C_4/1000$).

		C4/100				C4/1000			
	lane	4	5	6	7	4	5	6	7
Plus	TOPO	0	0	1	0	0	3	466	0
	hsp26	30687	5277	329	973	58208	26752	2901	3091
Minus	TOPO	195	18	0	0	4215	80	0	0
	hsp26	714	166	218	219	4874	101	175	194

Figure 4.22: Results from the real time PCR analysis for columns 3, 4, 7 and 8. They correspond to the results presented in figure 4.21. The numbers are target molecule numbers in 1 μl eluate. There is strong enrichment of hsp26 fragments in the "+" columns relative to the "−" columns (factor 10 to 50). Also for these columns, the results of the real time PCR are consistent with the *NIH Image* analysis numbers in figure 4.21.

The results of this experiment clearly show strong specific enrichment of hsp26 fragments. Enrichment factors reach up to 30687/718 = 43. Samples in lanes 6 and 7 "−" in figure 4.22 contained no detectable hsp26 molecules which means that the few molecules in these samples fell under the threshold for background in the real time PCR analysis. Enrichment

TOPO fragments were not enriched.

This experiment has clearly shown a highly efficient immunoaffinity separation from DNA samples and the concept of the fluidic setup has proven to be functional.

4.6 Experiments 6 - CHIP of GAGA-Factor in Capillaries

In the following sections, chromatin immunoprecipitation (CHIP) experiments in fused silica glass capillaries with 75 μm inner diameter are presented. They were carried out according to the protocol given in section 3.6. The following parameters were varied:

- Capillaries with 60 cm and 15 cm were compared.
- Several functional glass coatings were tested: protein A, ab#11, ab#12 and ab#13.
- Two blocking proteins to prevent non-specific adsorption were tested: BSA and milk protein. In one experiment a capillary was homogeneously coated with PEG-silane to test the polymer's properties to prevent non-specific adsorption.
- Experiments with incubation times (the time in which the sample is pumped through the column) of 20 minutes, 1 hour and 2 hours have been carried out.
- Two concentrations of the LiCl wash buffer were tested: 250 mM and 500 mM LiCl (see section 3.6 and 3.1).

A total of more than 15 experiments each involving 8 capillary columns (with a 1 : 1 ratio of positive samples to negative controls) were carried out. None of these experiments has shown any specific enrichment in hsp26, independent of the parameters listed above.

In the following, results from two representative experiments are shown. The first is a CHIP assay with protein A coated capillaries (section 4.6.1). The controls were saturated with BSA. The second experiment (section 4.6.2) involved PEG-silane coated capillaries, milk powder blocked capillaries, protein A functionalized (and BSA saturated) capillaries and capillaries functionalized with antibody#13 (saturated with milk protein).

4.6.1 Experiment 6a: Protein A Coated Capillaries

To stay as close as possible to the procedure of the large-scale CHIP experiments (section 4.3 and 4.4), a capillary-CHIP was performed with surface-bound protein A. The capillaries were coated following the protocol in section 3.6. The antibody solution was replaced by 1 mg/ml protein A (from Sigma, see section 3.1). 4 of the 8 eight capillaries were not coated with protein A but only saturated with BSA. The capillaries were 60 cm long.

3 μl from a 1 : 10 dilution of C_0 (for target concentrations in C_0 see section 3.3.1) in TE buffer were injected into the columns ("+" and "−" sample) and incubated for 1 hour. Injection, incubation and washing were carried out exactly as in the previous (anti-biotin - biotin) experiment.

After washing, the formaldehyde cross-links in the chromatin were reversed by heating the capillaries for 6 hours to 65°C. Then the free target molecules were washed out with TE buffer.

Fractions were taken every 10 μl from each column:

Fraction 1:	before sample injection	Fraction 5:	1st eluate
Fraction 2:	after sample injection	Fraction 6:	2nd eluate
Fraction 3:	1st wash	Fraction 7:	3rd eluate
Fraction 4:	last wash	Fraction 8:	4th eluate

From each sample, 4 μl were taken as template for the PCR detection reaction.

Figure 4.23 shows images of the agarose gels after electrophoresis. The images were obtained according to the gel electrophoresis protocol in section 3.7.2. Real time PCR was not carried out since quantification would not result in any more relevant information.

The results of this experiment show no detectable specific enrichment of hsp26 fragments.

4.6.2 Experiment 6a: Protein A versus Antibody Comparison

For this experiment, 2 capillary columns were coated with PEG-silane according to the protocol in section 3.5.2 and 2 columns were coated according to the standard protocol in section 3.5.1 but incubated with 5% milk powder in PBS instead of an antibody solution. These 4 capillaries were not specifically modified and used for

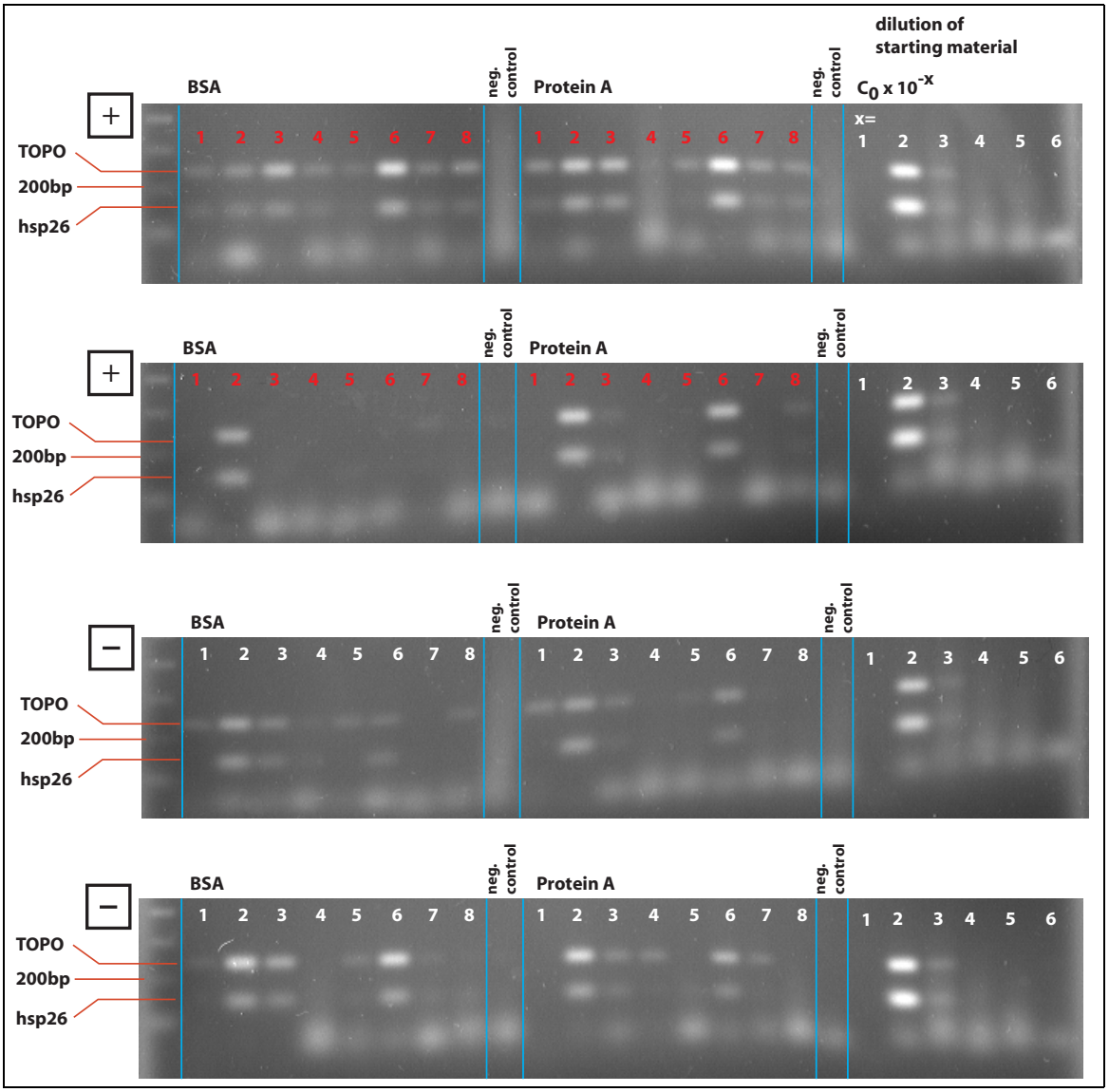

Figure 4.23: Agarose gel electrophoresis image of capillary CHIP with protein A coated columns. No specific enrichment of hsp26 fragments can be detected in the eluates (lanes 4-8). The band intensities are rather random. The only systematic feature in this figure is that most eluates in lanes number 6 seem to contain more DNA than other samples. But there is not difference between "+" and "−" samples and also not between BSA and protein A columns. Band intensities of TOPO fragments are similar to those of hsp26 fragments. This can only be explained by non-specific surface adsorption dominating over the specific antibody-antigen interaction.

testing for non-specific adsorption to compare them to the BSA saturated capillaries from the previously described experiment (section 4.6.1). Furthermore, 2 capillaries were coated with protein A exactly as described in the experiment in section 4.6.1

and 2 capillaries were coated with antibody number 13 ("ab #13", see section 3.1). These 8 capillaries were mounted on the fluidic setup (section 3.4) as follows:

column #	1	2	3	4	5	6	7	8
Coating	PEG	milk	protein A	ab#13	PEG	milk	protein A	ab#13
injected conc.	C_0	C_0	C_0	C_0	C_0	C_0	C_0	C_0
injected molec.	3×10^5	3×10^5	3×10^5	3×10^5	3×10^5	3×10^5	3×10^5	3×10^5
anti-GAF	+	+	+	+	−	−	−	−

Sample injection was identical to the experiment in section 4.6.1. Washes were also performed as in section 4.6.1 and the fractions were collected at the same experimental steps.

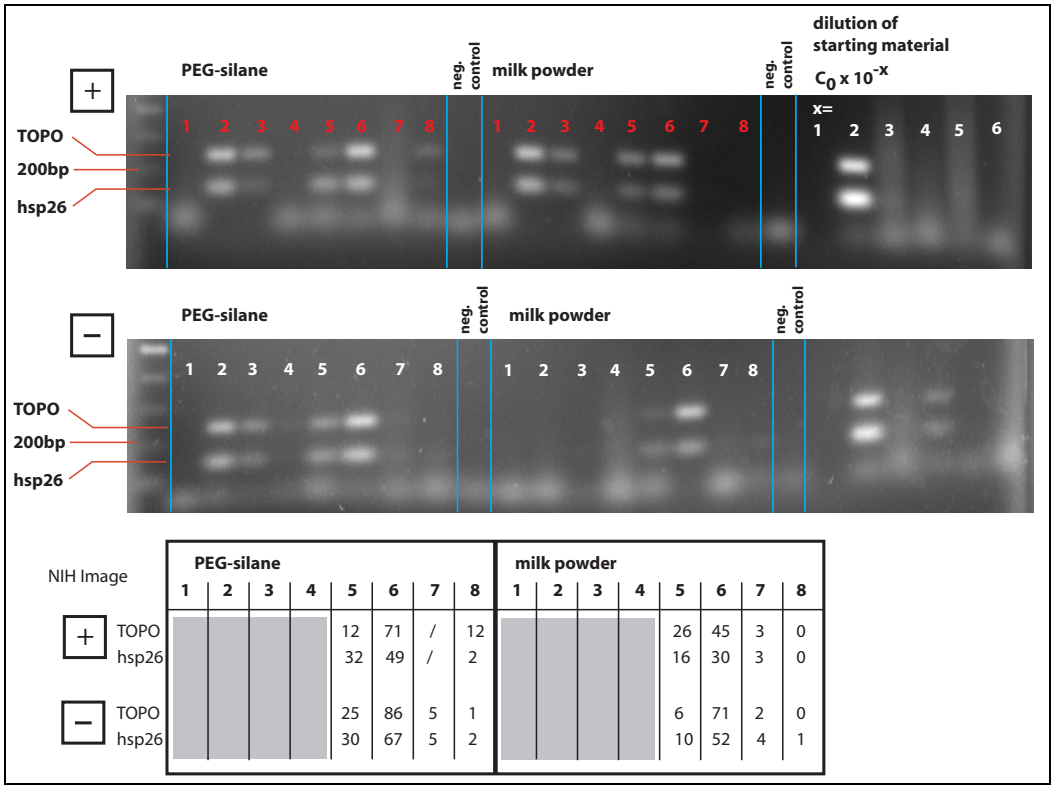

Figure 4.24: PCR products of eluates from PEG-silane and milk powder coated columns after gel electrophoresis: No specific enrichment should be seen since the columns were not specifically modified. However, non-specific signal (quite strong in some lane, such as lane 6) is randomly seen in the eluates. Eluates are represented in the lanes 4-8. The lower part of the figure shows the results from the *NIH Image* band intensity analysis. They are consistent with the quantitative analysis in real time PCR as represented in figure 4.25.

		PEG-silane				milk powder			
	lane	4	6	7	8	4	6	7	8
Plus	TOPO	11	887	48	31	42	480	16	7
	hsp26	22	699	55	18	18	288	0	2
Minus	TOPO	0	1308	28	46	9	208	11	12
	hsp26	28	1092	23	17	26	121	35	14

Figure 4.25: Real time PCR results corresponding to the gel electrophoresis analysis in figure 4.24. They confirm that there is quite high non-specific signal.

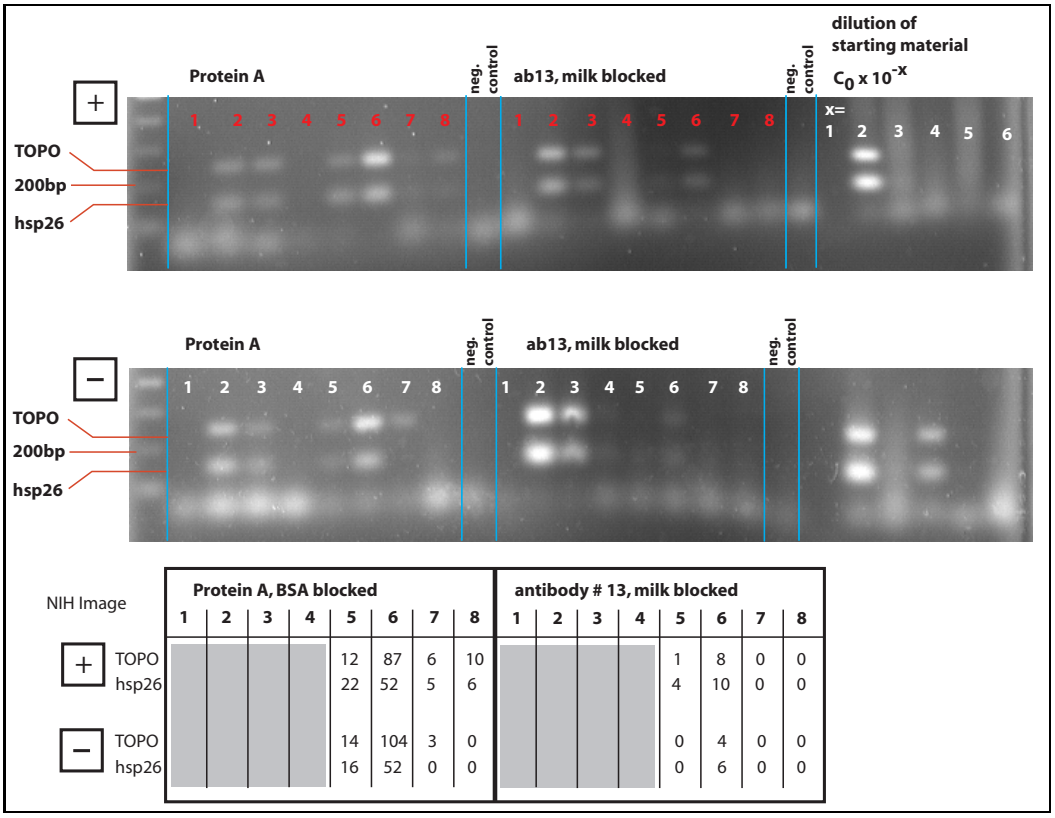

Figure 4.26: PCR products of eluates from protein A and ab #13 coated columns after gel electrophoresis: No specific enrichment of hsp26 is detected. Eluates are represented in the lanes 4-8. The lower part of the figure shows the results from the *NIH Image* band intensity analysis. They are consistent with the quantitative analysis in real time PCR as represented in figure 4.27

.

In the case of this experiment both the *NIH Image* analysis and real time PCR were carried out to demonstrate the qualitative equivalence between the two methods for DNA detection when only a yes/no signal is required. Quantitatively, real time PCR was more sensitive. Real time analysis of fraction 5 could not be carried out since no

		Protein A				ab13			
	lane	4	6	7	8	4	6	7	8
Plus	TOPO	13	555	21	0	10	57	0	0
	hsp26	14	394	27	21	0	54	0	15
Minus	TOPO	9	178	11	0	24	81	38	0
	hsp26	0	168	24	10	9	106	38	17

Figure 4.27: Real time PCR results corresponding to the gel electrophoresis analysis in figure 4.26. They confirm that there is no specific enrichment of hsp26 fragments. Non-specific signal seems to be slightly lower than in the eluates from PEG-silane and milk powder coated columns (compare numbers to the numbers in figure 4.25).

sample material was left after conventional PCR (for gel electrophoresis detection).

Figures 4.24, 4.25, 4.26 and 4.27 show the results of the described experiment. No specific enrichment of hsp26 fragments could be detected by neither analysis method. Generally, non-specific signal is stronger in eluates from columns with PEG-silane and milk powder coating compared to protein A and antibody coated capillaries.

Chapter 5

Discussion and Conclusions

In the presented work, the potential of fused silica micro-channels with specifically modified surface properties for the miniaturization of a chromatin immunoprecipitation (CHIP) assay of *Drosophila* GAGA transcription factor was investigated. To down-scale this particular immuno-separation technique, antibodies were attached to the walls of fused silica capillaries with an inner diameter of 75 μm. The biologically motivated goal of this project was to identify a DNA binding site of the GAGA transcription factor (GAF) *in vivo* by purifying the GAF protein with the associated DNA from *Drosophila* embryo chromatin. The antibody-functionalized surfaces were used as solid substrate (stationary phase) for the immunoaffinity-chromatographic separation of the protein-DNA complex from its cellular environment. From the literature, it is well known that the specificity of the separation method depends strongly on the successful prevention of non-specific adsorption of sample material to involved surfaces. To obtain such inert surfaces, the antibody-coated microchannel walls were saturated with the neutral protein BSA. The properties of the coating (antibodies plus blocking layer) with respect to sensitivity and selectivity of the resulting separation device were examined. A number of tests were carried out to verify if the coating can meet the demands of a capillary based micro-scale CHIP assay to study chromatin remodeling and gene expression regulation at the single cell level.

The following chapter summarizes the experimental results and discusses them with respect to the goal of this work (section 5.1). Conclusions from this project are drawn in section 5.2.

5.1 Summary and Discussion of Results

Experiments 1 and 2: Methods for Antibody Attachment

With the experiments in sections 4.1 and 4.2, two silane-based methods for antibody attachment to fused silica glass capillaries were tested with a particular focus on monitoring non-specific protein adsorption to the chemically modified micro-channel walls. Confocal fluorescence microscopy was employed to detect labeled probe proteins and to monitor binding of specific fluorescently labeled antigen to the immobilized antibodies. The two glass coating methods were a) the photo-patterned activation of a layer of custom-synthesized PEG-silane for covalent antibody attachment (section 3.5.3 and 4.1) and b) the homogeneous attachment of antibodies to glass with a mercapto-silane based protocol using heterobifunctional cross-linkers (section 3.5 and 4.2).

Method a) was analyzed only qualitatively. It showed remarkable contrast in specific binding signal between modified (i.e. antibody-coated) patches and the remaining PEG polymer layer (figures 4.1 to 4.5): The covalently immobilized antibodies bound significant amounts of antigen while at the surrounding PEG-coated surfaces no adsorbed protein could be detected. A critical parameter for a good coating has turned out to be UV irradiation intensity. Comparing two irradiation intensities (one with 20% higher primary laser power than the other, illuminated with a microscope-mounted N_2 laser, see section 3.5.3) it becomes evident that higher irradiation leads to more specific and at the same time to more non-specific binding. This observation can be explained by damage to the silane layer (and to the activated reactive group that forms the *Schiff base* in the covalent antibody attachment) caused by high UV intensities. On such damaged surfaces, non-specific interaction of the incubated proteins with the uncovered glass surface can result in the observed adsorption behavior. Thus, the irradiation intensity (laser power) needs to be optimized for an optimum ratio of specific binding to non-specific adsorption.

These - at least qualitatively - promising results of this technique for antibody (and protein) attachment are complemented by the flexibility in geometry of functionalized surfaces. It includes the possibility of creating multi-analyte purification on a single column by successive activation and coating of several patches with different antibodies (as demonstrated for a waveguide biosensor system by *Ligler et al.* (2002)).

A drawback of this photo-patterning based technique for antibody attachment is the complex and elaborate chemistry involved in its synthesis (*Eritja* (1999) and *Conrad et al.* (1997)). The insertion of the very sensitive UV linker between standard PEG and the silane group require considerable laboratory resources, extremely pure chemicals and special know-how. No laboratory, neither in industry nor in a research

institute could be found that would custom-synthesize the compound.

Therefore, after the stocks that were kindly provided by the developer of the NMPEG-silane, were used up, the antibody attachment strategy was changed to method b). This method relies only on commercially available chemicals. Although method b) is limited to homogeneous surface coating with antibodies, it allows an increase of immunoactive surface compared to the micrometer-sized patches created with method a). In section 3.5.1, the binding capacity has been estimated to about 1×10^{11} binding sites per 60 cm of a 75 μm ID capillary. Thus, with starting material concentrations of the IP in the order of 10^5 molecules, homogeneous antibody coating of capillary walls on a length of 60 cm ensures a considerable excess of binding sites which is not the case for small photo-patterned antibody patches.

Method b) is a commonly used method for protein attachment to glass, described in section 3.5.1. Blocking relies on BSA or other proteins that do not interact with the sample material. The quality of cured and not cured silane layers was compared: Ratios of specific binding to non-specific adsorption were $\frac{146}{38} = 3.8$ fold for not cured layers (washed with PBS buffer) and $\frac{114}{10} = 11.4$ fold (RIPA buffer wash) and $\frac{152}{7} = 21.8$ fold (PBS buffer wash) for cured layers (figures 4.9 and 4.11). Hence, curing significantly improves the ratio of specific binding to non-specific adsorption and was therefore incorporated in all following capillary wall coatings. Curing also produces smoother surfaces, reducing the number and size of defective areas that show high non-specific binding (figures 4.12 versus 4.10). PBS buffer washes give slightly better results (wash buffer is a very sensitive parameter as discussed in section 3.3.2).

Furthermore, the systematic variation of antibody performance from one supplier to another is striking. Specific binding varies from values of 146 (arbitrary fluorescence units) to 38, while non-specific binding (background) values are around 10. Thus, the most important parameter for successful immunoprecipitation is to find the best antibody for the particular experiment that keeps its function when attached to surfaces is.

In summary, these two experiments have achieved antibody attachment to glass substrates showing little non-specific adsorption of protein and good specific recognition of antigen. Non-specific adsorption was evaluated with pure protein solutions according to common practice (see e.g. *Alcantar et al.* (2000), *Piehler et al.* (1996) or *Anderson et al.* (1997)).

Quantitative comparison of the found ratios of specific to non-specific adsorption to published data can be done to a limited extend only. One reason is that there are only few studies available that actually quantify their data. Another reason is that surface modifications to prevent non-specific adsorption are commonly measured in terms of adsorption of a non-specific molecule to a coated surface relative to a not coated surface (*Alcantar et al.* (2000), *Piehler et al.* (1996)).

One of the few studies that compares binding of a specific molecule to an antibody modified surface directly with adsorption of the same molecule to the same surface without antibodies is presented in *Anderson et al.* (1997). They report an immobilization technique for antibodies involving protein A (see section 3.5.2 of this work). Covalent attachment of protein to the glass substrate is realized with the same GMBS-involving protocol as used in the experiments presented in this thesis, explained in detail in section 3.5.1, and they find non-specific adsorption to be 5% of the specific signal. This compares well to the quality of the coating produced in the discussed experiments ($\frac{7}{152} = 4.6\%$ for PBS and $\frac{10}{114} = 8.7\%$, see above).

Experiment 3 and 4: Large-Scale Reference CHIP-Experiments

The experiments in sections 4.3 and 4.4 show the enrichment of hsp26 achieved in large scale CHIP assays. Experiment 3 involved the lengthy well-established procedure described in detail in appendix B. Experiment 4 was carried out according to the shortened and simplified protocol given in section 3.3.2 and demonstrated that minor modifications to the protocol of experiment 3 did not adversely affect IP performance. Modifications were necessary to adapt the assay to the capillary format (see section 4.4).

Experiment 3 gave quantitative results on the performance of a "classical" large-scale CHIP assay with protein A agarose beads. Eluates from an IP experiment carried out in a collaborating laboratory were re-analyzed by the author using quantitative PCR and agarose gel electrophoresis. A 5 to 9.5 fold enrichment in the specific target hsp26 fragment could be shown (figure 4.14 and 4.15). Non-specific binding signal was in the range of 10% to 25% of the signal from specific target (see figure 4.14 and 4.15).

Reproduction of the classical CHIP could be achieved with paramagnetic styrene beads ("Dynabeads") and a slightly modified protocol (section 4.4). Quantitative analysis has shown that the protocol, which was transferred directly in the capillary format in section 4.6, was as efficient as the classical protocol for experiment 3. hsp26 enrichment of 11 fold (IP 1, protein A coated Dynabeads) and 9 fold (IP 2, sheep-anti-rabbit coated Dynabeads) could be shown (figure 4.18). However, non-specific enrichment of TOPO fragments in both IP 1 and IP 2 is indicated by real time PCR analysis (figure 4.18). This did not confirm the results from agarose gel electrophoresis analysis. But real time PCR data of the TOPO samples have to be considered with caution. TOPO fragment amplification has produced amplification plot curves that could indicate a sparsely efficient fluorescent probe, albeit still within the range of acceptable data for the integrated analysis software of the ABI Prism 7000 system. Whether an amplification plot can be analyzed by the real time PCR system or not

depends strongly on the threshold values which are set manually by the user to separate fluorescence background from signal (section 2.4.3). An inefficient specific probe results in highly fluctuating fluorescence intensities and, depending on threshold settings, could lead to wrong calibration and therefore, absolute quantitation would not be accurate. Fluctuations in target concentration in samples for the calibration curve could also result in such effects (concentrations are as low as 10 molecules/reaction volume for some samples). Therefore, real time PCR data should always be looked at in comparison to standard PCR analyzed by agarose gel electrophoresis. In any case, the agarose gel electrophoresis has shown insignificant or no enrichment of TOPO while hsp 26 is clearly enriched (see figure 4.17).

Experiment 5: Demonstration of Setup Functionality (Biotin-IP)

The functionality and efficiency of the newly developed fluidic setup and the surface coating were demonstrated in section 4.5. Capillaries were coated with anti-biotin antibodies to separate a biotinylated hsp26 fragment from non-biotinylated TOPO fragments. Highly specific enrichment of hsp26 is shown. Enrichment factors in some samples are up to 50 (figures 4.20 and 4.22). TOPO signals are very weak (figures 4.19, 4.21, 4.20 and 4.22), apart from the eluates from capillaries which were not coated with antibody but only passivated with BSA. These particular columns show very high signal which accounts for bad saturation efficiency of BSA (see figure 4.19).

This good performance of immunoaffinity columns was shown with starting concentrations of $C_4/10 \approx 10^8$ to $C_4/1000 \approx 10^6$ molecules (see section 4.5). It follows that the principle concept of performing an immunoseparation in micrometer sized fused silica capillaries has proven to be very efficient with pure DNA (protein free) samples.

Experiments 6: CHIP Assay in Capillaries

Experiments in section 4.6 put the immunoaffinity columns to test with chromatin sample material. More than 15 experiments were carried out, testing various parameters for their influence on immunoaffinity separation performance with capillaries coated after the same protocol as in experiment 2.

Towards the aspired goal of chromatin immunoseparation in a microchannel format, the following parameters have been screened:

- Two different types of neutral protein were incubated (i.e. BSA and milk powder) to block non-specific adsorption by saturation of remaining free binding sites after antibody attachment. A homogeneous PEG layer (commercial PEG-silane) was tested as well.

- Protein A and a number of anti-rabbit antibodies were tested for their suitability to fish a rabbit antibody with bound target protein-DNA complex from the sample.
- The capillary length (and thus the the binding capacity of the column) as well as incubation times were varied.
- Wash buffer conditions (i.e. the salt concentrations) were varied.

Also, care was taken that extensive washing of the column was carried out before elution. Elution was started after fractions from the last wash step were clean, i.e. did not contain any detectable target or control DNA fragments.

None of these experiments yielded any specific enrichment in hsp26, independent of the parameters listed above.

Detection limits were not a concern. In both experiments in section 4.6 bands of PCR products could be seen on the gel and real time PCR could determine target molecule numbers well below values of 100.

Thus, these experiments showed that specificity as well as sensitivity were clearly not sufficient for efficient separation of target from chromatin samples containing $\approx 10^5$ copies of the target molecule in the injected sample plug. As discussed with the coating evaluation for experiment 2, the coating quality met commonly achieved standards, indicating principal limitations for this kind of silane-based covalent antibody attachment methods with respect to micro-scale experiments involving complex protein samples.

5.2 Conclusions

A microfluidic setup for capillary based immunoaffinity chromatography was designed and a capillary coating procedure for antibody attachment was established.

In summary, the achieved coating showed good prevention of non-specific adsorption of proteins to the involved surfaces. The quality of the surface coatings with respect to non-specific protein adsorption was compared to the results of other research groups. Competitive coating quality could be demonstrated.

The newly designed experimental setup integrates the fabricated immunoaffinity columns in a parallel array of fluidic channels. The functionality of the system could be proven by successfully purifying a specific biotinylated DNA fragment from non-specific DNA. Enrichment-factors of ≈ 50 could be shown. But in immunoseparation assays from chromatin in capillaries, non-specific adsorption of sample material to the microchannel walls prohibited enrichment and resulted in rather random elution of target and control molecules.

However, from the results summarized above it becomes clear, that the antibody-modified fused silica surfaces, resulting from the surface modification technique employed, did not meet the challenge of separating a specific protein species from a nuclear extract, such as *Drosophila* chromatin, in micrometer-scale capillaries.

The sensitivity of the PCR protocol was pushed to a reliable detection of 100 target molecules per 4 microliter column eluate. This number is based on the estimate of target fragment concentration in section 3.3.1 which assumes the ideal case that there were no losses of DNA material during chromatin preparation. Adsorption of DNA to the walls of all involved containers, including the reaction tubes for PCR and real time PCR, reduces this number. Thus it is likely that the sensitivity of the PCR procedure used to detect immunoprecipitated PCR from chromatin IP experiments has reached the theoretical limit of identifying very few molecules.

In the particular case of the GAF-CHIP assay from *Drosophila* chromatin, the effects of non-specific binding of proteins and/or macromolecular chromatin-structures to microchannel walls clearly outweigh the function of the specifically designed layers of surface bound antibodies. Although the properties of the surface modifications with respect to specific binding of target and prevention of non-specific adsorption are comparable to published studies (discussed above), an efficient separation of the target protein-DNA complex from *Drosophila* chromatin could not be demonstrated. The variation of several important parameters involved in the fabrication of the described immunoaffinity column did not significantly improve the results.

Non-specific adsorption did not significantly affect the purification and detection of biotinylated DNA from a DNA mixture (see above and section 4.5). Therefore, the complex biochemical composition of the chromatin sample can be named as the major limiting factor. Chromatin handling in microchannels obviously makes considerably higher demands to coating properties compared to samples in other studies that have put antibody attachment methods to test. Chromatin is a highly complex mixture of highly charged molecules, consisting of DNA, histones and more nucleoprotein chromosomal material (see section 2.3.1). The exceptionally strong non-specific adsorption of chromatin is most likely caused by these heterogeneous properties. Thus, a qualitatively better concept for surface property control is required to improve the ratio of specific signal to non-specific adsorption. A promising example for such an better concept would be the replacement of the cross-linker GMBS in the coating procedure by a heterobifunctional PEG (see appendix A).

The levels of non-specific signal in the large-scale CHIP assays (up to 25% of the specific signal, see above) support the conclusion that the chemical nature of chromatin makes it very "sticky" compared to other biomolecular samples.

Furthermore, there could be steric accessibility restrictions of the wall-immobilized antibodies to their target antigen (i.e. the anti-GAF antibody) that could be bound

to a GAF molecule in the middle of a relatively large protein complex. If this was the case, beads as solid substrate would clearly have an advantage because of their mobility.

To conclude, the combined effects of non-specific adsorption and the low target concentration in the starting material ($\approx 10^5$ molecules, see section 3.3.1) prevented the application of the new miniaturized immunoaffinity separation tool to CHIP assays from *Drosophila* chromatin. Further research, that goes beyond the scope of the present thesis project, is required to improve the employed surface coatings or to develop novel coatings and materials. To perform biochemical analysis from single or few cells by purifying a particular complex of interest from nuclear or cellular extract, a new approach is definitely needed.

Potential strategies to overcome some of the problems revealed by the present work are further discussed in appendix A.

Appendix A

Alternative Strategies

Further experiments that could advance the idea of implementing a micro-scale CHIP assay from *Drosophila* chromatin in micrometer-sized glass channels are outlined in these final remarks. Alternative approaches and new concepts for fluidic handling in the sub-nanoliter range and their potential usefulness for the aims of this work are also considered.

Further Experiments

The following experimental strategies will provide further information on how ratios of specific binding to non-specific adsorption could be improved for protein-involving experiments in microchannels:

a) Packing a capillary column with magnetic beads similarly to the concept described in *Hayes et al.* (2001). The experiment could be carried out exactly as experiment 5 or 6 of this thesis. Beads will be held in place by a strong magnet and elution will take place by removing the magnet. Capillary surfaces will only be involved in terms of providing a micrometer-scale sample container and can be passivated against non-specific adsorption in a homogeneous manner. Passivation against sample-surface interaction without simultaneous functionalization offers much more flexibility in choice for chemical substrate modifications. This could help to obtain better blocking of non-specific adsorption compared to post-functionalization protein saturation of surfaces (*Bhatia et al.* (1993) and *Österberg et al.* (1995)). The most prominent molecule that can be used as a basis for such homogeneous coating is PEG (*Pan et al.* (2001), *Piehler et al.* (2000)).

The concept of inserting beads in microchannels has come up only recently (*Ruzicka and Hansen*, 2000) and mostly relies on mechanical trapping of the beads with frits

or barriers (*Jiang and Harrison* (2000) and *Oleschuk et al.* (2000)). Addressing the risk of channel clogging with mechanical barriers, *Hayes et al.* (2001) and *Choi et al.* (2002) have recently demonstrated magnetic bead capture in capillaries. This strategy was also envisaged at EMBL at an earlier stage but was not followed up because of lack of time.

b) Incorporation of an intermediate PEG layer between the glass and the NHS-ester link to the attached antibody. This is another approach to combine the chemical inertness of PEG (*Pan et al.* (2001), *Piehler et al.* (2000), *Zhang et al.* (1998) and *Zhang et al.* (2001)) with the covalent attachment of antibodies to a microchannel wall (*Shriver-Lake et al.*, 1997). In practical terms this means to replace the heterobifunctional cross-linker (in this thesis: GMBS) by a heterobifunctional PEG molecule for antibody attachment. Heterobifunctional PEG molecules as well as NHS-modified PEG-silanes are commercially available (e.g. from Shearwater Corporation).

Alternative Approaches to micro-scale CHIP Experiments

To work around the difficult task of controlling sample-surface interactions, new concepts have been brought up to transport, mix and analyze liquid samples in microstructures, avoiding surface contact of samples completely:

One approach is to avoid surface contact of the sample by sheath flow configurations. It relies on laminar flow in microchannels which persists up to very high flow rates and pressures (see section 2.1.3). In such a setup, the sample-carrying liquid is surrounded by buffer layers that prevent sample contact with the walls. The concept has been shown for example by *Blankenstein and Larsen* (1998). A similar concept was successfully applied to cell handling in microstructures by *Fuhr and Shirley* (1998) and *Müller et al.* (1999), exploiting dielectrophoretic control of cells and particles induced by high-frequency electromagnetic fields.

The newest concept is to prevent surface contact completely by guiding fluidic droplets along hydrophobic stripes on planar silicon chips in humidity saturated atmospheres (*Gau et al.* (1999) and *Grunze* (1999)). This very promising idea is already commercially exploited by the Advalytix AG, Munich.

Yet, the application of these no-contact techniques to solid substrate-based assays, such as affinity separation, bears some systematic challenges because they need surface interaction by definition.

Appendix B

Chromatin Immunoprecipitation (CHIP) Assay, Original Protocol

The original protocol for the Chromatin Immunoprecipitation (CHIP) assay, described in the following, was provided from Dr. Gregor Gilfillan and Prof. Peter Becker from the Adolf-Butenandt-Institute at the Ludwig-Maximilian-University in Munich. It is based on the work of *Orlando and Paro* (1993), *Orlando et al.* (1997), *Strutt and Paro* (1999) and *Cavalli et al.* (1999). The chromatin used in this work is formaldehyde cross-linked and isolated from the cells as described in these references.

1. Thaw a 0.5 ml aliquot chromatin and adjust to "RIPA-buffer" (see below) conditions by successive addition of the following reagents (on ice). Wait 2 minutes between each addition to allow the chromatin to adjust to the new conditions:

   - 100 μl 10% Triton-X-100
   - 100 μl 1% Na-deoxycholate
   - 100 μl 1% Sodium Dodecyl Sulfate (SDS)
   - 100 μl 1.4 M NaCl
   - 50 μl 0.1 M Tris pH8.0
   - 50 μl 10 mM EDTA
   - 10 μl 100 mM AEBSF

2. Pre-clear this chromatin solution with Protein A - agarose beads (this removes chromatin fragments that for some reason have high affinity to the Protein A - beads, so reduces background) by adding 40 μl beads (a 50 % slurry prepared in RIPA buffer) and rotating at 4°C for 1 hour.

3. Add anti-GAF antibody and rotate at 4°C over night ("o/n").

4. Purify antibody-chromatin complexes by adding another 40 μl protein A - beads and incubating at 4°C for 3 hours.

5. Wash to remove background binding to the beads. This can be done by spinning the beads down in an eppendorf tube, adding 1 ml RIPA buffer and rotating at 4°C for 10 minutes (repeated 5 times). This is then followed by a LiCl buffer wash (very high stringency) and a TE buffer wash (removes detergent).

6. The beads are finally resuspended in 100 μl TE buffer, ready for cross-link reversal.

   NOTE: From this point on, first an Rnase treatment and then a Proteinase K treatment is done before the cross-links are reversed (formaldehyde cross-linking reverse reaction is favored by a drop in pH caused by heating in a Tris-based buffer (see *Orlando et al.* (1997) and references cited therein). Be aware that Proteinase K will digest the antibodies and release everything from the beads.

7. Add Rnase to 50 $\frac{\mu g}{ml}$ final concentration and incubate at 37°C for 30 minutes.

8. Add SDS to 0.5% (from a 10% stock), and Proteinase K to 500 $\frac{\mu g}{ml}$ and incubate for 6 hours at 55°C, or o/n at 37°C.

9. Increase the temperature to 65°C for 6 hours (shaking the tubes hard in a heating block might help, but is not essential).

10. Finally do a phenol-chloroform extraction to remove proteins, and then ethanol precipitate the DNA using some glycogen (20 $\frac{mg}{ml}$, e.g. from Sigma) as a carrier to make the DNA pellet visible (the amount of DNA is tiny - supposed to be $1 - 10$ ng). Resuspend the dried pellet in 22 μl water - that gives enough for three ligation reactions using 7 μl a time, prior to PCR (in this case linker-mediated PCR).

RIPA buffer:

- 1% Triton-X-100
- 0.1% Na-deoxycholate
- 0.1% SDS
- 140 mM NaCl
- 10 mM Tris pH 8.0
- 1 mM EDTA
- add PMSF to 1 mM immediately before use.

LiCl buffer:

- 250 mM LiCl
- 10 mM Tris pH 8.0
- 1 mM EDTA
- 0.5% NP-40
- 0.5% Na-deoxycholate

TE buffer:

- 10 mM Tris pH 8.0
- 1 mM EDTA

Appendix C

The Sequence of the PCR Products and the respective PCR Primers and Probes

Figure C.1 shows the sequences of the primers used for multiplex PCR analyzed by agarose gel electrophoresis as well as the TaqMan probes used for Real Time PCR analysis together with the primers that have been changed to obtain ideal positions for the probes.

```
Primer for electrophoresis analyzed muliplex PCR:


 TOPO-NL:    5'- GCA GGG GAT CAA TCT CAA GAC C -3'    pos. 1-22, tm=55.0
 TOPO-NU:    5'- TTT TGG CTC CTT GGG CTC TTT G -3'    pos. 241-220, tm=54.8

 GAGA-5L:    5'- CGT CGC CCA GTT CAA GCC CAG TG -3'   pos. 150-128, tm=57.7
 GAGA-5U:    5'- CGC CTT GTA GCC ATC GGG AAC CT -3'   pos. 1-23, tm=56.3



Primer and TaqMan probes for Real Time PCR:

TaqMan probes:
hsp26 TaqMan :   5'-CAT GGT CGT CCT GGC GTT CCT CA-3'         pos. 57-79, tm=62.0
topo TaqMan:     5'-TCC CAG ATC CCG ATG GAG AAC CCG T-3'      pos. 111-128, tm=60.7

Primer:
TOPO-L-Taq, replacing TOPO-NL:  5'-TTA AGT CAA TGG GAG GCG GA-3'  pos. 72-91, tm=54.8
```

Figure C.1: Oligo sequences for PCR

Figure C.2 shows the amplified fragment sequences of both, the hsp26 and topo amplicon. The oligos are added to mark their positions and their 5' to 3' direction.

```
hsp26 fragment:
                                  G5U-Taq
GAGA-5U
CGCCTTGTAGCCATCGGGAACCT 23 -->   CACAAAGTGGCGCATGAT -->
cgccttgtagccatcgggaaccttgtagcggcgcacaaagtggcgcatgatgtgaccatggtcgtcctggcgttccttcatgcttgccctcgaccaagatg
                                                  CATGGTCGTCCTGGCGTTCCTCA -->
                                  GAGA-5L                 hsp26 TaqMan
      G5L-Taq
   <-- GTGGTGGAAGTGCAACTC  GTGACCCGAACTTGACCCGCTGC 1
gagtcgtccaccaccttcacgttgagctcactgggcttgaactgggcgacgtc
100
                                                                  TOPO-L-Taq
topo fragment:
                                                                    TTAAGTCAATGGGAGGCGGA -->
TOPO-NL
GCAGGGGATCAATCTCAAGACC -->
gcaggggatcaatctcaagaccgcgaaggctttgaagggccagaagtcggcctcagctaagggcagaaaggttaagtcaatgggaggcggagcgggtgcc
ggagacgtattcccagatcccgatggagaacccgtcgagtttaagatcaccgaagaaatcattaagaaaatggcagcggctgccaaggtagctcaggcgg
100     TCCCAGATCCCGATGGAGAACCCG -->
          topo TaqMan
                                  TOPO-NU
                <-- GTTTCTCGGGTTCCTCGGTTTT
ctaaggagccgaagaaacccaaagagcccaaggagccaaaa
200
```

Figure C.2: The sequence of both amplicons: topo and hsp26

Appendix D

Capillary Parameters

Capillary ID in μm	Volume per μm	Volume per m	Surface/Volume in $\frac{mm^2}{\mu l}$	Counter Pressure in bar	Diffusion Time in sec.
				flow: 1 μl/min length: 1 m	from $\bar{r}^2 = 6Dt$[1]
10	78.5 fl	78.5 nl	400	850	0.04 - 4
20	314 fl	314 nl	200	53	0.17 - 17
25	490 fl	490 nl	160	22	0.26 - 26
50	2 pl	2 μl	80	1.4	1 - 100
75	4.4 pl	4.4 μl	53.6	0.2	2.3 - 235
100	7.9 pl	7.9 μl	40	0.08	4 - 400
500	196 pl	196 μl	8	1.3×10^{-4}	104 - 10400

Table D.1: Capillary parameters for typical diameters of fused silica CE-capillaries. Counter Pressure and Diffusion times are discussed in section 2.1.3. Diffusion times for $D = 10^{-6}$ to 10^{-8} cm^2/sec are given.

[1]with $\bar{r}$ the mean diffusion distance, D the diffusion coefficient and t the time, see also section 2.1.3.

Appendix E

Abbreviations

BSA:	Bovine Serum Albumin
CHIP:	Chromatin Immunoprecipitation
DMF:	Dimethyl Formamide
DMSO:	Dimethyl Sulfoxide
dNTP:	deoxy nucleotide triphosphate
EMBL:	European Molecular Biology Laboratory
GAF:	GAGA-Factor (GAGA transcription factor protein)
GMBS:	N-succinimidyl 4-maleimidobutyrate
HPLC:	High Performance Liquid Chromatography
ID:	Inner Diameter
IP:	Immunoprecipitation
LSCM:	Laser Scanning Confocal Microscopy
MBS:	N-succinimidyl 3-maleimidobenzorate
μTAS:	Micro Total Analysis System
MTS:	3-Mercaptopropyl-trimethoxysilane
NHS:	N-hydroxy-succinimide
OD:	Outer Diameter
PBS:	Phosphate Buffered Saline
PDMS:	Polydimethylsiloxane
PEEK:	Polyetheretherketone
PEG:	Polyethylene Glycol
PMMA:	Polymethylmethacrylate
PTFE:	Polytetrafluorethylene
SDS:	Sodium Dodecylsulfate

Bibliography

B. Alberts, D. Bray, J. Lewis, M. Raff, K. Roberts and J. D. Watson (1994), Molecular biology of the cell. Garland, New York, third edition.

N. Alcantar, E. Aydil and J. Israelachvili (2000), Polyethylene glycol-coated biocompatible surfaces., *J. Biomed. Mater. Res.*, **51**(3), 343–351.

Amersham Pharmacia (2001), Affinity Chromatography, Principles and Methods. Handbook from Amersham Pharmacia Biotech, Edition AC.

G. Anderson, M. Jacoby, F. Ligler and K. King (1997), Effectiveness of protein A for antibody immobilization for a fiber optic biosensor, *Biosensors & Bioelectronics*, **12**, 329–336.

H. Andersson, W. van der Wijngaart and G. Stemme (2001), Micromachined filter-chamber array with passive valves for biochemical assays on beads., *Electrophoresis*, **22**(2), 249–257.

E. Baricheva, A. Katokhin and L. Perelygina (1997), Expression of Drosophila melanogaster gene encoding transcription factor GAGA is tissue-specific and temperature-dependent, *FEBS Lett*, **414**(2), 285–288.

H. Becker and C. Gärtner (2000), Polymer microfabrication methods for microfluidic analytical applications, *Electrophoresis*, **21**, 21–26.

P. Becker (1995), *Drosophila* Chromatin and Transcription, *Seminars in Cell Biology*, **6**, 185–190.

P. Becker (1998), personal communication.

E. Benjamini, R. Coico and G. Sunshine (2000), Immunology, A Short Course. Wiley, New York, fourth edition.

C. Benyajati, l. Mueller, N. Xu, M. Pappano, J. Gao, M. Mosammaparast, D.Conklin, H. Granok, C. Craig and S. Elgin (1997), Multiple Isoforms of GAGA Factor, a Critical Component of Chromatin Structure, *Nucleic Acids Research*, **25**(16), 3345–3353.

K. Bhat, G. Farkas, F. Karch, H. Gyurkovics, J. Gausz and P. Schedl (1996), The GAGA factor is required in the early Drosophila embryo not only for transcriptional regulation but also for nuclear division., *Development*, **122**(4), 1113–1124.

S. Bhatia, L. Shriver-Lake, K. Prior, J. Georger, J. Calvert, R. Bredehorst and F. Ligler (1991), Use of Thiol-Terminal Silanes and Heterobifunctional Crosslinkers for Immobilization of Antibodies on Silica Surfaces, *Analytical Biochemistry*, **178**, 408–413.

S. Bhatia, J. Teixeira, M. Anderson, L. Shriver-Lake, J. Calvert, J. Georger, J. Hickman, C. Dulcey, P. Schoen and F. Ligler (1993), Fabrication of Surfaces Resistant to Protein Adsorption and Application to Two-Dimensional Protein Patterning, *Analytical Biochemistry*, **208**, 197–205.

G. Blankenstein and U. Larsen (1998), Modular Concept of a Laboratory on a Chip for Chemical and Biochemical Analysis, *Biosensors & Bioelectronics*, **13**(3-4), 427–438.

E. Bonte (1998), personal communication.

T. Boone, Z. Fan, H. Hooper, A. Ricco, H. Tan and S. Williams (2002), Plastic Advances Microfluidic Devices, *Analytical Chemistry*, **74**(3), 78A–86A.

A. Brecht and G. Gauglitz (1995), Optical probes and transducers, *Biosensors and Bioelectronics*, **10**, 923–936.

M. Brischwein, W. Baumann, R. Ehret, A. Schwinde, M. Kraus and B. Wolf (1996), Mikrosensorische Systeme in der zellbiologischen Grundlagenforschung und der medizinischen Diagnostik, *Naturwissenschaften*, **83**, 193–200.

W. Burnette (1981), 'Western Blotting': Electrophoretic transfer of proteins from sodium dodecyl sulfate-polyacrylamide gels to unmodified nitrocellulose and radiographic detection with antibody and radioiodinated protein A, *Analytical Biochemistry*, **112**, 195.

M. Burns, B. Johnson, S. Brahmasandra, K. Handique, J. Webster, M. Krishnan, T. Sammarco, P. Man, D. Jones, D. Heldsinger, C. Mastrangelo and D. Burke (1998), An Integrated Nanoliter DNA Analysis Device, *Science*, **282**, 484–487.

D. Campbell, E. Luescher and L. Lerman (1951), Immunologic Adsorbents. I. Isolation of Antibody by Means of a Cellulose-Protein Antigen, *Proc. Natl. Acad. Sci.*, **37**, 575–578.

J. Campos-Ortega and V. Hartenstein (1997), The embryonic development of Drosophila melanogaster. Springer Verlag, Berlin, 2nd edition.

K. Catt and H. Niall (1967), Solid phase radioimmunoassay., *Nature*, **213**, 825–827.

G. Cavalli, V. Orlando and R. Paro (1999), Mapping DNA target sites of chromatin-associated proteins by formaldehyde cross-linking in *Drosophila* embryos, in: *Chromosome Structural Analysis: A Practical Approach*, herausgegeben von W. Bickmore, pp. 20–37. Oxford University Press.

W. Chan and J. Delabie (1996), Single Cell Analysis of H/RS Cells, *Annals of Oncology*, **7 (Suppl.4)**, S41–S43.

N. Chiem and D. Harrison (1998), Monoclonal Antibody Binding Affinity Determined by Microchip-Based Capillary Electrophoresis, *Electrophoresis*, **19**, 3040–3044.

Chipping Forecast (1999), The Chipping Forecast, Supplement to Nature Genetics.

J.-W. Choi, K. Oh, J. Thomas, W. Heineman, H. Halsall, J. Nevin, A. Helmicki, H. Henderson and C. Ahn (2002), An integrated microfluidic biochemical detection system for protein analysis with magnetic bead-based sampling capabilities, *Lab Cip*, **2**, 27–30.

T. Chovan and A. Guttman (2002), Microfabricated devices in biotechnology and biochemical processing, *Trends in Biotechnology*, **20**(3), 116–122.

D. Conrad, A. Davis, S. Golightley, J. Bart and F. Ligler (1997), Photoactivatable Silanes for the Site-Specific Immobilization of Antibodies, *SPIE*, **2978**, 12–21.

D. Conrad, S. Golightley and J. Bart (1998), US Patent No 5773308.

C. Crane-Robinson, F. A. Myers, T. R. Hebbes, A. L. Clayton and A. W. Thorne (1999), Chromatin immunoprecipitation assays in acetylation mapping of higher eukaryotes., *Methods Enzymol*, **304**, 533–47.

J. Cras, C. Rowe-Taitt, D. Nivens and F. Ligler (1999), Comparison of chemical cleaning methods of glass in preparation for silanization, *Biosensors & Bioelectronics*, **14**, 683–688.

P. Cuatrecasas and M. Wilchek (1968), Single-step purification of avidine from egg white by affinity chromatography on biocytin-Sepharose columns., *Biochem. Biophys. Res. Commun.*, **33**, 235–239.

R. Daniels, C. Holding, E. Kontogianni and M. Monk (1996), Single-Cell Analysis of Unstable Genes, *J. Assist. Reprod. Genet.*, **13**(2), 163–169.

A. de Mello and R. Wootton (2002), But what is it good for? Applications of microreactor technology for the fine chemical industry., *Lab Chip*, **2**, 7N–13N.

Y. Dong, S. Pappu and Z. Xu (1998), Detection of Local Density Distribution of Isolated Silanol Groups on Planar Silica Surfaces Using Nonlinear Optical Molecular Probes, *Analytical Chemistry*, **70**(22), 4730–4735.

C. Effenhauser, A. Manz and H. Widmer (1993), Glass Chips for High-Speed Capillary Electrophoresis Separations with Submicrometer Plate Hights, *Analytical Chemistry*, **65**(19), 2637–2642.

K. Ensing and A. Paulus (1996), Immobilization of Antibodies as a Versatile Tool in Hybridized Capillary Electrophoresis, *J. of Pharmaceutical and Biomedical Analysis*, **14**, 305–315.

R. Eritja (1999), personal communication.

G. Farkas, J. Gausz, M. Galloni, G. Reuter, H. Gyurkovics and F. Karch (1994), The Trithorax-like gene encodes the Drosophila GAGA factor, *Nature*, **371**, 806–808.

E. Florin, V. Moy and H. Gaub (1994), Adhesion forces between individual ligand-receptor pairs., *Science*, **264**, 415–417.

S. Fodor, J. Read, M. Pirrung, L. S. andA.T. Lu and D. Solas (1991), Light-Directed, Spatially Adressable Parallel Chemical Synthesis, *Science*, **251**, 767–773.

G. Fuhr and S. Shirley (1998), Biological Applications of Microstructures, in: *Microsystem Technology in Chemistry and Life Sciences*, herausgegeben von A. Manz and H. Becker, Topics in Current Chemistry. Springer.

G. Fuhr, T. Schnelle, R. Hagedorn and S. Shirley (1995), Dielectrophoretic Field Cages: Technique for Cell, Virus and Macromolecule Handling, *Cellular Engineering*, **1**, 47–57.

Q. Gadgil, H. Jurado and H. Jarrett (2001), DNA Affinity Chromatography of Transcription Factors, *Analytical Biochemistry*, **290**, 147–178, Review.

M. Garrison and B. Ratner (1997), Scanning probe microscopy for the characterization of biomaterials and biological interactions., *Ann. N. Y. Acad. Sci.*, **831**, 101–113.

H. Gau, S. Herminghaus, P. Lenz and R. Lipowsky (1999), Liquid Morphologies on Structures Surfaces: From Microchannels to Microchips, *Science*, **283**, 46–49.

G. Gauglitz, A. Brecht, G. Kraus and W. Nahm (1993), Chemical and biochemical sensors based on interferometry at thin (multi-)layers., *Sensors and Actuators B*, **11**, 21–27.

C. Gerthsen (2001), Physik. Springer, Berlin.

G. Gilfillan (2000), personal communication.

S. Gilman and A. Ewing (1995), Analysis of Single Cells by Capillary Electrophoresis with On-Column Derivatization and Laser-Induced Fluorescence Detection, *Analytical Chemistry*, **67**(1), 58–64.

A. Giulietti, L. Overbergh, D. Valckx, B. Decallonne, R. Bouillon and C. Mathieu (2001), An Overview on Real-Time Quantitative PCR: Applications to Quantify Cytokine Gene Expression, *Methods*, **25**, 386–401.

H. Granok, B. Leibovitch, C. Shaffer and S. Elgin (1995), Ga-ga over GAGA factor, *Current Biology*, **5**(3), 238–241.

P. Gravesen, J. Branebjerg and O. Jensen (1993), Microfluidics - A Review, *J. Micromech. Microeng.*, **3**, 168–182.

N. Green (1975), Avidin., *Adv. Protein Chem.*, **29**, 85–133.

R. Green, R. Frazier, K. Shakesheff, M. Davies, C. Roberts and S. Tendler (2000), Surface plasmon resonance analysis of dynamic biological interactions with biomaterials., *Biomaterials*, **21**, 1823–35.

M. Grunze (1999), Driven Liquids, *Science*, **283**, 41–42.

D. Hage and M. Nelson (2001), Chromatographic Immunoassays, *Analytical Chemistry*, **73**(7), 199A–205A.

C. Halliwell and A. Cass (2001), A Factorial Analysis of Silanization Conditions for the immobilization of Oligonucleotides on Glass Surfaces, *Analytical Chemistry*, **73**(11), 2476–2483.

E. Harlow and D. Lane, Editor (1988), Antibodies - A Laboratory Manual. Cold Spring Harbor Laboratory.

D. Harrison, K. Fluri, K. Seiler, Z. Fan, C. Effenhauser and A. Manz (1993), Micromachining a Miniaturized Capillary Electrophoresis-Based Chemical Analysis System on a Chip, *Science*, **261**, 895–897.

D. Harrison, C. Wang, P. Thibeault, F. Ouchen and S. Cheng (2000), The Decade's Search for the Killer Ap in μTAS, in: *Micro Total Analysis Systems 2000*.

P. L. D. Harrison (1997), Transport, manipulation and reaction of biological cells on-chip using electrokinetic effects., *Analytical Chemistry*, **69**, 1564–1568.

M. Hayes, N. Polson, A. Phayre and A. Garcia (2001), Flow-based Microimmunoassay, *Analytical Chemistry*, **73**, 5896–5902.

A. Hecht and M. Grunstein (1999), Mapping interaction sites of chromosomal proteins using immunoprecipitation and polymerase chain reaction., *Methods Enzymol*, **304**, 399–414.

C. Heid, J. Stevens, K. Livak and P. Williams (1996), Real time quantitative PCR, *Genome Research*, **6**, 986–994.

R. Higuchi, C. Fockler, G. Dollinger and R. Watson (1993), Kinetic PCR Analysis: Real-time Monitoring of DNA Amplification Reactions, *Biotechnology*, **11**, 1026–1030.

C. Horak, M. Mahajan, N. Luscombe, M. Gerstein, S. Weissmann and M. Snyder (2002), GATA-1 binding sites mapped in the β-globulin locus by using mammalian chIp-chip analysis, *Proc. Natl. Acad. Sci.*, **99**(5), 2924–2929.

S. Jakeway, A. de Mello and E. Russel (2000), Miniaturized total analysis systems for biological analysis, *Fresenius Journal of Analytical Chemistry*, **366**, 525–539.

C. Janeway, P. Travers, M. Walport and M. Shlomchik (2001), Immunobiology. Garland Publishing, New York, fifth edition.

G. Jiang and D. Harrison (2000), mRNA isolation in a microfluidic device for eventual integration of cDNA library construction., *Analyst*, **125(12)**, 2176–2179.

U. Jönsson, M. Malmqvist, G. Olofsson and I. Rönnberg (1988), Surface immobilization techniques in combination with ellipsometry., *Methods Enzymol*, **137**, 381–8.

R. Jung, K. Soondrum and M. Neumaier (2000), Quantitative PCR., *Clin. Chem. Lab. Med.*, **38**(9), 833–836.

J. Khandurina and A. Guttman (2002), Bioanalysis in Microfluidic Devices, *Journal of Chromatography A*, **943**, 159–183, Review.

M. Kopp, H. Crabtree and A. Manz (1997), Developments in Technology and Applications of Microsystems, *Current Opinion in Chemical Biology*, **1**, 410–419.

M. Kopp, A. Mello and A. Manz (1998), Chemical Amplification: Continuous-Flow PCR on a Chip., *Science*, **280**, 1046–8.

M. Krishnan, V. Namasivayam, R. Lin, R. Pal and M. Burns (2001), Microfabricated reaction and separation systems, *Current Opinion in Biotechnology*, **12**, 92–98.

L. Kuhn, E. Bassous and R. Lane (1978), Silicon charge electrode array for ink jet printing, in: *IEEE Transactions for Electronic Devices*, Band ED-26, pp. 1918–1920.

M. Küpper, U. Loftin, F. von Bonin, M. Pfreundschuh, H. Daus and L. Trümper (1996), Single Cell PCR for the Analysis of Hodgkin's Disease: Four Years Later, *Annals of Oncology*, **7 (Suppl.4)**, S35–S39.

N. Lacher, K. Garrison, R. Martin and S. Lunte (2001), Microchip capillary electrophoresis/electrochemistry., *Electrophoresis*, **22**, 2526–2536.

E. Leyden, Editor (1986), Silanes, Surfaces and Interfaces. Gordon and Breach, New York.

J. Li, T. Tremblay, C. Wang, S. Attiya, D. Harrison and P. Thibault (2001), Integrated system for high-throughput protein identification using a microfabricated device coupled to capillary electrophoresis/nanoelectrospray mass spectrometry., *Proteomics*, **1**(8), 975–986.

Y. Lie and C. Petropoulos (1998), Advances in quantitative PCR technology: 5' nuclease assays, *Current Opinion in Biotechnology*, **9**, 43–48.

F. Ligler (2001), personal communication.

F. Ligler, M. Breimer, J. Golden, D. Nivens, J. Dodson, T. Green, D. Haders and O. Sadik (2002), Integrating waveguide biosensor., *Analytical Chemistry*, **74**, 713–719.

P. Lindberg and J. Roeraade (1998), A new technique for stripping of polyimide coating from fused-silica capillaries, *Electrophoresis*, **19**, 2445–2446.

Q. Lu, L. Wallrath, H. Granok and S. Elgin (1993), (CT)n (GA)n repeats and heat shock elements have distinct roles in chromatin structure and transcriptional activation of the Drosophila hsp26 gene., *Molecular Cell Biology*, **13**, :2802–2814.

Y. Lyubchenko, R. Blankenship, A. Gall, S. Lindsay, O. Thiemann, L. Simpson and L. Shlyakhtenko (1996), Atomic force microscopy of DNA, nucleoproteins and cellular complexes: the use of functionalized substrates., *Scanning Microsc. Suppl.*, **10**, 97–107.

A. Manz, N. Graber and H. Widmer (1990), Miniaturized Total Chemical Analysis Systems: A Novel Concept for Chemical Sensing, *Sensors and Actuators B, Chemical*, **1**, 244–248.

P. Matejtschuk, Editor (1997), Affinity Separations - A Practical Approach, The Practical Approach Series. Oxford University Press, Oxford.

P. Mazur, U. Schneider, K. Jacobsen and A. Mahowold (1988), Survival of intact *Drosophila* eggs at various stages of embryonic development as a function of the extent of dehydration on intraembryonic freezing., *Cryobiology*, **25**, 543–544.

M. McPherson and S. Møller (2000), PCR, The Basics, from background to bench. BIOS Scientific Publishers Ltd, Oxford.

M. McPherson, P. Quirke and G. Taylor, Editor (1996), PCR1, A Practical Approach, PAS The Practical Approach Series. IRL Press at Oxford University Press, Oxford, New York, Tokyo.

M. Minsky (1961), Microscopy Apparatus, US Patent No 3013467, Filed 1957.

M. Mitchell, V. Spikmans, F. Bessoth, A. Manz and A. de Mello (2000), Towards Organic Synthesis in Microfluidic Devices: Multicomponent Reactions for the Construction of Compound Libraries., in: *Micro Total Analysis Systems 2000*.

H. Morgan, D. Pritchard and J. Cooper (1995), Photo-patterning of sensor surfaces with biomolecular structures: characterisation using AFM and fluorescence microscopy, *Biosensors and Bioelectronics*, **10**, 841–846.

V. Moy, E. Florin and H. Gaub (1994), Intermolecular forces and energies between ligands and receptors., *Science*, **266**, 257–259.

M. Mrksich and G. Whitesides (1996), Using Self-Assembled Monolayers to Understand the Interactions of Man-Made Surfaces with Proteins and Cells, *Annu.Rev.Biophys.Biomol.Struct.*, **25**, 55–78.

T. Müller, G. Gradl, S. Howitz, S. Shirley, T. Schnelle and G. Fuhr (1999), A 3-D microelectrode system for handling and caging single cells and particles., *Biosensors and Bioelectronics*, **14**, 247–256.

K. Mullis, F. Faloona, S. Scharf, R. Saiki, G. Horn and H. Erlich (1986), Specific enzymatic amplification of DNA *in vitro*: The polymerase chain reaction., *Cold Spring Harb. Symp. Quant. Biol.*, **51**, 263–273.

V. Muronetz, M. Sholukh and T. Korpela (2001), Use of protein-protein interactions in affinity chromatography., *J. Biochem. Biophys. Methods*, **49**, 29–47.

U. Narang, G. Anderson, F. Ligler and J. Burans (1997), Fiber Optic-Based Biosensor for Ricin, *Biosensors & Bioelectronics*, **12**(9-10), 937–945.

M. Nisnevitch and M. Firer (2001), The solid phase in affinity chromatography: strategies for antibody attachment, *J. Biochem. Biophys. Methods*, **49**, 467–480.

M. Northrup, B. Benett, D. Hadley, P. Landre, S. Lehew, J. Richards and P. Stratton (1998), A Miniature Analytical Instrument for Nucleic Acids Based on Micromachined Silicon Reaction Chambers, *Analytical Chemistry*, **70**(5), 918–922.

T. O'Brien, R. Wilkins, C. Giardina and J. Lis (1995), Distribution of GAGA protein on Drosophila genes in vivo., *Genes and Development*, **9**(9), 1098–1110.

R. Oleschuk, L. Shultz-Lockyear, Y. Ning and D. Harrison (2000), Trapping of bead-based reagents within microfluidic systems: on-chip solid-phase extraction and electrochromatography, *Analytical Chemistry*, **72**(3), 585–590.

J. Omichinski, P. Pedone, G. Felsenfeld, A. Gronenborn and G. Clore (1997), The solution structure of a specific GAGA factor-DNA complex reveals a modular binding mode, *Nat. Struct. Biol.*, **4**(2), 122–132.

V. Orlando and R. Paro (1993), Mapping Polycomb-Repressed Domains in the Bithorax Complex Using In Vivo Formaldehyde Cross-Linked Chromatin, *Cell*, **75**, 1–20.

V. Orlando, H. Strutt and R. Paro (1997), Analysis of Chromatin Structure by in Vivo Formaldehyde Cross-Linking, *Methods: A Companion to Methods in Enzymolgy*, **11**, 205–214.

E. Österberg, K. Bergström, K. Holmberg, T. Schuman, J. Riggs, N. Burns, J. Van Alstine and J. Harris (1995), Protein-Rejecting Ability of Surface-Bound Dextran in End-on and Side-on Configurations: Comparison to PEG, *Journal of Biomedical Materials Research*, **29**, 741–747.

V. Pan, Y. Hanein, D. Leach-Scampavia, K. F. Böhringer, B. Ratner and D. Denton (2001), A Precision Technology for Controlling Protein Adsorption and Cell Adhesion, in: *BioMEMS, Proc. IEEE Workshop on Micro Electro Mechanical Systems (MEMS)*, Interlaken, Switzerland.

P. Paul, M. Garguilo and D. Rakestraw (1998), Imaging of Pressure- and Electrokinetically Driven Flows through Open Capillaries., *Analytical Chemistry*, **70**(13), 2459–2467.

K. Petersen (1982), Silicon as a Mechanical Material, *Proceedings of the IEEE*, **70**(5), 420–457.

J. Piehler, A. Brecht, K. Geckeler and G. Gauglitz (1996), Surface Modification for Direct Immunoprobes, *Biosensors and Bioelectronics*, **11**(6/7), 579–590.

J. Piehler, A. Brecht, R. Valiokas, B. Liedberg and G. Gauglitz (2000), A high-density poly(ethylene glycol) polymer brush for immobilization on glass-type surfaces., *Biosensors and Bioelectronics*, **15**(9/10), 473–481.

D. Polla, A. Erdman, W. Robbins, D. Markus, J. Diaz-Diaz, R. Rizq, Y. Nam, H. Brickner, A. Wang and P. Krulevitch (2000), Microdevices in medicine., *Annual Rev. Biomed. Eng.*, **2**, 551–576.

N. Polson and M. Hayes (2001), Microfluidics: Controlling Fluids in Small Places, *Analytical Chemistry*, **73**(11), 313A–319A.

D. Pritchard, H. Morgan and J. Cooper (1995), Micron-Scale Patterning of Biological Molecules, *Angew. Chem. Int. Ed. Engl.*, **34**(1), 91–93.

B. Ratner (1995), Surface modification of polymers: chemical, biological and surface analytical challenges, *Biosensors and Bioelectronics*, **10**, 797–804.

C. Rowe, L. Tender, M. Feldstein, J. Golden, S. Scruggs, B. MacCraith, J. Cras and F. Ligler (1999), Array biosensor for simultaneous identification of bacterial, viral, and protein analytes., *Anal Chem*, **71**(17), 3846–52.

J. Ruzicka and E. Hansen (2000), Flow injection analysis: from beaker to microfluidics., *Analytical Chemistry*, **72**, 212A–217A.

R. Saiki, D. Gelfand, S. Stoffel, S. Scharf, R. Higuchi, G. Horn, K. Mullis and E. H.A (1988), Primer-directed enzymatic amplification of DNA with a thermostable DNA polymerase., *Science*, **239**, 487–491.

J. Sambrook, E. Fritsch and T. Maniatis, Editor (1989), Molecular Cloning - A Laboratory Manual, Topics in Current Chemistry. Cold Spring Harbor Laboratory Press.

H. Seehofer (1997), Adsorption von Plasmaproteinen aus wäßrigen Lösungen auf Festkörperoberflächen, Diplomarbeit, Universität Heidelberg.

R. Seigel, P. Harder, R. Dahint, M. Grunze and F. Josse (1997), On-Line Detection of Nonspecific Protein Adsorption at Artificial Surfaces, *Analytical Chemistry*, **69**, 3321–3328.

D. Sheehan (2000), Physical Biochemistry: Principles and Applications. Wiley, Chichester.

Y. Shi, P. Simpson, J. Scherer, D. Wexler, D. Skibola, M. Smith and R. Mathies (1999), Radial capillary array electrophoresis microplate and scanner for high-performance nucleic acid analysis., *Analytical Chemistry*, **71**, 5354–5361.

L. Shriver-Lake, B. Donner, R. Edelstein, K. Breslin, S. Bhatia and F. Ligler (1997), Antibody Immobilization using Heterobifunctional Crosslinkers, *Biosensors & Bioelectronics*, **12**(11), 1101–1106.

M. Solomon and A. Varshavsky (1985), Formaldehyde-mediated DNA-protein crosslinking: A probe for *in vivo* chromatin structures, *Proc. Natl. Acad. Sci. USA*, **82**, 6470–6474.

J. Stevens, L. Mills and J. Trogadis, Editor (1994), Three-Dimensional Confocal Microscopy: Volume Investigation of Biological Systems. Academic Press, London.

H. Strutt and R. Paro (1999), Mapping DNA target sites of chromatin in vivo by formaldehyde crosslinking., *Methods in Molecular Biology*, **119**, 455–467, Review.

H. Strutt, G. Cavalli and R. Paro (1997), Co-localization of Polycomb protein and GAGA factor on regulatory elements responsible for the maintenance of homeotic gene expression, *EMBO Journal*, **16**(12), 3621–3632.

L. Stryrer (1995), Biochemistry. Freeman, New York, fourth edition.

S. Sundberg, R. Barrett, M. Pirrung, A. Lu, B. Kiangsoontra and C. Holmes (1995), Spatially-Addressable Immobilization of Macromolecules on Solid Supports, *J. Am. Chem. Soc.*, **117**(49), 12050–12057.

S. Terry (1975), A Gas Chromatography System Fabricated on a Silicon Wafer Using Integrated Circuit Technology, Ph.D. thesis, Stanford University, Stanford, CA, USA.

H. Towbin, T. Staehelin and J. Gordon (1979), Electrophoretic transfer of proteins from polyacrylamide gels to nitrocellulose sheets: Procedure and some applications., *Proc Natl. Acad. Sci.*, **76**, 4350.

G. Truskey, F. Yuan and D. Katz (2000), Transport Phenomena in Biological Systems: A Textbook for Biomedical Engineers. Duke University, Durham, USA, Draft, pre-published at http://www.duke.edu/ gtruskey/book.html.

E. Vandenberg, L. Bertilsson, B. Liedberg, K. Uvdal, R. Erlandsson, H. Elwing and I. Lundström (1991), Structure of 3-Aminopropyl Triethoxy Silane on Silicon Oxide, *Journal of Colloid and Interface Science*, **147**, 103–118.

J. Wang (2000), From DNA biosensors to gene chips., *Nucleic Acids Research*, **28(16)**, 3011–3016.

L. Waters, S. Jacobson, N. Kroutchinina, J. Khandurina, R. Foote and J. Ramsey (1998), Microchip Device for Cell Lysis, Multiplex PCR Amplification, and Electrophoretic Sizing, *Analytical Chemistry*, **70**(1), 158–162.

M. Weller (2000), Immunochromatographic techniques–a critical review., *Fresenius J. Anal. Chem.*, **366**(6-7), 635–645.

P. Wilding and L. Kricka (1999), Micro-microchips: just how small can we go?, *Trends in Biotechnology*, **17**, 465–468.

P. Wilding, M. Shoffner and L. Kricka (1994), PCR in a Silicon Microstructure, *Clinical Chemistry*, **40**(9), 1815–1818, Oak Ridge Conference.

R. Wilkins and J. Lis (1997), Dynamics of potentiation and activation: GAGA factor and its role in heat shock gene regulation, *Nucleic Acids Research*, **25**(20), 3963–3968.

R. Wilkins and J. Lis (1998), GAGA factor binding to DNA via a single trinucleotide sequence element, *Nucleic Acids Research*, **26**(11), 2672–2678.

T. Wilson, Editor (1990), Confocal Microscopy. Academic Press, London.

A. Woolley, D. Hadley, P. Landre, A. deMello, R. Mathies and M. Northrup (1996), Functional Integration of PCR Amplification and Capillary Electrophoresis in a Microfabricated DNA Analysis Device, *Analytical Chemistry*, **68**(23), 4081–4086, Accelerated Article.

D. Wylie, D. Lu, R. Carlson, K. Babacan, S. Schuster and F. Wagher (1992), Monoclonal antibodies specific for mercury ions., *Proc. Natl. Acad. Sci. USA*, **89**, 4101–4108.

F. Zhang, E. Kang, K. Neoh, P. Wang and K. Tan (2001), Surface modification of stainless steel by grafting of poly(ethylene glycol) for reduction in protein adsorption., *Biomaterials*, **22**(12), 1541–1548.

M. Zhang, T. Desai and M. Ferrari (1998), Proteins and Cells on PEG Immobilized Silicon Surfaces, *Biomaterials*, **19**, 953–960.

Acknowledgements

I would like to thank:

Prof. Dr. Christiane Ziegler for supervising and supporting my thesis and for her unquestioning moral support;

Christian Boulin, Peter Becker and Heinrich Hörber for initiating and supervising the project and for their dedicated help during the harder periods of my time at EMBL;

Jürgen Zimmermann and Vladimir Benes for teaching me the nuts and bolts of molecular biology work and for all the questions they were asking;

Matthias Hentze and Tiziana Novarini who take care of the EMBL Ph.D. programme;

Simon Sheldon, Gregor Gilfillan, Ario de Marco, Jens Rietdorf, small Sabine and tall Sabine and the people from the EMBL mechanical workshop;

Stefania, Stephanie, François, Ann, Arnd, Pete, Corinna, Renaud, Sandra, HG, Frank, Doris, Rick, Holger and Elena, Anton, Irmtraud and the whole group, Ralph, Bianca

and Elke.

In particular I want to express my thankfulness to Tor Erik, Birgit, Michi, Katrin and Josefa who were there when I needed help.

Finally, this work was possible thanks to the generous financial support of the European Molecular Biology Laboratory.

Erklärung

Hiermit erkläre ich, daß ich diese Dissertation selbständig angefertigt habe und keine anderen als die angegebenen Quellen und Hilfsmittel benutzt sowie Zitate kenntlich gemacht habe.

Lebenslauf

Name:	Olaf Selchow
Geburtsdatum:	24. April 1970
Geburtsort:	Stuttgart
Familienstand:	ledig
Anschrift:	Beethovenstraße 1, 69121 Heidelberg
	Tel: 06221 411815, email: selchow@embl-heidelberg.de

Schulbildung:

August 1976 – Juli 1980	Grundschule Stuttgart-Kaltental
August 1980 – Mai 1989	Hegel-Gymnasium Stuttgart-Vaihingen
9.5.1989	Abitur, Gesamtnote: 1,5 (sehr gut)

Hochschulausbildung:

Oktober 1989 – März 1992	Studium der Physik TH Darmstadt
	17.12.1991 Diplomvorprüfung, Gesamtnote: befriedigend
April 1992 – September 1993	Studium der Physik TU München
Oktober 1993 – Juli 1994	Auslands-Studium Frankreich, Universit Montpellier II
	4.7.1994 "Maîtrise de Physique", Note: assez bien (≈ gut)
	April 1994 - Mai 1994: Praktikum am Institut für
	Biomechanik des INSERM (Unit 103), Montpellier.
Oktober 1994 – Januar 1997	Studium der Physik TU München
	1.12.1995 – 2.12.1996: Diplomarbeit am Max-Planck-Institut
	für Kolloid- und Grenzflächenforschung in Teltow bei
	Berlin, Prof. Dr. R. Lipowsky in Zusammenarbeit mit
	der TU München (Prof. Dr. E. Sackmann)
	21.1.1997: Diplom in Physik, Gesamtnote: 1,4 (sehr gut)
Juli 1997 – März 2002	Doktorand am European Molecular Biology Laboratory (EMBL)
	in Heidelberg, betreut von Prof. Dr. Ch. Ziegler,
	Fachbereich Physik der Universität Kaiserslautern

Weitere Tätigkeiten:

Oktober 1992 – Januar 1993	Studentische Hilfskraft an der TU München
Mai 1993 – Juli 1993	Studentische Hilfskraft an der TU München
Januar 1995 – März 1995	Studentische Hilfskraft an der TU München
Dezember 1996 – April 1997	Wissenschaftliche Hilfskraft am Max-Planck-Institut
	für Kolloid- und Grenzflächenforschung in Teltow bei Berlin